School of Mining Engineering

UNIVERSITY OF THE WITWATERSRAND, JOHANNESBURG

SUPPORT DESIGN APPROACH FOR CRUSHER CHAMBERS: A CASE STUDY OF PALABORA MINING COMPANY

Nyeleti Venus Masole

A research report submitted to the Faculty of Engineering and the Built Environment, University of the Witwatersrand, Johannesburg, in partial fulfilment of the requirements for the degree of Master of Science.

Johannesburg, 2023

DECLARATION

I declare that this report is my own, unaided work. I have read the University Policy on Plagiarism and hereby confirm that no plagiarism exists in this report. I also confirm that there is no copying nor is there any copyright infringement. I willingly submit to any investigation in this regard by the School of Mining Engineering and I undertake to abide by the decision of any such investigation.

Nyeleti Masole

Signature of Candidate

09/01/2024

Date

“Discovery consists of seeing what everybody has seen and thinking what nobody has done”.

Albert von Szent-Gyorgyi

ABSTRACT

This report project aimed to design a support system for crusher chambers at Palabora. The research project focused mainly on the two crusher chambers (12m wide by 25m high and 61m long) planned for the Lift 2 project as part of the ore handling system. The main research questions that the researcher sought to answer were; what are the differences between Lift 1 & Lift 2 in rock mass characterisation, classification and the ground control district?; how suitable is the Lift 1 crusher chamber support system for Lift 2?; what could be support requirements for Lift 2 crusher chambers in terms of empirical, analytical and numerical design methods and what are the recommended support design approaches for Lift 2 crusher chambers?

The methodology used to design support for the Lift 2 crusher chambers was based on determining the expected failure mode first and then selecting suitable design methods to cater for the extent of failure. This study combined empirical and analytical methods to determine the failure mode and required support system. The results were then validated using Finite Element Method numerical modelling software called RS2 (Phase 2) from RocScience.

Research findings revealed that the ground control district, classification and characterisation of rock masses differ slightly between Lift 1 and Lift 2. Jointing in dolerite dykes (DOL) was slightly dense in Lift 2 compared to Lift 1 and was associated with increased mining depth. Furthermore, the Lift 1 crusher chamber support system was found to be suitable for Lift 2 but must incorporate dynamic support. Unwedge (RocScience) analysis simulated wedge type of failure in the crusher chamber walls. The empirical and analytical design approach proposed cable bolt lengths of between 6m and 9 m and 3-4 m for roof bolts with bolt spacing of 1.4 m and 1.0 m respectively. The simulation results using RS2 confirmed that the cable bolt length and spacing were appropriate. The recommended support system was expected to provide sufficient support to the crusher chamber in terms of controlling rock mass deformation and yielding.

The general conclusion was that the design approach selected for crusher chambers must be able to adequately represent rock mass behaviour and the support required to maintain long-term stability.

PUBLICATIONS AS PART OF THIS RESEARCH

No publication emanating from this research work has been prepared so far:

ACKNOWLEDGMENTS

I am beyond grateful for the invaluable patience and feedback my supervisor gave me. You have been a reliable source of knowledge and expertise, enabling me to embark on this journey. In addition, I appreciate the peer editing assistance and constructive criticism. I appreciate the support of my parents, husband and children. They have inspired me throughout this process and kept me motivated.

TABLE OF CONTENTS

DECLARATION i

ABSTRACT iii

PUBLICATIONS AS PART OF THIS RESEARCH iv

ACKNOWLEDGMENTS v

LIST OF FIGURES ix

APPENDIX LIST OF FIGURES xii

LIST OF ABBREVIATIONS xiii

LIST OF SYMBOLS xiv

1 INTRODUCTION 1

1.1 Research Background and Context 2

1.2 Problem Statement 2

1.3 Justification for Research 3

1.4 Research Aim and Objectives 4

1.5 Research Methods 4

1.6 Sources of Data 6

1.7 Research Validation 6

1.8 Mine Background 7

1.9 Structure of the Research Report 11

2 LITERATURE REVIEW 13

2.1 Introduction 13

2.2 Geology of the Study Area 13

2.3 Geological Structures 14

2.4 Lift 2 Geotechnical Zones 16

2.5 Support Design Approach 18

2.6 Benchmarking 44

2.7 Chapter Summary 45

3 RESEARCH APPROACH 46

3.1 Introduction 46

3.2 Desktop Study 46

3.3 Field Observations and Measurements 46

3.4 Laboratory Analysis 47

3.5 Empirical Analysis 48

3.6 Numerical Analysis 49

3.7 Research Design 50

3.8 Data Collection Process 51

3.9 Data Validation Process 52

3.10 Data Analysis Approach 52

3.11 Chapter Summary 54

4 DATA COLLECTION AND ANAYSIS 55

4.1 Introduction 55

4.2 Field Observations and Measurements 55

4.3 Geological Mapping 60

4.4 Core Logging 63

4.5 In-situ Stress 71

5 SUPPORT DESIGN FOR LIFT 2 CRUSHER CHAMBERS 75

5.1 Introduction 75

5.2 Kinematic Analysis 75

5.3 Numerical Modelling Analysis 78

5.4 Rock Mass Rating and Support Selection 85

5.5 Support Calculations..87

6 CONCLUSIONS AND RECOMMENDATIONS 92

6.1 Recommendation for Future Work 94

REFERENCE LIST 95

A. APPENDIX...107

LIST OF FIGURES

Figure 1-1: Locality plan of the Palabora Mining Company (Google)....................7
Figure 1-2: Illustration of the Lift 1 production footprint (Palabora, 2015) 9
Figure 1-3: Illustration of the PMC open pit and the underground operation.......10
Figure 1-4: Schematic view of the undercut and production level (Palabora, 2015)...10
Figure 1-5: A typical isometric overview of the lift 2 crusher chamber 11
Figure 2-1: Local geology of PMC (Diering et al., 2018)....................................14
Figure 2-2: Illustration of the geological structures of PMC (Palabora, 2015).....16
Figure 2-3. Illustrates Lift 2 ground control districts...17
Figure 2-4: A Plan View of the production level and Crusher location 18
Figure 2-5: Support Design Methodology as cited by (Pakalnis, 2015) 20
Figure 2-6: Wheel of Design (Stacey, 2009) 21
Figure 2-7: Maximum unsupported span vs stand-up time as a function of RMR and Q (Stacey, 2001)..29
Figure 2-8: Maximum unsupported span vs Q (Barton et al., 1974) 30
Figure 2-9: Unsupported span as a function of RMR as cited by Bieniawski & Lowson (2013)..30
Figure 2-10: Unsupported span vs FoS as a function of RMR/Q (Stacey, 2001)..31
Figure 2-11: Support design chart (NGI, 2022) 34
Figure 2-12: Illustration of support conditions for (A) gravity fall and (B) sliding instability for wedge within the back of tunnel (Pakalnis, 2015)..36
Figure 2-13: Illustration of the support of a potentially falling roof wedge (Li, 2017) 37
Figure 3-1: The methodology followed to design support for Lift 2 crusher chambers..50
Figure 4-1: Heading with FOS host rocks and calcite veins (Site A)...................56
Figure 4-2: Shows Site a jointed rock mass 57
Figure 4-3: Illustrates influence of water on stability of excavations 57
Figure 4-4: Illustrates an excavation with loose shotcrete held by mesh 58
Figure 4-5: Illustrates an excavation supported with shotcrete and roof bolts.....59
Figure 4-6: Illustrates shotcrete detachment and cracks in Lift 1 Production footprint 60

Figure 4-7: Illustrates mapped face in Site A.... 61
Figure 4-8: Illustrates drill hole HD020 discing and fractured zone (Palabora, 2017).... 65
Figure 4-9: Illustrates a jointed dolerite zone (Palabora, 2017).... 66
Figure 4-10: Illustrates HD020 highly jointed dolerite zone (Palabora, 2017).... 66
Figure 4-11: Illustrates HD020 crushed zone of MFOS (Palabora, 2017).... 67
Figure 4-12: Illustrates HD039 discing and fractured zone (Palabora, 2017).... 68
Figure 4-13: Illustrates HD039 a highly weathered FOS (Palabora, 2017).... 68
Figure 4-14: Illustrates HD039 dolerite dyke intersected (Palabora, 2017).... 69
Figure 4-15: Illustrates drill hole HD051 fractured zone (Palabora, 2017).... 70
Figure 4-16: Illustration of HD051 discing and fracture zones (Palabora, 2017).... 70
Figure 4-17: Illustrates borehole camera assessment at Site A (Masole, 2022).... 73
Figure 4-18: Illustrates borehole camera assessment at Site B (Masole, 2022).... 74
Figure 5-1: Great circle representing the three joint sets.... 77
Figure 5-2: Simulated wedges in the rock mass surrounding the Lift 2 crusher chambers.... 77
Figure 5-3: RS2 Model Outline.... 80
Figure 5-4: Contours of Strength Factor.... 81
Figure 5-5. Simulated Yield Zone.... 82
Figure 5-6. Major Principal Stress.... 83
Figure 5-7: Minor Principal Stress.... 83
Figure 5-8: Vertical Displacement.... 84
Figure 5-9: (a) Maximum shear strain, (b) Total displacement, $\sigma 1$ (c), $\sigma 3$ (d), Yield zone (e).... 85
Figure 5-10: Support design chart as a function of Q (NGI, 2022).... 86
Figure 5-11: Unsupported span vs Q/RMR of the 12 and 25m span (from Stacey, 2001).... 87
Figure 5-12: Proposed Support Standard for Lift 2 Crusher Chambers.... 91

LIST OF TABLES

Table 2-1: Major faults intersecting Lift 2 orebody (Palabora, 2015)..................15
Table 2-2: Rock quality based on RQD (Deere, 1964)......................................23
Table 2-3: Recommended ESR Values (NGI, 2022)..25
Table 2-4: Rock quality based on Q (NGI, 2022)...26
Table 2-5: Rock Mass Quality Based on (Bieniawski, 1989)..............................27
Table 4-1: Mapped joint data (Masole, 2022)...61
Table 4-2. Drill hole information (Palabora, 2017)...64
Table 4-3. Summary of major structure log (Palabora, 2017)............................64
Table 4-4: Lift 2 in-situ stress data (Handley & Piper, 2017)..............................71
Table 4-5: Definition for stress damage assessment (Martin et al., 1998)..........72
Table 5-1: Summary of prominent joint sets analysis..76
Table 5-2: Strength and limitations of RS2 (Rocscience, 2021b).......................78
Table 5-3. Rock material properties applied in the model (Palabora, 2015)........79
Table 5-4. Rock Mass Rating for Each Rock Type...85
Table 5-5: Selected Ground Support for Lift 2 Crusher Chambers.....................91

APPENDIX LIST OF FIGURES

Figure A- 1: Q system (NGI,2022) 107
Figure A- 2: Orientation Guide (Bieniawski, 1989) 107
Figure A- 3: Typical loding deformation curve of a 25mm threaded bar. 110
Figure A- 4: Strength /strain curve for 18mm 7 strand cable bolt...................... 111

APPENDIX LIST OF TABLES

Table A-1: RMR Parameters and Rating (Bieniawski, 1989)............................ 108
Table A-2: Cont... RMR Parameters and Rating (Bieniawski, 1989)................. 109
Table A-3: : Geological summary of HD020 111
Table A-4: Summary of major structure log of HD020 112
Table A-6: Geological summary of HD039 113
Table A-7: Summary of Major Structure log of HD039 113
Table A-7: Geological Summary of HD051 114
Table A-8: Summary of Major Structure log of HD051 115
Table A-9: Table codes description... 115

LIST OF ABBREVIATIONS

Abbreviation	Description
2D	Two dimensions
3D	Three dimensions
3DEC	Universal discrete element method in three dimensions
B	The excavation span
BCB	Banded Carbonatite
CFZ	Central Fault Zone
D	Disturbance factor
De	Equivalent Dimension
DEM	Distinct Element Method
DOL	Dolerite dyke
DRMS	Design Rock Mass Strength
ESR	Excavation Support Ratio
FDM	Finite Difference Method
FEM	Finite Element Method
FLAC	Fast Lagrangian Analysis of Continua in two dimensions
FLAC3D	Fast Lagrangian Analysis of Continua in three dimensions
FOS	Foskorite rock
FoS	Factor of safety
GSI	Geological Strength Index
Ja	Joint alteration number
Jc	Joint condition
Jn	Joint set number
Jr	Joint roughness number
Js	Joint spacing
Jv	Volumetric joint count
Jw	Joint water reduction factor
LHDs	Laud Haul Dumpers
LEM	Limit equilibrium method
MFOS	Micaceous Foskorite
MFZ	Mica Fault Zone
MPY	Micaceous Pyroxenite
MRMR	Mining Rock Mass Rating

NX	Core size with a diameter of 54 mm
PMC	Palabora Mining Company
PPV	Peak Particle Velocity
Q	Tunnelling Quality Index
RMR	Rock Mass Rating
SRF	Stress reduction factor
SWFZ	Southwest Fault Zone
TCB	Transgressive Carbonatite
TCP	Triaxial Compression tests with post-failure behaviour
TCS	Triaxial Compressive Strength
TFZ	Tree Fault Zone
TQI	Tunnel Quality Index
UCS	Uniaxial Compressive strength
UCM	Uniaxial compressive strength test with elastic modulus, Young's modulus and Poisson's ratio
UCP	Uniaxial pre- and post-failure test with axial and lateral deformation.
UDEC	Universal discrete element method

LIST OF SYMBOLS

Symbol	Description	Units
σ_1	Major Principal stress	MPa
σ_2	Medium Principal stress	MPa
σ_3	Minor Principal Stress	MPa
σ_c	Uniaxial compressive strength of intact rock	MPa
σ_{cm}	Uniaxial compressive strength of rock mass	MPa
σ_t	Tensile Stress	MPa
γ	Safety factor	
B	Exaction width	m
C	Parameter with value about 0.2–0.3 for design purposes	
R	Is the distance to the source	m
R_0	Is the source	
d_f	Depth of failure	m

E	Young's Modulus of intact rock	GPa
E_{ab}	The energy absorption of each bolt	J
E_{ej}	Kinetic energy	J
E_{rm}	Young's Modulus of a rock mass	GPa
g	Gravitational Acceleration	m/s^2
Ln	Natural Logarithm	
m_L	Local Magnitude	
n	Number of bolts	
ρ	Rock density	kg/m^3
P_{ult}	The ultimate load of the rock bolt	kN
s & m	Material constant of Hoek-Brown Failure criterion	
S	Span	m
v	Ejection velocity	m/s
V	Poisson's ratio of intact rock	MPa
V_{rm}	Poisson's ratio of a rock mass	
W	The deadweight force of the block or wedge	N

1 INTRODUCTION

Palabora Mining Company (PMC) is expanding its underground operation through a second block cave (Lift 2), 450m below Lift 1 and 1650m below the surface. The Lift 2 horizontal development work has commenced, establishing the required cave footprint. Additionally, various large excavations such as crusher chambers are required to service the mine. The crusher chambers are designed with the following dimensions: 12m in width, 25m in height and 61m in length. These crusher chambers usually have operating lives of up to 40 years and their long-term stability is critical.

At the mining depth of Lift 2, seismic activity is expected to increase. According to Hutchinson & Diederichs (1996), rock masses are subject to time-dependent deterioration near excavations. Underground excavations may initially be stable but degrade over time and eventually become unstable. Moss & Kaiser (2022a) show that a strategic ground control element is critical for uninterrupted production and timely construction of underground excavations.

PMC requires a study to examine the stability of these critical infrastructures (crusher chambers). The study area is located in the Palabora Igneous Complex, where the rock mass is weak, extensively jointed and weathered. Additionally, the rock mass conditions for the Lift 2 crusher chambers are expected to change due to the increase in mining depth. The stress-induced failure becomes more dominant than geological (structural) controlled failure with increasing depth. It is, therefore, necessary to review the existing design methods to make them suitable for Lift 2 crusher chambers.

The financial and operational implications of the failure of critical mine infrastructure, such as a crusher chamber, necessitated the need to develop site-based guidelines for the Lift 2 crusher chambers. This research report describes the analysis and design approach to be carried out to evaluate the stability and support required for the two crusher chambers in Lift 2. This approach will guide PMC's future large excavations and can be used as a design methodology for mines with similar conditions.

1.1 Research Background and Context

Ground support design is essential for stable excavations; historically, the numerical modelling and empirical design approach has been successfully applied at several caving operations worldwide (Speakman, 2022). Despite PMC's documented support standards for Lift 1 crusher chambers, no appropriate support standards have been explicitly designed for Lift 2. An appropriate ground support system must be designed for Lift 2 to cater for the anticipated stress and deformation changes experienced over the crusher chamber for its life span. Within this context, using the most efficient support system is extremely important to maintain the integrity of the rock mass and mitigate risk.

Several factors influence the ground support design, such as excavation dimensions, rock mass ratings, dominant structures and anticipated induced stress conditions. These support requirements for underground excavations may change due to variations in the listed factors mentioned earlier. The vertical virgin stress due to the overburden weight tends to increase with depth. It is essential to cater for this change and the support design should also consider the risk of seismicity and deformation which may occur. In this research study, empirical, analytical and numerical methods are integrated to assess the stability of the crusher chambers at Lift 2 and design an appropriate support system for the expected instability. This approach could enhance the understanding and predicting of the failure mechanism and instability.

1.2 Problem Statement

PMC is expanding its underground block caving project from 1200m (Lift 1) below the surface to 1650m (Lift 2). Large excavations, such as crusher chambers, have been planned to service the mine in Lift 2. Crusher chambers were developed for Lift 1. However, the rock mass characteristics in Lift 2 differ slightly from Lift 1. Moreover, the rock mass in Lift 2 is disintegrated and weak due to the mica content. Therefore, a support system that caters for disintegrated and weak rock mass will be required. An increase in the mining depth will increase the in-situ stress and deformation around underground excavations, which may increase the risk of seismicity, ground closure and fall of ground. Furthermore, Lift 2 may be classified as a brittle rock mass requiring special treatment to maintain stability. The design approach used in Lift 1 may need to be revised to maintain the long-term stability of Lift 2. PMC is also associated with intermediate mining depth, which is known to have moderate to high in-situ stress and seismic activity. Therefore, a combination of the brittleness of the rock mass and seismicity may jeopardise the production rate and the safety of employees. Considering the knowledge gap mentioned above, it is crucial to undertake this study to maintain the mine's safety and production.

1.3 Justification for Research

The failure of large excavations such as crusher chambers can inevitably lead to the loss of production and increased operating costs. In the worst cases, it can result in fatal injuries and damage to infrastructure. The mine could lose considerable revenue when excavations such as crusher chambers fail. An appropriate ground support design will lead to a safe and productive working environment and this study will develop a proper ground support design approach to maintain long-term stability.

Lift 2 has four ground control district and the rock mass conditions vary for each ground control district. Considering the various ground control districts. The study will contribute to developing an appropriate ground support system for Lift 2. Furthermore, various ground control districts may behave differently. For Lift 2, a specific support system must be designed for the ground control districts. If an appropriate support system is not in place within these various ground control districts, extensive ground deformation and ground failures are expected, which may affect the safety and productivity of the mine. This is the motivation of this study, to mitigate the risk and promote safety and productivity.

Ground support design is essential for stable excavations; historically, the numerical modelling and empirical design approach has been successfully applied at several caving operations worldwide (Speakman, 2022). Despite PMC's documented support standards for Lift 1 crusher chambers, no appropriate support standards have been explicitly designed for Lift 2. An appropriate ground support system must be designed for Lift 2 to cater for the anticipated stress and deformation changes experienced over the crusher chamber for its life span. Within this context, using the most efficient support system is extremely important to maintain the integrity of the rock mass and mitigate risk. Several factors influence the ground support design, such as excavation dimensions, rock mass ratings, dominant structures and anticipated induced stress conditions. These support requirements for underground excavations may change due to variations of the listed factors. The vertical virgin stress due to the overburden weight tends to increase with depth. It is essential to cater for this change and the support design should also consider the risk of seismicity and deformation which may occur.

1.4 Research Aim and Objectives

The long-term stability of crusher chambers is controlled mainly by the performance of its support system. Previous studies, including Barton *et al.* (1974) and (Bieniawski, 1989), documented that an effective support system and rock mass conditions can maintain the life span of these crusher chambers. Therefore, this study aims to develop a support system for Lift 2 crusher chambers.

The specific objectives of this project are:

- To collect geotechnical data for rock mass characterisation and classification and compare the ground control districts of Lift 1 and Lift 2;
- Review Lift 1 crusher chambers support and determine if it is suitable for Lift 2 crusher chambers;
- To evaluate support requirements using empirical, analytical and numerical design methods; and
- To recommend an optimum support design approach for Lift 2 crusher chambers.

1.5 Research Methods

This study included both qualitative and quantitative research methods. Limited research has been conducted in the context of support design for underground Lift 2 crusher chambers at PMC. Stress-induced and structurally controlled failures are the common failures in Lift 2 and there is high stress related to overburden due to increase in mining depth. Poor rock mass quality, close jointing and weathering is evident where the rock mass is intersected by geological structures such as dolerite dykes and faults. Lift 2 crusher chambers were analysed using RS2 software from RocScience (2021). A support system for the Lift 2 Crusher chambers is recommended based on analytical, empirical and numerical design methods.

1.5.1 Qualitative Research

Qualitative research is a detailed approach to studying social reality (Bless & Higson-Smith, 2000). It uses descriptive language to analyse the subject matter and aims to provide a comprehensive understanding of the phenomenon being studied. For this study, it involved obtaining primary data through visual observations such as identification of critically unstable areas; structural orientation i.e., dip angle and dip direction, geological contacts and major structures such as faults, dolerite, fracture zones, shear zones and highly jointed rock masses. Equipment such as cameras and computers for geological and geotechnical mapping was used for geological and geotechnical characterisation. This included monitoring of the boreholes for depth of failure assessment. Preliminary work involved secondary data collection by reviewing existing literature on the support design approach for crusher chambers. Literature review related to the geology and geotechnical conditions of PMC mine including the support performance of the Lift 1 crusher chambers. Literature review also related to rock mass classification, empirical, analytical and numerical modelling to evaluate and analyse crusher chamber stability.

1.5.2 Quantitative Research

It is the researcher’s view that a research approach that makes use of figures and numbers is quantitative research, while qualitative study is based on non numerical data. Bless & Higson-Smith (2000) define quantitative research as research in which aspects of social reality are recorded and investigated using a variety of methods. According to Leedy & Ormrod (2005), quantitative research is generally used to explain, predict and control phenomena through the investigation of relationships among measured variables. Field measurement and face mapping of blasted exposures near the crusher chamber site were conducted to assess the stability of the rock mass. The process of face mapping of blasted excavations was enhanced by a digital photogrammetry equipment, commonly referred to as AdamTech. This technology captures photographs of the excavations, which allow for a more accurate analysis and interpretation of the rock mass quality and the rock mass behaviour. Data collection involves obtaining geological data such as rock types and geological structures and the stress regime of the study area. The collected data included the lithological units, discontinuity sets and their orientations, spacing and conditions and the presence of groundwater. The collected data is presented in figures and tables. The mapped excavations were mostly 5 m wide by 5 m high. The stability analysis was carried out using empirical, analytical and numerical simulation and the rock mass was characterized using empirical classification such as Bieniawski's RMR (Bieniawski, 1989), Barton's Q system (NGI, 2022) and Laubscher's rock mass classification system (Laubscher & Jakubec, 2001). Joint data was processed using DIPS software from RocScience to identify the prominent joint sets that will be encountered when developing the crushers (RocScience, 2021a). Analytical analysis was conducted using UNWEDGE software from Rocscience to evaluate wedge formation and their mode of failure. Numerical analysis was conducted using finite element (FEM) software RS2 (RocScience,2021b), formerly known as Phase2, to evaluate the stress levels and validate analytical and empirical results. Support system requirements will be proposed accordingly, in terms of the rock mass classification for the different ground control districts.

1.6 Sources of Data

The data used for this study is based on the field work conducted at the project site (underground observations), a desktop study conducted on the research topic, including peer-reviewed journals, geotechnical data collected from laboratory tests conducted and core logging data.

1.7 Research Validation

Mine data was utilised for this research project. The data collection included operational data based on daily production and will be available upon request. Numerical models will be validated as data becomes available during the development process. Peer-reviewed journals were used to compare the study's results with the previous work. Therefore, a correlation or disagreement was outlined and the reason for such were documented.

1.8 Mine Background

1.8.1 Locality and General Background

The project area is approximately 3km east of Phalaborwa town in South Africa's Limpopo Province (*Figure 1-1*). The Palabora Mining Company (PMC) also operates smelters and refineries in addition to its copper mine. In the region, the Palabora Igneous Complex is a unique rock formation. Most of PMC's refined copper is sold locally, while the rest is exported. PMC's primary product is copper, but it also produces and exports magnetite, vermiculite, sulphuric acid, anode slimes and nickel sulphate by-products.

Figure 1-1: Locality plan of the Palabora Mining Company (Google)

1.8.2 Mining Methods

Palabora Mining Company commenced mining in 1956 as an open pit that operated to a maximum depth of 800 m. In 2001, the mine transitioned from surface to underground, utilising the block-cave mining method. Caving is initiated by an undercut where a large area of rock below the mining block is removed. Gravity induces stress in the rock, causing it to fracture. The fracturing process is successive and affects the entire rock mass. Gravity and stress act on the continuous zone of broken rock created by an undercut at the base of the block cave orebody. This eventually causes the rock mass to fracture progressively (Fernandez *et al*., 2010). This process allows a continuous cave to be sustained by removing the broken rock. Van As & Guest (2020) show that to propagate the cave and reach steady state production, block caving requires complete undercutting of the mine footprint. The caveability of an orebody is dependent on the strength of the rock to be caved and the area available to be undercut. Drawbells are developed between the undercut and the production level and the fractured rock gravitates through the drawbells to draw points on the production level. The broken ore is transported from the draw points to the crusher using Laud Haul Dumpers (LHDs) and hoisted from the mine. Block caving mining is a large-scale method for low-grade massive ore bodies that can cave. Undercutting corresponds to the initial stages of caving in a block cave mine (Fernandez *et al.,* 2010).

Lift 1 production footprint is equipped with four crusher chambers. These crusher chambers are located at the northern side of the Lift 1 production footprint (Figure 1-2). Each crusher chamber has the following dimensions: a width of 9.5 m, height of 30 m and length of 54.9 m. The types of ground support employed at Lift 1 crusher chambers are: 2.4 m long rock bolts, 6 m cable anchors and 100 mm layer of fibre reinforced shotcrete. Large excavations at PMC typically exceed a span of 6 m. The support systems required for these excavations are highly dependent on their projected service life. Permanent excavations, such as crusher chambers, workshops, shafts, draw points and ramps, differ from temporary excavations, which include undercut-level excavations. The quality of rock mass within these excavations was determined through the use of Q, RMR and MRMR system. Rock bolt support reinforces the rock mass against both structurally controlled and stress defined failures (Cai & Kaiser, 2018). Lift 2 has been designed to operate with two jaw-gyratory crushers in contrast to the four jaw crushers that were installed on Lift 1. The Lift 2 crusher complex design and layout incorporates four tipping points compared to one per crusher on Lift 1. The two crushers are located on the northern perimeter of the Lift 2 footprint. The silo chambers are orientated 90 degrees, designed with a 6 m diameter and a total length of 24 m. These crushers are positioned 170 m apart and at least 80 m from the ore body perimeter.

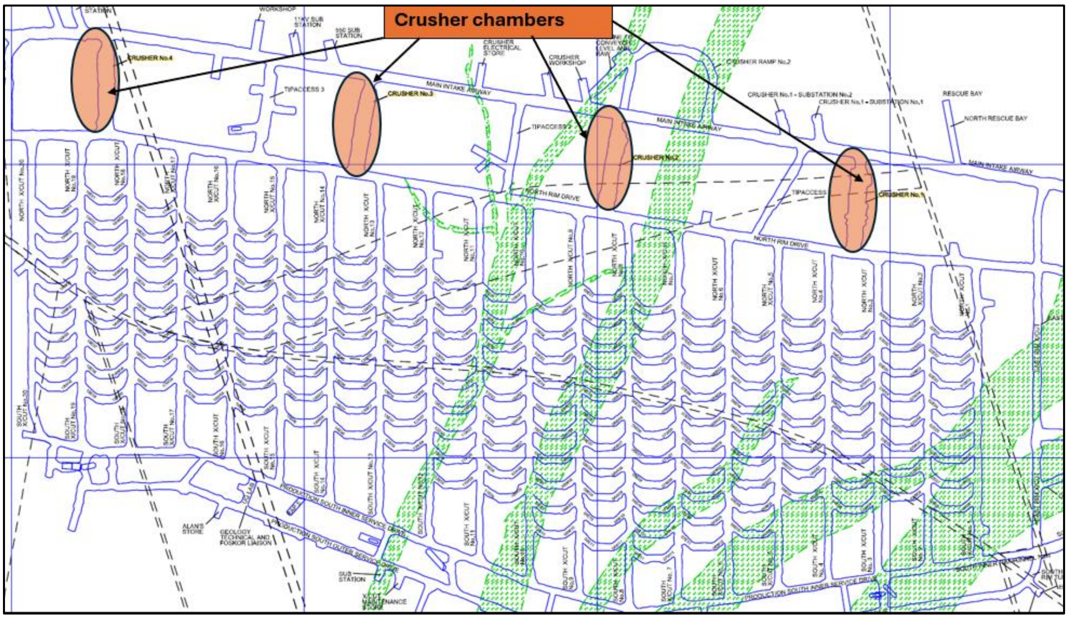

Figure 1-2: Illustration of the Lift 1 production footprint (Palabora, 2015)

Figure 1-3 shows a conceptual view of the open pit and the underground mine and the Lift 2 development footprint is located approximately 1650 m below the surface.

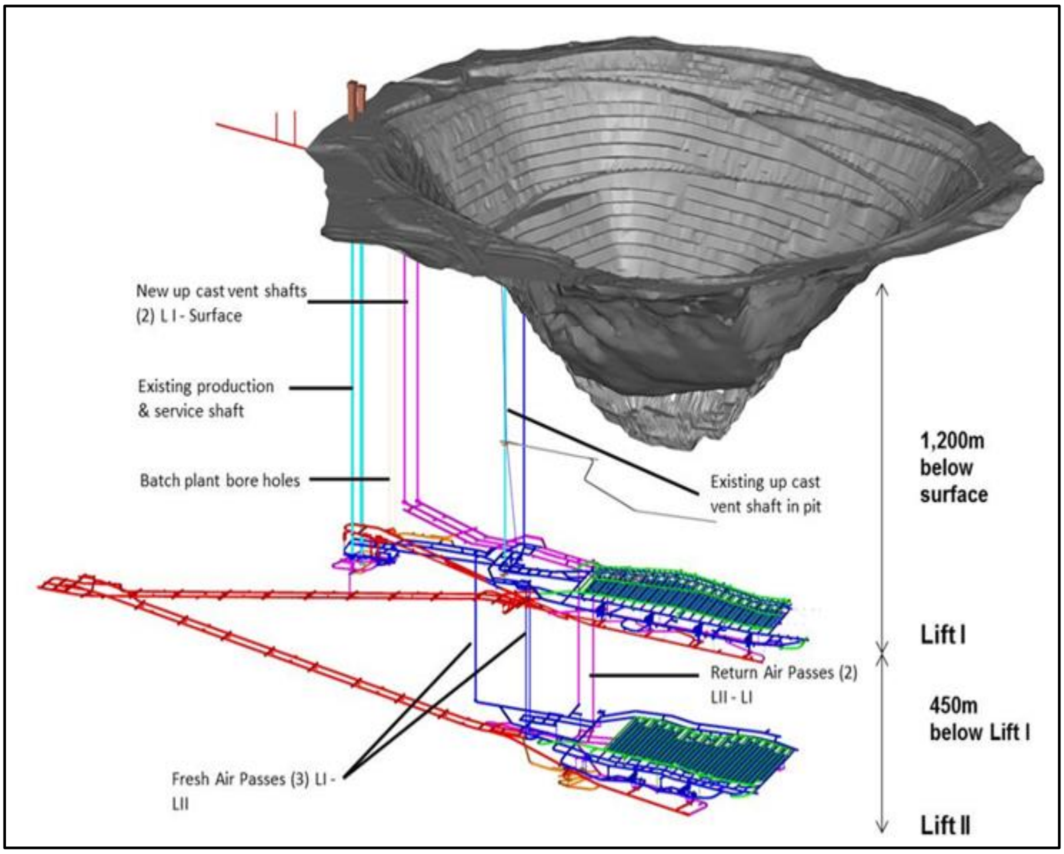

Figure 1-3: Illustration of the PMC open pit and the underground operation

Figure 1-4 illustrates the crosscuts, draw points and draw bells relative to the undercut. A typical view of the Lift 2 crusher chambers is shown in Figure 1-5.

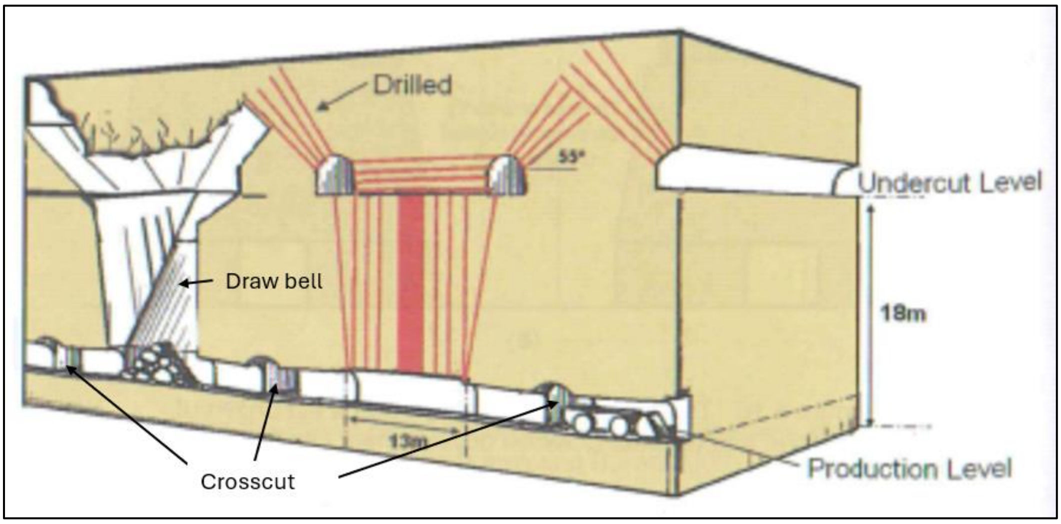

Figure 1-4: Schematic view of the undercut and production level (Palabora, 2015)

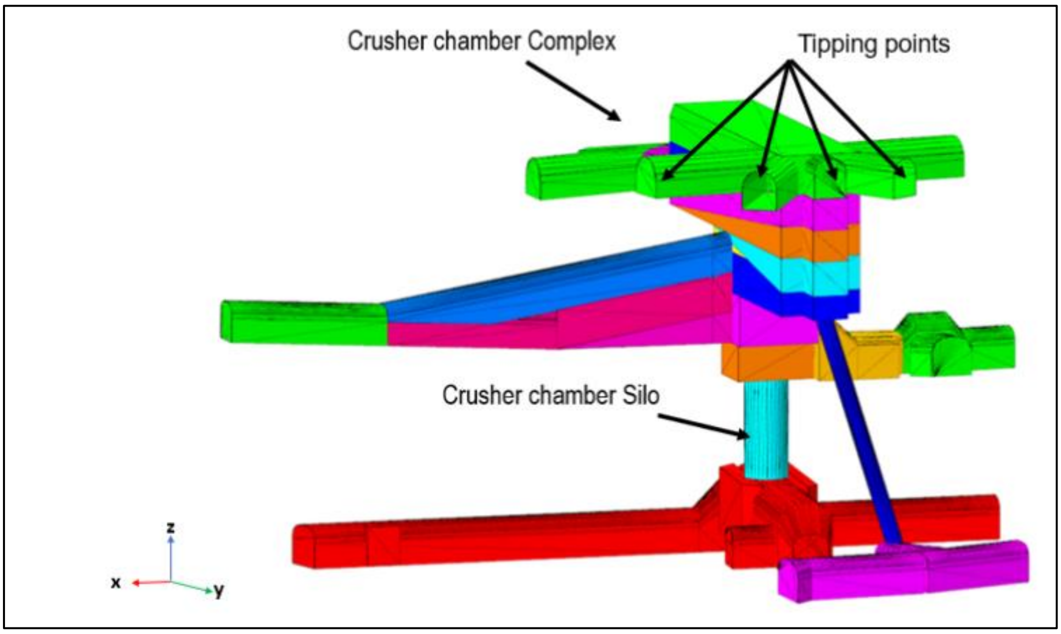

Figure 1-5: A typical isometric overview of the lift 2 crusher chamber

1.9 Structure of the Research Report

This research report is composed of six chapters. The first chapter serves as an introduction, providing important context for the study. Included in this chapter is the problem statement, which outlines the specific issue that the research aims to address. Additionally, the justification for the research is presented to provide insight into why this topic is important. The research objectives are also included in this chapter, outlining the specific goals that the study seeks to achieve. Furthermore, the research methodologies that were utilised in the study are introduced, along with the sources of information that were used to obtain data. To ensure the validity of the research, the validation criteria are discussed in this chapter. Finally, the contribution to knowledge that this study makes is explored, highlighting the ways in which it adds to the existing body of knowledge on the topic.

Overall, this first chapter provides a thorough and detailed overview of the research that is to follow. Chapter 1 also presents a background of the study area, detailing the mining methods and geotechnical conditions. Chapter 2 presents a critical literature review of the research topic: the types and functions of support systems, support design methods, rock mass classification systems and numerical modelling.

Chapter 3 discusses the methodology followed. In Chapter 4 discusses data collection and analysis. Support design for the Lift 2 crusher chambers is presented in Chapter 5. An interpretation and discussion of the results is also discussed in Chapter 5. Chapter 6 presents the conclusions that the author derived from the research project, including the additional research work that needs to be done to address the issues highlighted in the study. The research report reference list is included.

2 LITERATURE REVIEW

2.1 Introduction

A thorough understanding of the rock mass is essential for any rock engineering analysis. This chapter presents literature related to the description of the geology of PMC, the support design approach for crusher chambers and rock mass classification. Literature related to research work on the application of the existing design methods is presented in this chapter. This is relevant to the research work in terms of empirical and analytical methods. A brief description of numerical methods and their application to underground structures is also provided to determine the stability and estimate support requirements. This section will also establish a relationship between literature knowledge and the study's objectives.

2.2 Geology of the Study Area

Lift 2 crusher chambers are located within the Palabora Igneous Complex. The Palabora Igneous Complex is an elliptically shaped, vertically dipping volcanic pipe measuring approximately 1,400 m by 800 m in plan, with resources extending up to 1,800m in depth (Southwood & Cairncros, 2017). It is located in the Archean Shield of the Limpopo Province; as one of the unique African alkaline complexes in the Archean Shield, this complex is unique in that its carbonatite member has an economic deposit of copper ore (Verwoerd,1986). A concentrically zoned, alkaline intrusion, the Palabora Igneous Complex is ancient. While copper surface mining has existed in the Palabora area for centuries, early European prospectors only discovered the potential for larger-scale mining in the late nineteenth century (Southwood & Cairncross, 2017).

Southwood & Cairncross (2017) further state that the modern, open-pit copper mining began in the mid-1960s, exploiting a significant, low-grade resource hosted by the carbonatite and foskorite rocks at the core of the complex, originating from the outer ultramafic rocks. Apatite and vermiculite mines had been established by the mid-twentieth century in the outer ultramafic rocks. The carbonatite rock is at the centre of the igneous intrusion and is further geologically subdivided into transgressive (TCB) and banded carbonatites (BCB). For rock engineering purposes, they are treated as a single formation with uniaxial compressive strength

(UCS) of 120 MPa. Foskorite (FOS) surrounds the TCB core of the deposit and has an average UCS of 100 MPa and it has shown evidence of weathering following years of exposure to atmospheric conditions. FOS is, in turn, surrounded by the micaceous pyroxenite (MPY), which has an average UCS of 90 MPa and follows a similar jointing pattern to the TCB and FOS (see Figure 2-1).

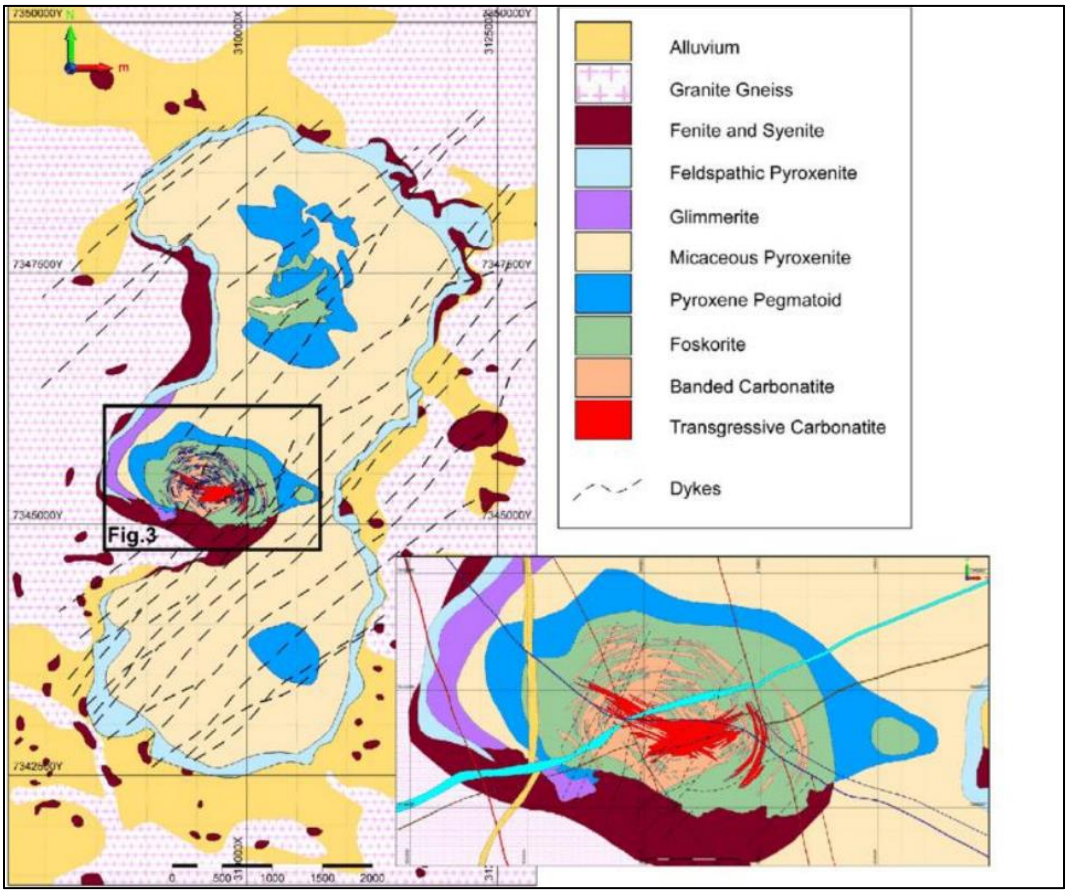

Figure 2-1: Local geology of PMC (Diering et al., 2018)

2.3 Geological Structures

The PMC ore body is traversed by a series of northeast and southwest-trending dolerite dykes (DOL). The dykes vary in thickness from 60 m to narrow stringers. The dolerites are typically very hard, with uniaxial compressive strength of 330 MPa, but the strength and the fracturing of the dykes and the associated degree of weathering varies considerably by location. These dolerite dykes often act as channels for water, it is prone to stress concentration and it is mostly highly jointed creating blocky ground. The dykes in the east and south of the ore body are generally strong and less fractured, with a mean fracture spacing of 350 mm.

The dolerite is more weathered at the centre of the ore body and the uniaxial compressive strength drops to 80 MPa with close fracturing at a mean spacing of 40mm. Similarly, the contacts between the dolerite and country rock are variable. Typically, the contact is a narrow zone of weathering and close fracturing even where the centre of the dyke is strong and less fractured, but the contact can be tight and cemented.

The Central Fault Zone (CFZ), North-northwest Fault Zone (NNWFZ), Southwest Fault Zone (SWFZ), Glimmerite Fault Zone (GFZ) and Mica Fault Zone (MFZ) are major geological structures contained in the orebody. The fault zones are characterized as breccia zones between 1 and 20 metres wide (Palabora, 2015). There is often evidence of lateral slickenside combined with chrysolite, serpentinite and valleriite surface coating. Underground exposures of the main faults of the Palabora Igneous Complex have shown sympathetic structures running parallel to them. Figure 2-2 illustrates the study area's geology showing the major structures and their orientation is shown in Table 2-1.

Table 2-1: Major faults intersecting Lift 2 orebody (Palabora, 2015).

Fault Name	Width (m)	Orientation (^{0})
MFZ	1 to 30	Dips at 70^0 to 80^0, to the east.
CFZ	0.5 to 3	Vertical to sub-vertical
GFZ	1 to 20	Sub-vertical dip.
NNWFZ	1 to 20	Subparallel to the GFZ.
SWFZ	1 to 20	Sub-vertical dip.

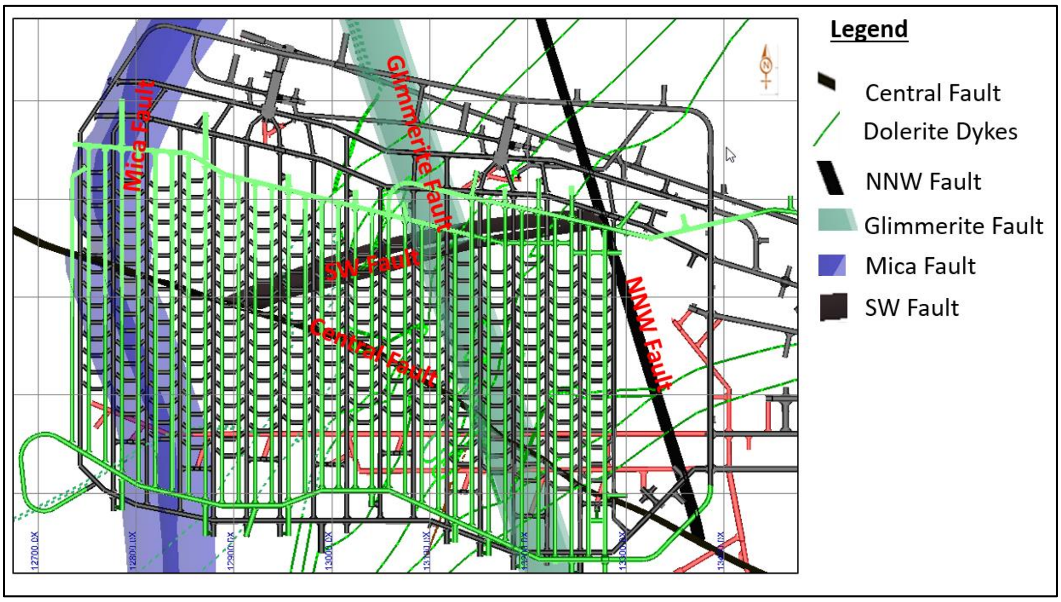

***Figure 2-2*: *Illustration of the* geological structures of PMC (Palabora, 2015)**

2.4 Lift 2 Geotechnical Zones

Lift 2 Geotechnical areas have been defined according to rock mass properties that are primarily a function of rock type and major structures.These were then grouped into four zones, where unaltered or less jointed rock mass was grouped as ground control district (GCD) Zone 1, GCD Zone 2 is bounded by major faults, GCD Zone 3 rock mass bounded by both major faults with intense jointing and GCD Zone 4 where the rock mass is characterised by faults and dykes. Figure 2-3 illustrates the Lift 2 ground control districts.

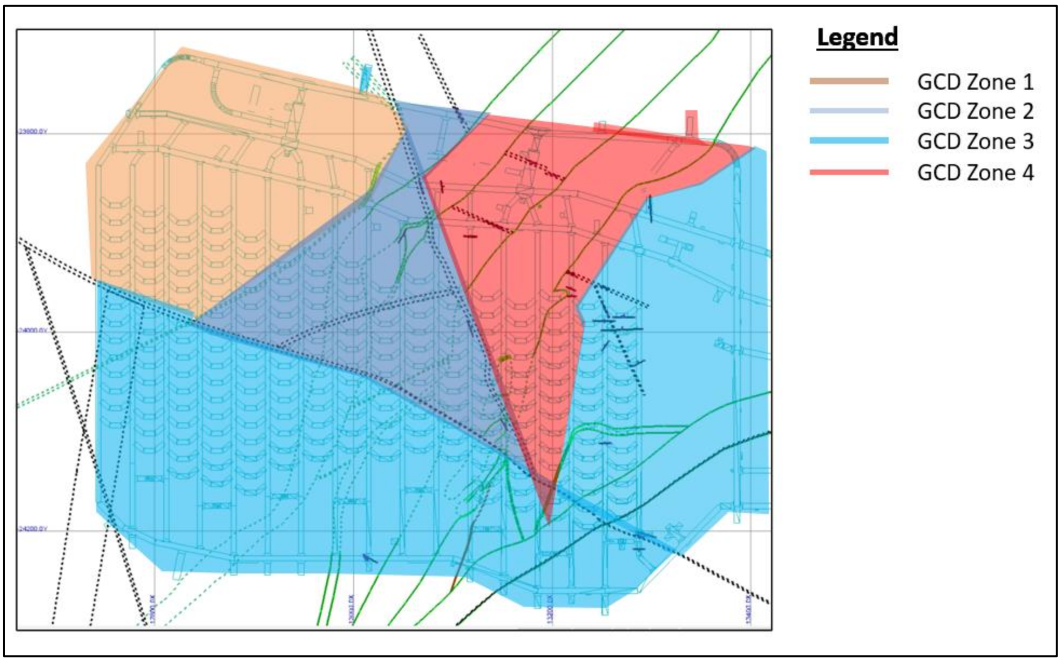

Figure 2-3: Illustrates Lift 2 ground control districts

The crusher chamber excavations are situated in a relatively competent rock mass. The east crusher chamber (Crusher 5) is bounded by two Dolerite dykes (see Figure 2-4). Foskorite dominates the geology of Crusher 5 and Crusher 6 is dominated by carbonatite. Carbonatite has an average uniaxial compressive strength (UCS) of 120 MPa and the rock mass was classified as well-jointed with an average spacing of 1.5m. Foskorite has an average UCS of 100 MPa and jointing is similar to that found in the carbonatite material. The foskorite has also shown evidence of weathering for some years after exposure to atmospheric conditions. Figure 2-4 shows a plan view of the Lift 2 production level with two crusher chambers planned for Lift 2 as part of the ore handling system.

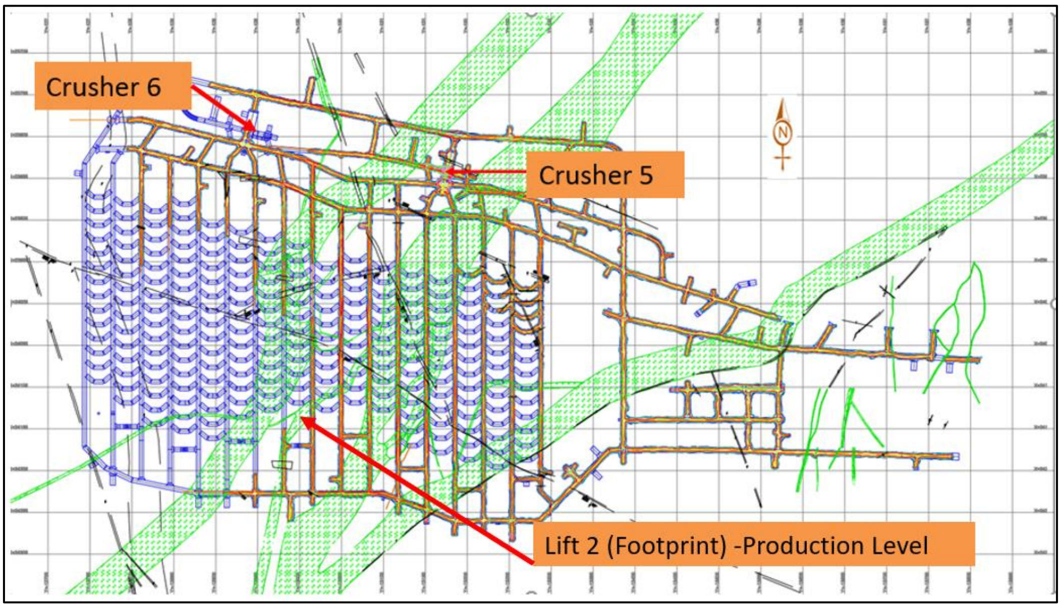

Figure 2-4: A plan view of the production level and crusher location

2.5 Support design approach

The design of underground structures has evolved over time, but it is still relatively new compared to the practice of mining underground. The support design recommendations are often based mainly on empirical design methods or experience. Obert (1973) urges that simple rule-of-thumb, approaches are still commonly used in the design process despite advancements in technology and engineering. The Mining Hard Rock Handbook provides guidelines that assist in the design process (De la Vergn, 2014). As safety concerns have become more prominent in recent years (Moss & Kaiser, 2022b), there is an increased need for reliable and practical approaches to designing underground structures.

This has led to the implementation of higher safety factors and greater mining efficiencies in the design process, which are critical for ensuring workers' safety and the success of underground mining operations (Obert, 1973). Similarly, Potvin & Hadjigeorgiou (2015) show that most mines rely on Norwegian tunnelling ground support recommendation linked with rules of thumb and wedge analysis forms part of support selections mostly at prefeasibility stage. Potvin & Hadjigeorgiou (2015) also highlight the need to review ground support when more data becomes available to suit the ground conditions.

Studies have shown that there are different categories of design approaches. Bieniawski (1992) classified methods into analytical, observational and empirical. Meanwhile, Choquet & Hadjigeorgiou (1993) categorised design approaches into empirical, observational and rational. When designing structures in rock, empirical methods employ rock mass classification. This approach is based on extensive research and experience. It comes with a set of design recommendations or rules that are considered acceptable practice in the field, as shown by Potvin & Hadjigeorgiou (2020). The rational design approach involves using analytical solutions and numerical modelling to anticipate how different support designs will impact the overall stability of an excavation (Cai & Kaiser, 2018). Observational methods recommend installing monitoring instruments in the excavation and implementing support as the design is developed.

Fernandez *et al.* (2010) demonstrates that ground support is quantified using empirical methods and empirical design methods are verified through numerical modelling methods. Kaiser & Cai (2013) showed that the general design procedure used for rock support design in underground construction focuses mainly on checking how much load a rock bolt can support. In addition, it checks how much energy a rock bolt can dissipate. Stacey (2015) shows that a thorough design will ensure that reliability and safety are at acceptable levels and that all likely hazards have been satisfactorily addressed. Several authors have established a workflow or a methodology for designing excavations, a typical example is shown in Figure 2-5.

A detailed discussion of the design process is found in Bieniawski (1992) and the Wheel of Design by Stacey (2009) summarises it well (Figure 2-6). Similarly, Stacey & Page (1986) suggest that underground excavations should be designed according to the following approach:

- Select an appropriate excavation size and shape for crusher chambers. This will depend on the orebody geometry, the mining method chosen and the equipment used;
- Determine the most effective excavation method for the project;
- Considering the properties of the rock mass where the excavation is to be placed is essential to;
    - Evaluate the stability of the excavation;

- Identify the mode of instability;
- Check for stress-induced failure around openings;
- Check for block instability and;
- Assess the rock mass stability and classify it.

- If necessary, optimise design, e.g., modify the size, shape, orientation, or location, when unstable ground conditions such as wedges are predicted to occur. If the excavations remain unstable even after modification, determine the support required to promote and maintain stability.

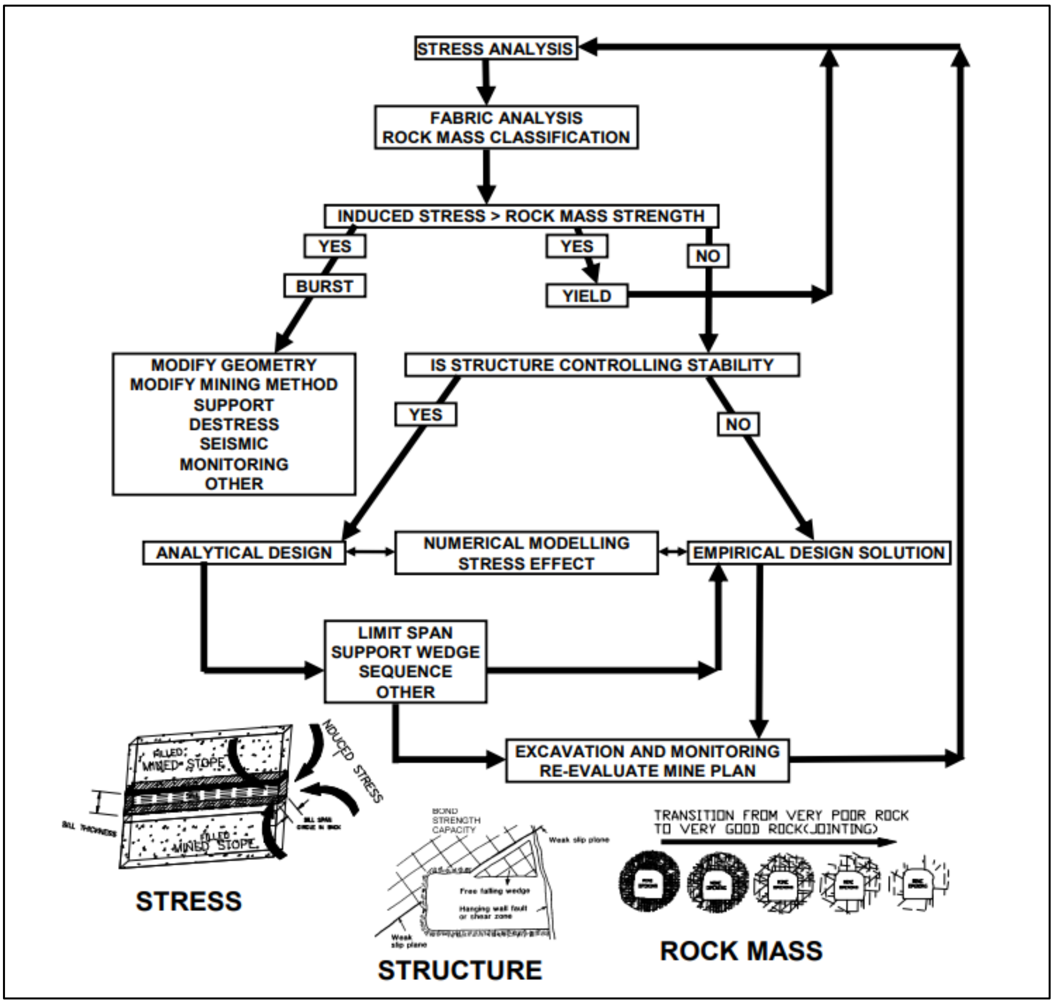

Figure 2-5: Support design methodology as cited by (Pakalnis, 2015)

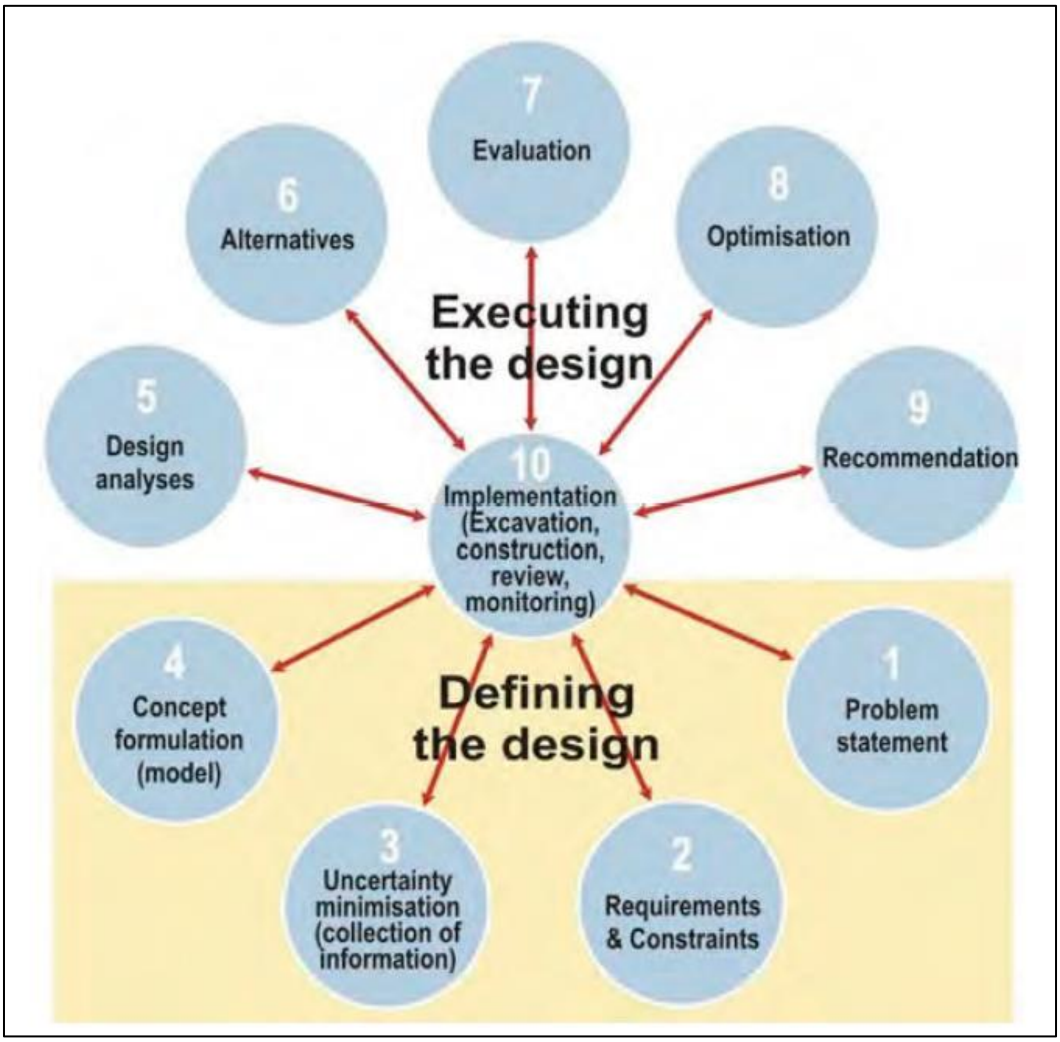

Figure 2-6: Wheel of design (Stacey, 2009)

2.5.1 Empirical design based on rock mass classification

Rehman *et al.* (2018) describe rock mass characterisation as a process of measuring crucial factors that affect the behaviour of rock masses during tunnelling. On the other hand, rock mass classification evaluates the quality of rock masses based on a predetermined system (Palmström, 2009). The empirical approach is based on a collection of experience-based site data as the basis for interpreting behaviour (Mikula & Lee, 2007); (Terron-Almenara *et al.,* 2023). Empirical design is applied at any stage of the design process when data is limited. According to Budavari (1983), the empirical design approach is entirely based on the premise that methods that work in similar situations will be effective again. However, assessing the similarity of different situations is challenging because mining depth is continually changing. Rock mass classification can be obtained from the structural mapping of blasted excavations and core logging data. Empirical design systems have the advantage of being economical, reliable and straightforward (Rehman *et al.,* 2018). Palmstrom & Broch (2006) argue that rock mass classifications alone present limitations to addressing permanent ground support and predicting rock mass behaviour in poor ground conditions.In the field of mining and tunnelling, several empirical design methods have been developed to assess the rock masses' stability and quality. These include the Rock Mass Rating (RMR) system by Bieniawski (1989), the Mining Rock Mass Rating (MRMR) System by Laubscher and Taylor (1976), the Laubscher block caving rules (Laubscher, 1994), the Q-system or Tunnelling Quality Index (TQI) developed initially by in 1974 by Barton, Lien and Lunde (NGI, 2022). The Stability Graph described in Mathews *et al.* (1981) publication, includes equations used for designing pillars.

Rock mass classification schemes such as those by Barton and others (NGI, 2022); (Bieniawski, 1976) and Bieniawski (1989) were developed to estimate support. However, these schemes may only serve the purpose in some mines; therefore, a critical analysis of rock mass behaviour is required to develop an appropriate support system. Laubscher's rock mass rating system (Laubscher, 1990) was designed to cater for diverse mining situations and therefore based on the conditions encountered in mines. Mining rock mass rating (MRMR) considers the effect of weathering and mining, including stresses, joint orientation and blasting, to adjust the RMR for a particular mining environment. The MRMR is further applied to derive an empirical rock mass strength (RMS) which is subsequently adjusted to arrive at a Design Rock Mass Strength (DRMS).

Rock Quality Designation

Deere introduced the Rock Quality Designation (RQD) as an index for assessing and quantifying rock quality in 1964 (Deere, 1964). RQD is an input for Q and RMR classification systems. An RQD value can be obtained by adding pieces of the core with a length of more than 10cm (Equation 2-1) and it can also be calculated from the number of joints or discontinuities per unit volume (Jv) on the rock surface using Equation 2-2 (Palmström, 1982). Previous research has shown that RQD is not a reliable measure of rock mass quality at joint spacings close to 10 cm, as it returns an RQD value of 100%, which classifies the rock mass as excellent (Table 2-2).

$$RQD = \sum \left(\frac{Length\ of\ core\ pieces \geq 10cm}{Total\ core\ run} \right) x\ 100\% \qquad \textbf{Equation 2-1}$$

$$RQD = 115 - 3.3J_V \qquad \textbf{Equation 2-2}$$

Table 2-2: Rock quality based on RQD (Deere, 1964)

RQD (%)	**Class**
<25	Very poor
25-50	Poor
50-75	Fair
75-90	Good
90-100	Excellent

Norwegian Geotechnical Institute (NGI) Q-System

The Q-System also known as Tunneling quality index is a rock mass classification system developed in 1974 by Barton and others, based on case histories (NGI, 2022). It is used to determine the quality of rock for engineering purposes. It takes into account factors such as rock strength, joint orientation and spacing and the presence of groundwater. The Q-system is widely used in the mining and tunneling industries to assess the potential stability of rock masses and to design support systems (NGI, 2022). Several revisions have been made of the Q-system, the latest work is found in NGI (2022).

The initial work by Barton *et al.* (1974) showed that the Q value is calculated using Equation 2-3 and the most recent work reference Equation 2-4 (NGI, 2022). In Equation 2-4, a normalisation factor is applied for a modified Qc due to the significance of intact rock UCS as stated by Barton (2002), (Rehman *et al.,* 2018). Barton (2002) shows that Equation 2-5 can also be used to estimate the unconfined compressive strength of the rock mass (σ_{cm}). Barton *et al.* (1974) provides more details on the origin of the Q rating and the latest update is found in NGI (2022).

$$Q = \frac{RQD}{J_n} \times \frac{J_r}{J_a} \times \frac{J_w}{SRF}$$ **Equation 2-3**

$$Q_c = \frac{RQD}{J_n} \times \frac{J_r}{J_a} \times \frac{J_w}{SRF}\ x\ \frac{\sigma_c}{100} \quad \text{or} \quad Q_c = Q\ x\ \frac{\sigma_c}{100}$$ **Equation 2-4**

$$\sigma_{cm} = 5\rho Q^{\frac{1}{3}}$$ **Equation 2-5**

Where:

RQD is the Rock Quality Designation;

Jn is the joint set number (the number of discontinuity sets);

Jr is the joint roughness number (the roughness of the discontinuity surfaces);

Ja is the joint alteration number (the degree of alteration or weathering of the discontinuity surfaces);

Jw is the joint water reduction factor (groundwater inflow);

SRF is the stress reduction factor (stress condition) and it can be calculated using Equation 2-6 and Equation 2-7;

ρ is the rock density measured in kg/m^3;

σ_{cm} is the uniaxial compressive strength of the rock mass;

σ_c is the uniaxial compressive strength of intact rock measured in MPa and the *value of σc is its rating on Equation 2-4*;

$$SRF_Q = \left(\frac{RQD}{Jn}\right) * \left(\frac{Jr}{Ja}\right) * \left(\frac{Jw}{Q}\right)$$ **Equation 2-6**

$$SRF_{Q_c} = \left(\frac{RQD}{Jn}\right) * \left(\frac{Jr}{Ja}\right) * \frac{Jw}{Q_c} * \frac{\sigma_c}{100}$$ **Equation 2-7**

NGI (2022) shows that wall support can also be obtained by applying the adjustment to the Q value as shown in Equation 2-8 to Equation 2-10.

For Q> 10	$Q_{wall} = 5Q$	**Equation 2-8**
For 0.1< Q <10	$Q_{wall} = 2.5\ 5Q$	**Equation 2-9**
For Q<0.1	$Q_{wall} = Q$	**Equation 2-10**

Excavation support ratio

NGI (2022) defined an additional parameter called the Equivalent Dimension (De), of the excavation to relate the Q value to the underground excavations' stability and support requirements. In order to calculate De, the span, diameter, or wall height of the excavation is divided by the Excavation Support Ratio (ESR). ESR value relates to the intended use of the excavation and the degree of security demanded by the support system installed to maintain the stability of the excavation. Crusher chambers fall into the category of very critical underground openings without access for maintenance once developed. The ESR value of 0.5 is recommended as indicated in Table 2-3 (NGI, 2022).

Table 2-3: Recommended ESR values (NGI, 2022)

Type of Excavation		ESR
A	Temporary mine openings, etcetera	ca. 3-5
B	Vertical shafts*: i) circular section ii) rectangular section *Dependant of the purpose. It may be lower than the given values	ca. 2.5 ca. 2.0
C	Permanent mine openings, water tunnels for hydropower (exclude high-pressure penstocks), pilot tunnels, drifts and headings for large openings, surge chambers	1.6
D	Storage caverns, water treatment plants, minor road and railway tunnels, access tunnel	1.3
E	Power stations, major road and railway tunnels, civil defence chambers, portals, intersections	1
F	Underground nuclear power stations, railway stations, public facilities and sports, factories, major gas pipeline tunnel	0.8
G	Very important caverns and underground openings with long lifespan of 100 years or without access for maintenance.	0.5

Rock Quality Based on Q-system

The Q value ranges from 0.001 to 1000 on a logarithmic scale (NGI, 2022). Table 2-4 classifies the rock mass based on the Q value, where higher values indicate stable conditions and lower values indicate instability requiring extensive support.

Table 2-4: Rock quality based on Q (NGI, 2022)

Q	Group	Class
400-1000 100-400 40-100 10-40	1	Exceptionally good Extremely good Very good Good
4-10 1-4 0.1-1	2	Fair Poor Very poor
0.01-0.1 0.001-0.01	3	Extremely poor Exceptionally poor

Rock Mass Rating

Geomechanics classification, also known as RMR, was developed by Bieniawski in 1972-1973 to assess tunnel stability and support requirements (Bieniawski & Lowson, 2013). The system has been refined and improved as more case histories have been examined. The RMR system is a numerical (0-100) rock mass classification that has been reviewed since and the latest being Bieniawski (1989), and RMR_{14} as cited by Celada et al. (2014). As part of the RMR system, five basic parameters are used to classify rock masses (Bieniawski, 1989), with an adjustment for joint orientation. RMR parameters are given in Table A-1 and Table A-2. Orientation guide is Given in Figure A-1 (see APPENDIX). Table 2-5 illustrates the rock mass quality based on RMR.

- Uniaxial compressive strength of intact rock (UCS)
- Rock Quality Designation (RQD)
- Spacing of discontinuity
- Condition of discontinuity surfaces
- Groundwater conditions

Table 2-5: Rock mass quality based on Bieniawski (1989)

RMR	Class
0-20	Very poor
21-40	Poor
41-60	Fair
61-80	Good
81-100	Very good

Correlation Between RMR, Q and Geological Strength Index (GSI)

In order to examine the correlation between Barton's rock mass quality Q and Bieniawski's RMR, Bieniawski in 1984 analysed 117 case histories. These included 21 documented case histories from the United States, 28 South African and 68 Scandinavian. The data covered the complete range of Q and RMR and resulted in the formulation of Equation 2-11 (Goel *et al.,* 1996).

$\mathrm{RMR} = 9\ln\mathrm{Q} + 44$ **Equation 2-11**

GSI, which was developed by Hoek (1994), is widely used to estimate the strength reduction from intact rock to rock mass. From a geological perspective, Carter & Marinos (2014) demonstrate that the GSI system can be used to characterize rock masses. This allows reliable input data on properties that affect mechanical behaviour of rock masses to be obtained. Similarly, Hoek *et al.*(1995) suggest that GSI is five points below the RMR as given by Equation 2-12. Following further research Hoek, *et al*. (2013) proposed Equation 2-13 for calculating the GSI as cited by Somodi *et al*. (2021).

$\mathrm{GSI} = RMR_{89} - 5$ for $RMR_{89}>23$ **Equation 2-12**

$\mathrm{GSI} = 0.5\,\mathrm{RQD} + 1.5\,\mathrm{Jc}$ **Equation 2-13**

Where

Jc is the joint wall conditions as described by Bieniawski (1989) and RQD is the rock quality designation.

Mining Rock Mass Rating System (MRMR)

Laubscher (1990) adopted an RMR specifically for mining applications (block caving) called the mining rock mass rating (MRMR). It considers the same parameters as RMR (Bieniawski, 1989) but combines joint condition (JC) and groundwater. The MRMR is obtained by summing up the four parameters namely, intact rock strength (IRS), RQD, Joint spacing (JS) and JC. The MRMR value is then adjusted to account for the rock mass disturbances caused by mining activities. These include in situ and induced stresses, stress changes, blasting and weathering effects. The adjusted MRMR rating is the product of the MRMR and the adjustments. These adjustments have been thoroughly documented in Laubscher & Page (1990) and the latest update can be found in the Laubscher & Jakubec (2001).

Stand-Up Time and Unsupported Span

In the context of excavation techniques, drilling and blasting are often employed, which require an excavation to remain stable and unsupported for a certain period after a blast, until the installation of ground support. It is crucial to determine the length of time that an excavation can remain unsupported and stable for mine logistics purposes. This information is highly valuable for planning and executing mining operations efficiently. This means that the excavation should be left unsupported for some time because it usually takes around 3 hours or half a shift to remove the blasted material and prepare the heading for the installation of support. When the rock mass that has been excavated is left unsupported for a prolonged period, it can lead to instabilities which may ultimately result in the failure and collapse of the excavation (Rehman *et al.,* 2018). For that reason, it is important to determine the stand-up time for all underground excavations. The maximum stable unsupported span can be determined using design charts shown in Figure 2-7 to Figure 2-10.

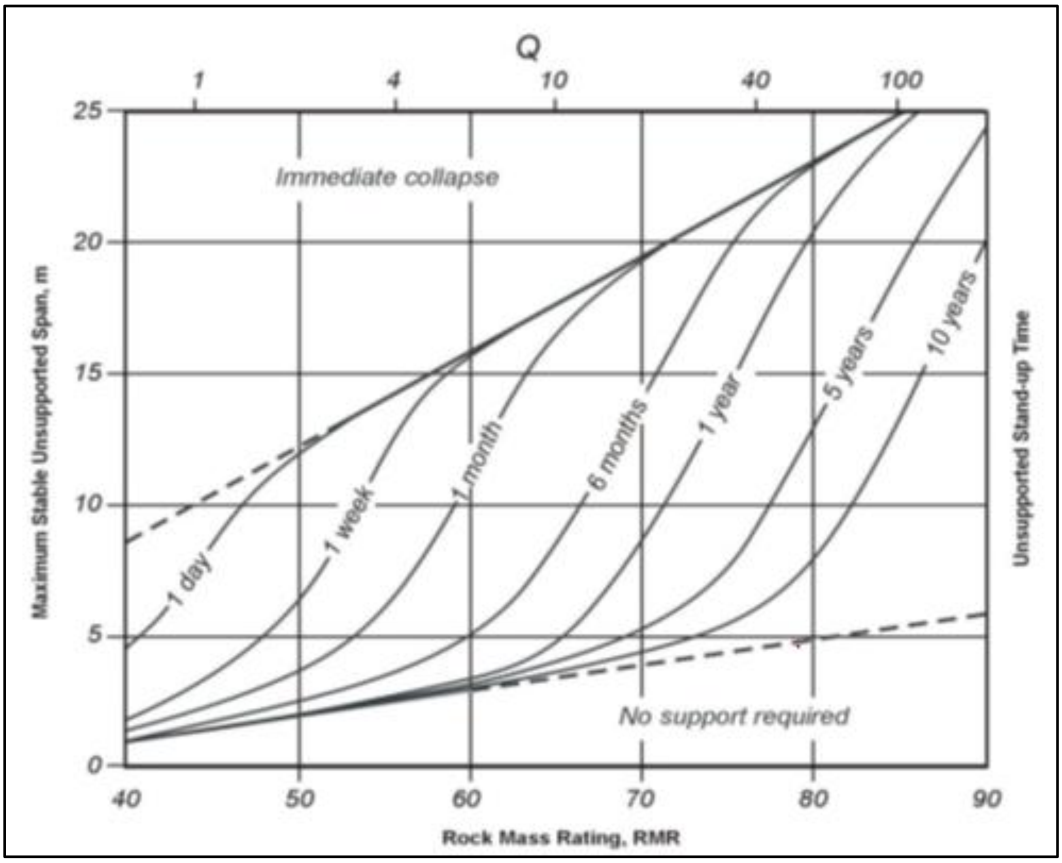

Figure 2-7: Maximum unsupported span vs stand-up time as a function of RMR and Q **(Stacey, 2001)**

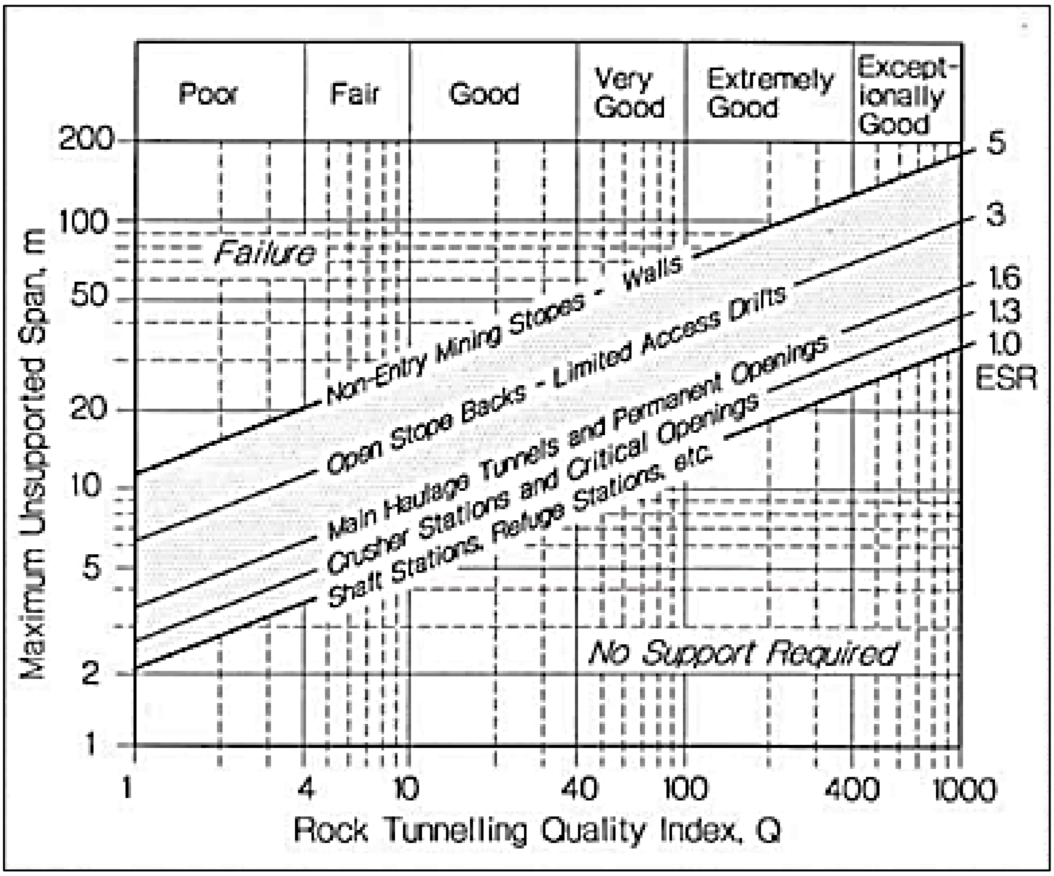

Figure 2-8: Maximum unsupported span vs Q **(Barton** ***et al.,*** **1974)**

The unsupported span as a function of RMR is given in *Figure 2-9*.

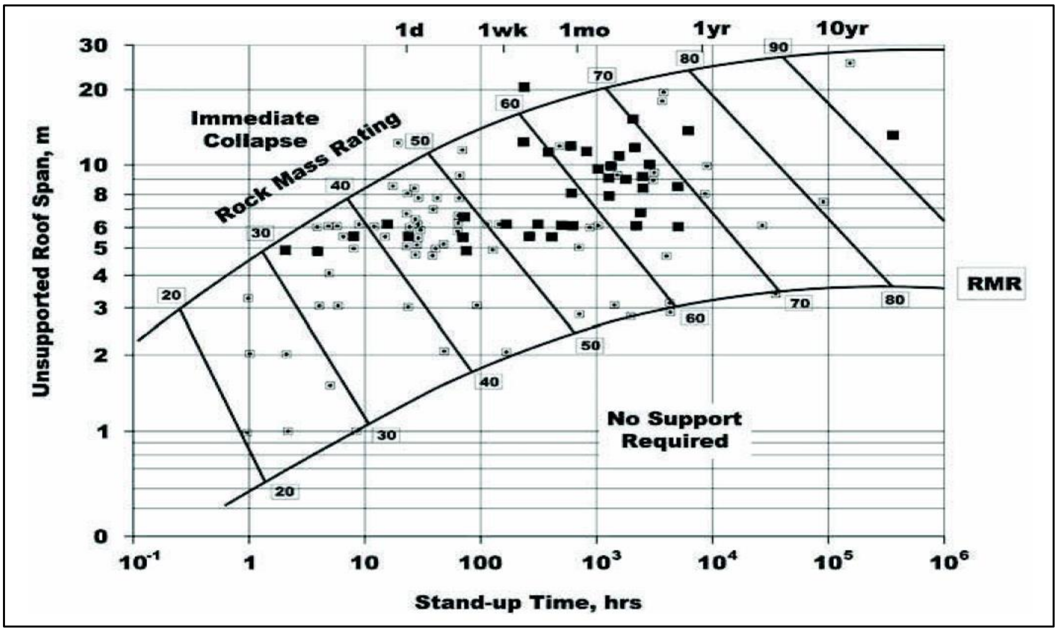

Figure 2-9**: Unsupported span as a function of RMR as cited by Bieniawski & Lowson (2013)**

The recommended safety factor for large excavation according to the industry best practice is 1.5. FOS can be obtained by plotting the Q or RMR value against unsupported span as shown in Figure 2-9.

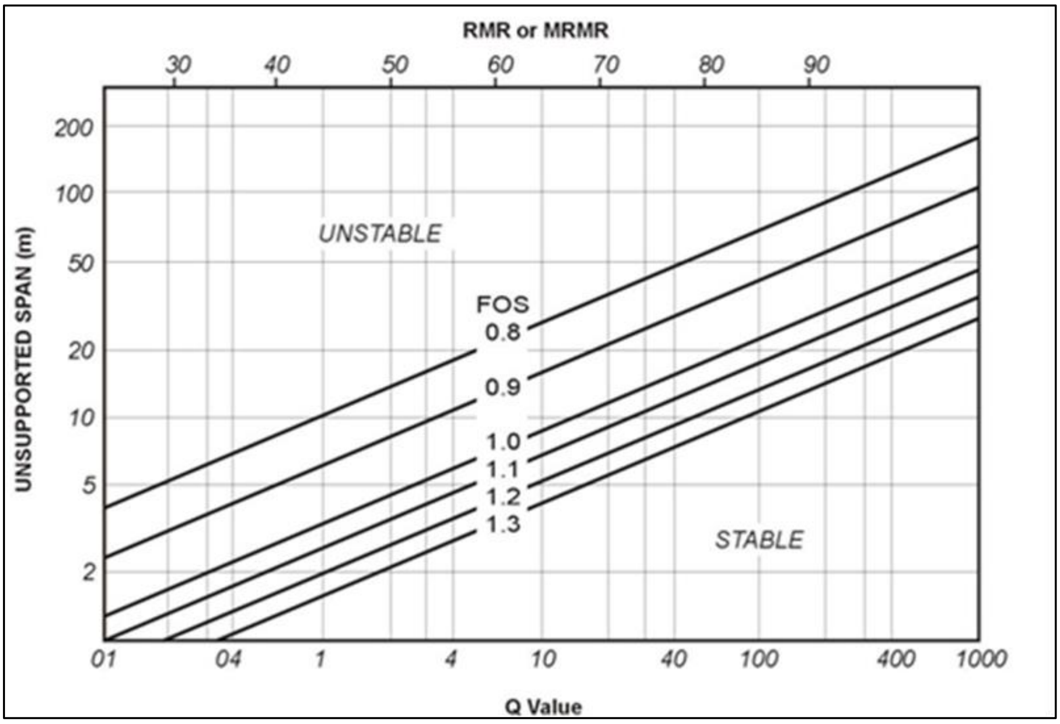

Figure 2-10: Unsupported span vs FoS as a function of RMR/Q **(Stacey, 2001)**

Bolt Length Estimation

In the context of bolting, the length of the bolt (referred to as L_b) plays a crucial role in ensuring that the loose block or rock mass is secure and stable. The bolting principle dictates that the bolt length should be carefully selected to ensure that it extends beyond the unstable block, allowing for proper tensioning of the loose rock mass. When the hanging wall geometry results from stratification, its stability depends on the stability of the beam of hanging wall rock. The length of rock bolts and cables used for stabilisation should be appropriate to support the thickness of the beam. The bolts should be 0.33 times the span or wall height under reasonable rock conditions (Stacey, 2001). For very good rock mass conditions, this multiplier could be as low as 0.25; for poor-quality rock mass, it could be as high as 0.5 (or even higher). Cables may be required in larger excavations; typical lengths are 0.4 times the span or wall height. Preliminary rock bolt or cable lengths for crusher chambers can also be estimated from empirical relationships proposed by NGI (2022) and Bieniawski (1989) and using rules of thumbs. NGI (2022) shows that the rock bolt and cable bolt length can be calculated using Equation 2-14 and Equation 2-15 respectively, where B is the excavation span.

L = 2 + 0.15B/ESR **Equation 2-14**

L = 0.4 B/ESR **Equation 2-15**

According Bieniawski & Lowson (2013) the bolt length varies with RMR and span and Equation 2-16 can be used to calcuate bolth length. Where L_b is the bolt length and Span is the width of the exavation.

$$Span = \frac{(L_b+2.5)^{\frac{RMR+25}{52}}}{3.6}$$ **Equation 2-16**

Hutchinson and Diederichs (1996) have suggested that the length should be adjusted for cable bolts by adding 2 m of embedment length such that the length is related to the span (S) by Equation 2-17.

L = $0.7S^{0.7}$ + 2 m **Equation 2-17**

If the failure zone is relatively shallow, the bolt length should be at least one metre longer than the depth of the failure zone to provide anchorage (Li, 2017). This is calculated using Equation 2-18, where d_f is the depth of the failure zone.

$$l_b = d_f + 1$$ **Equation 2-18**

Number of cables required to support a loosened zone

Using the empirical tool described by Hills *et al.* (2015), the number of cable bolts required to support the crusher chambers can be calculated using Equation 2-19.

$$\boldsymbol{N}umber\ of\ Cables\ = \frac{Mass\ x\ FoS}{Cable\ bolt\ strength}$$ **Equation 2-19**

Where the mass can be calculated using Equation 2-20 as defined by Hills *et al.* (2015).

$$M\ =\ Density\ x\ \frac{(\ Drive\ width\ or\ span^2)}{3}(tons)$$ **Equation 2-20**

Support Capacity

Rock bolt capacity can be calculated using Equation 2-21, where F_b is the bolt ultimate tensile strength and γ is the safety factor as described by Bieniawski & Lowson (2013).

$$F_{bd} = \frac{F_b}{\gamma} * \left(\frac{RMR}{85}\right)^{\frac{40}{RMR}}$$ **Equation 2-21**

When the rock mass is subjected to high levels of stress, it may break apart if not properly held together with reinforcing, retaining or holding elements (Cai & Kaiser, 2018). Common retaining elements include wire mesh, reinforced shotcrete, straps, steel arches and cast-in-place concrete. Shotcrete is used in the jointed and blocky rock mass environment to hold potential pieces which might fall out between bolts and prevent instability from developing. Bieniawski & Lowson (2013) state that the capacity of shotcrete support is designed based on the simple concept that it acts as an arch in compression using Equation 2-22. Where F_{ck} is the shotcrete cylinder strength and γ_s is the partial factor as described by Bieniawski & Lowson (2013).

$$F_{cd} = \frac{F_{ck}}{\gamma_s} * \left(0.2 + 0.8 * \left(\frac{RMR}{100}\right)^{\frac{3}{2}}\right)$$ **Equation 2-22**

Support requirements can also be obtained using support charts where the excavation span is plotted against the Q value (NGI, 2022). Support design based on Q is shown in Figure 2-11. The excavation span of 12 m in the case of the Lift 2 crusher chambers 12 m was divided by the excavation support ratio in order to obtain the equivalent dimension. For empirical rock support recommendation, the equivalent dimension is then plotted together with the Q rating on NGI (2022) support chart given in Figure 2-11.

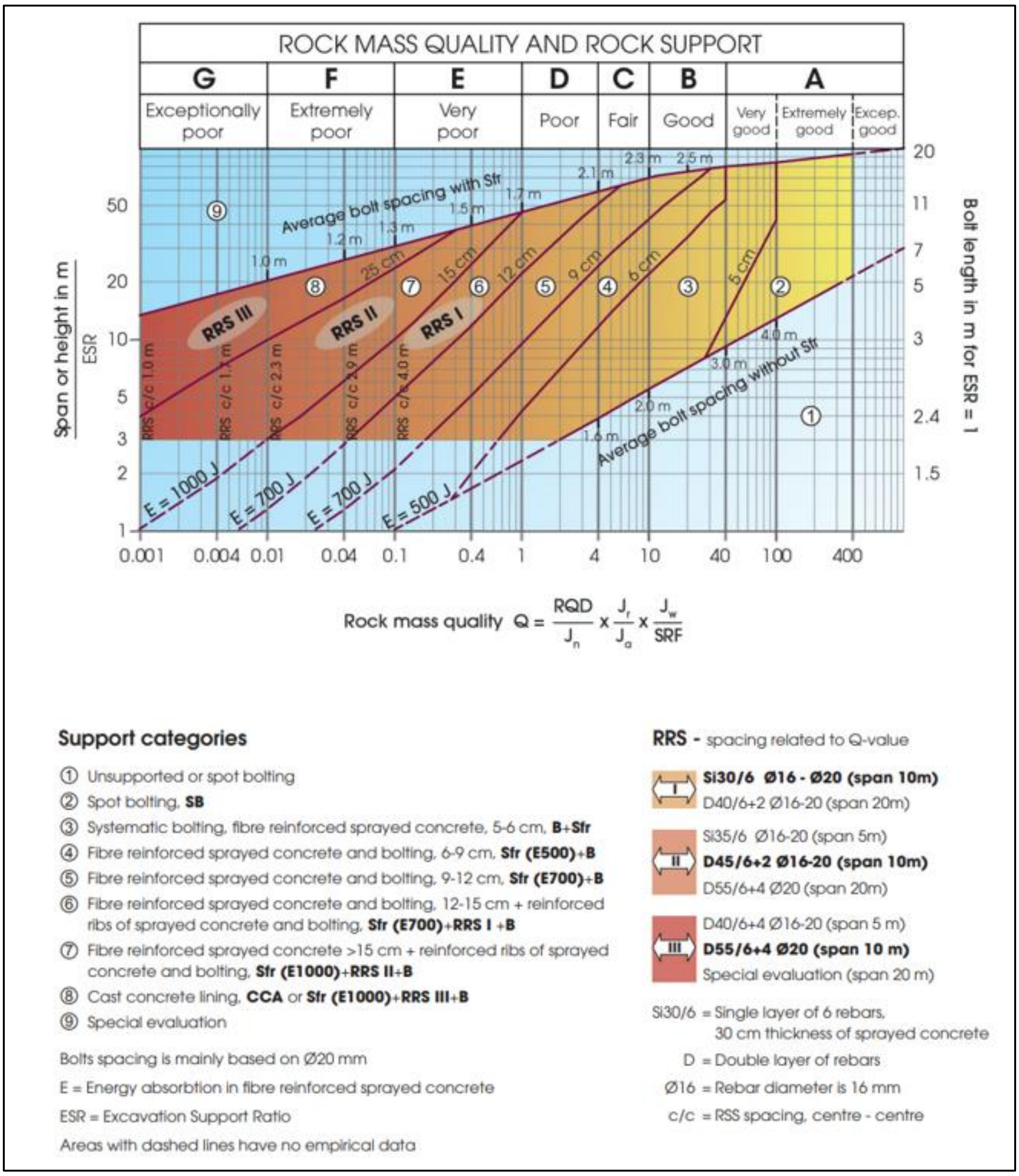

Figure 2-11: Support design chart **(NGI, 2022)**

2.5.2 Analytical Design Approach

As part of designing effective support systems, it is necessary to consider various stress conditions (static and dynamic) and failure mechanisms, such as gravity-driven wedge failures, stress-driven rock fractures and seismicity (Ortlep & Stacey, 1998). Identifying possible and likely rock failure mechanisms is important for geotechnical engineering designs. It is common for underground mines to experience wedge failures, also known as structurally controlled failures. When developing large underground chambers, it is inevitable to encounter complex geological discontinuities (including faults, cracks and joints). As a result, rock blocks can form and local collapses can occur. Analytical design methods include closed-form solutions, simple limit equilibrium techniques, elastic modelling and physical modelling. These methods usually involve simplifying the excavation geometry and rock properties. Simple limit equilibrium methods (LEM) techniques that can be used for wedge stability are available in several rock mechanics textbooks and calculations can be done for each wedge (Lorig & Varona, 2013).

Software called Dips, created by Rocscience, is often used for stereographic projections (RocScience, 2021a). With this software, users can quantify the rock mass based on joint frequency, joint spacing and RQD analysis collected along scanlines or boreholes. This can provide valuable insights into the major joint sets encountered when developing an excavation. This data can be utilised for structural interpretation and analysis through Unwedge. Unwedge is usually used for three-dimensional stability analyses to determine the maximum size of unstable wedges in the back or roof of openings (RocSience, 2022). Excavation geometry, joint strength properties and joint pattern are input into the analysis. Structure-mapping data is needed for the analysis. An excavation intersected by geological structures may fail. Stereonet projection also allows quick analysis of potential failures.

Hoek & Brown (1980) demonstrate that the first step is to determine the orientations of the dominant sets that are prevalent in the area. Figure 2-12 shows that failure can occur by falling or sliding from the back. Failure can also occur by sliding from the side wall. The size and shape of rock wedges or blocks surrounding tunnel openings exhibit considerable variability, dependent upon the tunnel profile, orientation, as well as the frequency, persistence, and number of joint sets. Wedge stability is also affected by the stress imposed on the excavation.

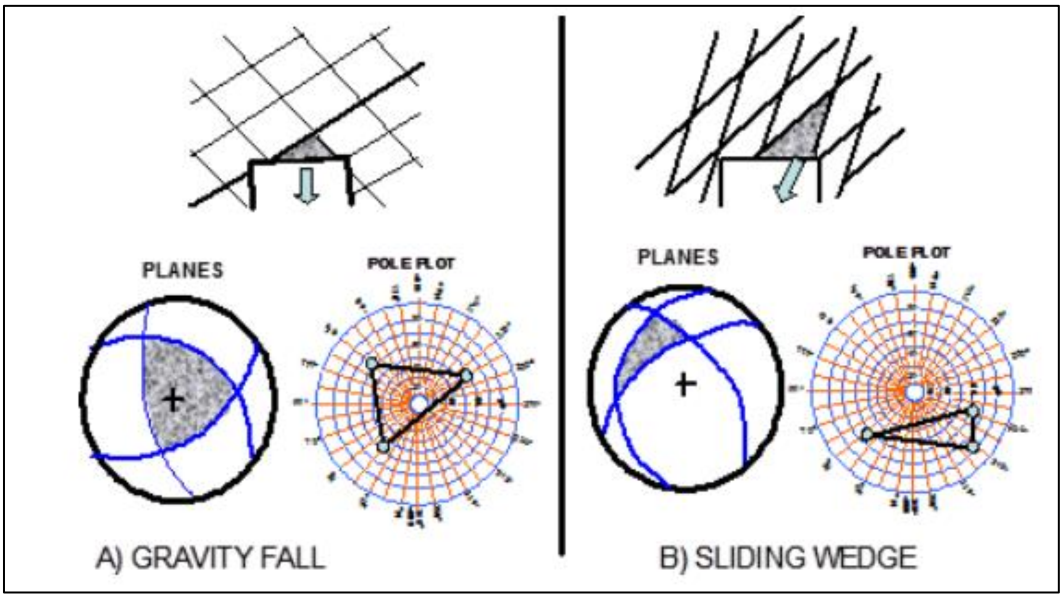

Figure 2-12: Illustration of support conditions for (A) gravity fall and (B) sliding instability for wedge within the back of tunnel **(Pakalnis, 2015)**

When the rock mass depth is shallow to intermediate, the in-situ rock stresses are usually low or moderate and well-developed joint sets often occur. After tunnel creation, wedge blocks can be formed on the tunnel's hanging wall or sidewall. As a result, the major issue with instability is caused by loose blocks. As illustrated in Figure 2-13, rock support acts as a barrier to prevent loosening blocks from falling.

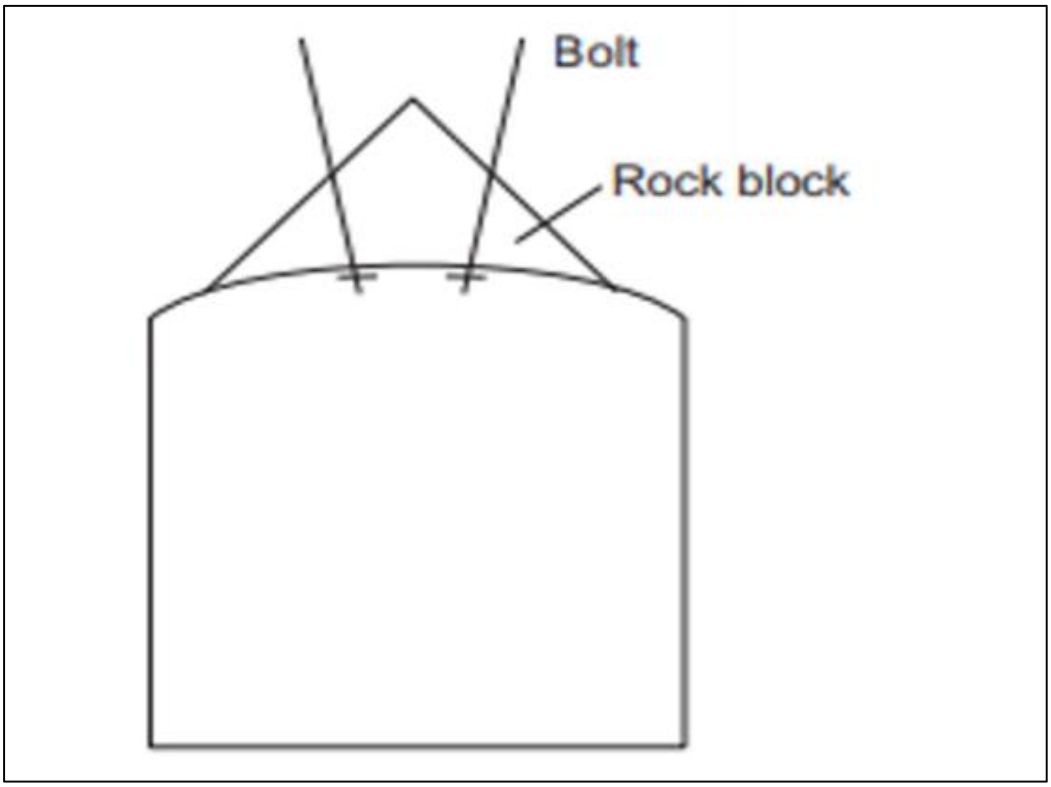

***Figure 2-13: Illustration of the support of a potentially falling roof wedge* (Li, 2017)**

Factor of safety in gravitational falls of ground

A crucial aspect of stability analysis and designing ground support for a rock mass is the factor of safety (Rahimi *et al.,* 2020). According to Pariseau (2007), a large excavation should not have a load that exceeds half the strength of its support. It is common for structurally controlled failures in large chambers to be designed to have an acceptability factor of safety of 1.5 to 2.0 (Hoek, 2007). According to Li (2017), in cases of gravitational falls, the support must be able to withstand a load, this mean that the strength of the bolt must be more than the load it has to carry to ensure stability. The factor of safety (FoS) for gravitational fall of ground is defined by Equation 2-23 as described by Li (2017):

$$Fos = \frac{Load\ capacity\ of\ the\ support\ system}{Total\ load\ on\ the\ support\ system}$$ **Equation 2-23**

Ground support demand required to support the dead weight under static conditions can be calculated using Equation 2-24 as described by Cai & Kaiser (2018).

$Ground\ support\ demand = \rho g d_f$ **Equation 2-24**

Where

ρ is the density of rock (kg/m^3);
g is the gravitational acceleration (m/s^2) and;
d_f is the depth of failure or the displacement of the rock (m)

Factor of safety in burst prone rock

According to Li (2017), rock burst events can occur when a highly stressed rock mass suddenly releases stored strain energy. The rock bolts must have a higher energy absorption capacity than the kinetic energy of the ejected rock. To calculate the factor of safety for dynamic rock support (Equation 2-25), the energy absorption capacity of the rock bolts and the energy released in the rock burst event must be considered (Li, 2017).

Morissette & Hadjigeorgiou (2019) state that a reliable ground support system is essential in underground mines subjected to seismic activity. This means that support system must have the ability to maintain confinement and manage rock mass dilation around reinforcement elements. Additionally, the ground support system should be able to absorb the kinetic energy released when rock ejection or rock mass failure occurs.

$Fos = \frac{nE_{ab}}{E_{ej}}$ **Equation 2-25**

Where
n *is the number of roof bolts;*
E_{ab} *is the energy absorption of each bolt and;*
E_{ej} *is the kinetic energy (calculated using* Equation 2-26 as described by Li (2017);

$E_{ej} = \frac{1}{2}mv^2$ **Equation 2-26**

Where
m is the mass of the ejected rock and;
v is the ejection velocity;

In cases where bursts occur in walls, the ejection velocity can be calculated based on the horizontal distance of the dislodged rock (Kaiser et al., 1996).

The ejection velocity can be calculated using Equation 2-27 (Potvin *et al.,* 2010).

$$v(PPV) = \frac{C10^{\frac{1}{2(m_L+1.5)}}}{R+R_0}$$ **Equation 2-27**

Where

C i*s the parameter with value about 0.2–0.3 for design purposes;*

R is the distance to the source R_0 *can be calculated using Equation 2-28 (* (Rahimi *et al.,* 2020)*;*

m_L *is the magnitude event;*

$\propto$ *is the parameter with value of 0.53-1.14.*

$$R_0 = \propto \frac{10^1}{3(m_L+1.5)}$$ **Equation 2-28**

Li (2017) shows that mesh and yielding roof bolts are usually used to deal with excessive rock deformation in the mines. The rock bolts mainly carry the support load while the mesh restrains the dilation of the rock surface. To minimize shear failure, it is suggested by Stacey (2016) to install additional rock bolts at an acute angle (less than 30 degrees) to the orientation of discontinuities.

Number of bolts required to support a wedge

The number of rock bolts required to stabilise a wedge can be calculated using Equation 2-29 (Li, 2017).

$$N_{bolt} = FoS\frac{W_g}{P_{ult}}$$ **Equation 2-29**

Where

W_g *is the deadweight force of the block or wedge* and;

P_{ult} *is the ultimate load of the rock bolt.*

2.5.3 Numerical Modelling

Due to structural complexities, standard rules of thumb and empirical calculations may not adequately provide reliable solutions for the design of large excavations. By simplifying rock properties and excavation geometry, analytical methods cannot accurately calculate complex compressive stresses on blocks with complex geological conditions (RocScience, 2020). Alternatively, numerical methods are more suitable for complex block problems (RocScience, 2020). In particular, when more data is available and a deeper understanding of fundamental mechanics is required, numerical modelling provides a valuable function (Sjöberg, 2020).

Numerical modelling is crucial for ground support and can be classified into three categories, each of which necessitates different techniques and data types (Potvin & Hadjigeorgiou, 2020). In the early to mid-1960s, the application of numerical methods, specifically the finite element method, to rock engineering began. Since then, it has been successfully applied to analyse stress and deformation around mining openings (Brown, 2012). There are two ways to model a rock mass: the continuum approach and the discontinuum approach, as explained by Unteregger *et al.* (2015). If there are only few fractures, the continuum approach can be used (Unteregger *et al.,* 2015). However, for moderately fractured rock masses, where there are too many fractures for the continuum-with-fracture-elements approach or where large-scale displacements of individual blocks are possible, the discontinuum approach, is more suitable.

Many underground excavations are designed using numerical simulations based on boundary element method (BEM), distinct element (DEM), finite difference (FDM) and finite element methods (FEM) (Cai & Kaiser, 2018). Examine 2D, Examine3D and Map3D are examples BEM based numerical methods, where only the boundary of the model is discretised. FLAC3D is an example of FDM based numerical method and the whole domain or model is discretised. RS2 is a FEM based numerical method where the whole domain is discretised.

Elastic Models

According to Kaiser *et al.* (1995), elastic models assume that rock masses surrounding underground excavations behave elastically. Young's Modulus, Poisson's ratio, excavation geometry and stress field are required for elastic model analysis. Several common packages that model rock masses and elastic media include Examine2D, Map3D and Examine3D (Kaiser et al., 1995). Examine 2D is a boundary element program that calculates displacements and stresses around two-dimensional (2D) excavation geometries (Kaiser *et al.* 1995). The model assumes that the rock mass behaves in an elastic manner and that the rock mass is isotropic. The calculated stress results are dependent on the modelled geometry, in-situ stresses and the Poisson's ratio. The displacement results are dependent on the value of the Young's Modulus used. Kaiser *et al.* (1995) showed that since failure is not represented in the model, the application of elastic models is limited to situations where the extent of failure is confined in the immediate vicinity of an opening. This limitation causes elastic models not to be suitable for modelling for example, failure propagation or movement of blocks, yielding pillars and asperity shearing on faults, as described by Kaiser *et al. (*1995)

Examine 3D as a boundary element program that calculates displacements and stresses in three-dimensional (3D) excavation geometries (RocScience, 2020). The rock mass is modelled as a single elastic material. Modelling results consist of stresses, displacement, strength factors and energy in the form of planar or spatial contours. Kaiser *et al.* (1995) describe Map3D as a boundary element program that calculates displacements and stresses around two-dimensional excavation geometries in 3D. Multiple elastic materials, faults and backfill can be represented in Map3D. Modelling results consist of stresses, displacements and strength factors.

Non-Elastic Models

As Kaiser *et al.* (1995) point out, numerical models allow for exploring non-elastic or discontinuous rock masses under more complex geometries and it is possible to categorise numerical models as elastic or non-elastic based on their function. The post-failure properties of the rock mass are often input into non-elastic models. Cohesion and internal friction angle must be input if the rock mass is modelled as a plastic material. Kaiser *et al.* (1995) also show that RS2, Fast Lagrangian Analysis of Continua (FLAC) or Fast Lagrangian Analysis of Continua in Three Dimensions (FLAC3D), universal discrete element method in two dimensions (UDEC) or universal discrete element method in three dimensions (3DEC) are non-elastic models. Discontinuum programs such as UDEC/3DEC are used where the behaviour of joints or geological structures, such as faults or joints influences rock mass stability (Lorig & Varona, 2013). In contrast, continuum programs such as FLAC/FLAC3D are better suited to studying rock mass failure through inelastic constitutive models (Kaiser *et al.*,1995).

Model Input Parameters

An in-situ stress magnitude and orientation are crucial information when performing numerical analysis. This can be determined by measuring stress and reading literature on general estimates from different mines. The modeller can use observations of breakouts along an excavation or tunnel without stress measurement data to determine the principal stress direction. The modulus of elasticity and the Poisson ratio need to be known even for simple numerical analysis, as Kaiser *et al.* (1995) demonstrated. Laboratory tests can be conducted on an intact rock to determine these properties. Based on empirical rock mass classification techniques such as those specified by Hoek *et al*. (1995), various methods can be used to calculate the rock mass modulus of elasticity.

Poisson's ratio is usually taken to be between 0.2 and 0.3. The rock mass strength properties are required for numerical modelling analysis to determine the likelihood of failure. The failure criteria Mohr-Coulomb and Hoek-Brown can be used for this purpose (Kaiser *et al*.,1995). The intact rock tensile strength, uniaxial compressive strength and friction angles can be determined by laboratory testing of intact rock. The unconfined compressive strength, modulus of elasticity and tensile strengths of the rock mass can be determined from Equation 2-30, Equation 2-31 and Equation 2-32 respectively (Lorig & Varona, 2013).

$$\sigma_c = \sigma_{ci} s^a$$ **Equation 2-30**

$$\sigma_t = -\frac{s\sigma_{ci}}{m_b}$$ **Equation 2-31**

$$E_{rm}\,(\mathrm{MPa}) = E_i\left(0.02 + \frac{1-\frac{D}{2}}{1+e^{\left(\frac{75+25D-GSI}{11}\right)}}\right)$$ **Equation 2-32**

The Hoek–Brown envelope is known to overestimate the tensile strength of intact or unjointed rock mass. However, a more accurate assessment of the tensile strength can be determined by finding the intersection of a line passing through the origin with a -3:1 slope and the Hoek–Brown envelope (Hoek & Bieniawski, 1965). Equation 2- 33 expresses the generalised Hoek-Brown failure criterion for the estimation of rock mass strength as described by Hoek & Brown (2019)

$$\sigma_1 = \sigma_3 + \sigma_{ci}\left(m_b \frac{\sigma_3}{\sigma_{ci}} + s\right)^a$$ **Equation 2-33**

Hoek-Brown failure parameters *m* and *s* of the rock mass can be determined from estimates of the disturbance factor (D) and Geological Strength Index (GSI). Hoek *et al.* (2002) proposed the D factor to account for blast damage and stress relaxation around excavations. A rock mass that is undisturbed has a value of 0 while a rock mass that is extremely disturbed has a value of 1 (Lorig & Varona, 2013). and the rock mass material constants mb, s and a are given by Equation 2-34 to 2-36.

$$s = e^{\left(\frac{GSI-100}{9-3D}\right)}$$ **Equation 2-34**

$$m_b = m_i e^{\left(\frac{GSI-100}{28-14D}\right)}$$ **Equation 2-35**

$$a = \frac{1}{2} + \frac{1}{6}\left(e^{-\frac{GSI}{15}} - e^{-\frac{20}{3}}\right)$$ **Equation 2-36**

For very poor rock mass conditions, Hoek & Diederichs (2006) showed that the Young's Modulus of a rock mass (E_{rm}) can be estimated based on the simplified method shown in Equation 2-37. The Poisson's ratio of a rock mass ($\mathcal{V}_{rm}$) can be estimated from Equation 2-38.

$$E_{rm}\,(\mathrm{MPa}) = 1e5\left(\frac{1-\frac{D}{2}}{1+e^{\left(\frac{75+25D-GSI}{11}\right)}}\right)$$ **Equation 2-37**

$$\mathcal{V}_{rm} = 0.32 - 0.0015\ x\ GSI$$ **Equation 2-38**

2.6 Benchmarking

According to Stacey & Wesseloo (2022), there are two ways that empirical and analytical methods can be utilised in rock engineering applications to design and predict the behaviour of rock masses. It was necessary to benchmark the design approach used in other mines when developing the crusher chambers. This section discusses support design approaches used in other mines.

The Finsch Mine crusher chamber with dimensions: 10 m wide, 38 m high and 78 m long has been developed in Northen Cape in South Africa (Talu & Wilson, 2004). The support design approach applied consisted of a combination of analytical, empirical and numerical modelling. Talu & Wilson (2004) used FLAC3D package to model the stress and deformation imposed on the excavation. The Ernest Henry Mine crusher chamber was developed 1000 m below the surface in the Eastern Fold Belt of the Mount Isa Inlier in Australia. The crusher chamber measured 9.5 m wide by 25 m high by 35 m long and is considered a large excavation (Campbell et al., 2013). An empirical kinematic analysis and benchmarking with crusher chambers at similar mines led to the development of the support design, as cited by Campbell et al. (2013).

A large excavation (Panel 2 crusher chamber) has been developed at Oloy Tolgoi in the South Gobi region of Mongolia, located 1300 m below the surface. The chamber measured 21 m wide, 34 m high and more than 50 m long (Sharrock *et al.*, 2022). Sharrock *et al.* (2022) showed that the ground support design approach for the Panel 2 crusher chamber was based on analytical, empirical and kinematic assessment. It also applied a factor of safety of 1.5 for all load and deformation calculations. Fu *et al.* (2013) and Zhao *et al.* (2016) examined the failure modes of blocks as part of a large underground excavation process. In a study by Chen et al. (2020), the interaction between blocks was analysed using the discrete element method.

Ground support and reinforcement systems for these crushers were designed to withstand static and dynamic loads. The case studies further outlined the importance of geotechnical data collection for a practical design approach. As illustrated by these case studies, the proposed methodology combined analytical, empirical and kinematic assessments to analyse and design the reinforcement for their crusher chambers. The results of comparing the published works show that an integrated design approach that incorporates numerical simulation produces a more conservative and reliable design.

2.7 Chapter Summary

In order to mitigate a risk, it is important to be aware of the important factors affecting stability. Empirical, analytical, numerical design methods were reviewed. Analytical methods involve using numerical codes, closed-form solutions and classical physical and strength models. Empirical methods assess stability based on past practices and existing mine behaviour to predict future outcomes (Pakalnis, 2015); (Bieniawski, 1992). Barton's Q system (NGI, 2022) and (Bieniawski, 1989) are widely used for support selection and rock mass classification. The Q-system was developed mainly from experience in hard rock tunnels and a few cases in weak rocks and weak zones (NGI, 2022).

The empirical analyses are based on case histories and hence tend to achieve conservative practice and their limitations must be noted (Palmstrom & Broch, 2006). Lorig & Varona (2013) show that DEM codes are particularly well suited to modelling tunnels in jointed rock masses where the geological structure dominates instability. Input parameters play a major role in the analysis and design approach. It is crucial that care is taken to ensure the reliability of data. It is the author's view that the best approach is one that integrates empirical, analytical and numerical simulation. This approach has been successfully applied in most mines. Solving a problem from two or more approaches provides confidence in the design. One approach can be used to check and validate the other approach. For example, the challenge of relying solely on experience is that changing rock mass conditions as the mine progresses to greater depth may affect the support performance over time. The stresses induced due to greater mining depth may require increased support capacities to satisfy the rock demand.

3 RESEARCH APPROACH

3.1 Introduction

Leedy & Ormrod (2005) define research methodology as the approach a researcher employs to conduct a research project. This approach dictates the tools that the researcher will use. Various methods employed in the collection and analysis of the data were presented in this chapter. The process involved a combination of preliminary work, fieldwork and desktop study to ensure the comprehensive gathering of all necessary information. Additionally, a thorough literature review was conducted to determine the most effective support system for large excavations based on the research findings.

3.2 Desktop Study

The commencement of the research study was marked by a thorough desktop study of the study area and its relevant aspects. The primary objective of the desktop study was to gain a comprehensive and in-depth understanding of the support design approaches relevant to the design of crusher chambers. Additionally, an analysis of the mechanisms and geological factors responsible for rock mass instability was conducted to understand better the challenges that need to be addressed. The literature review conducted in the initial stages of the research study played a pivotal role in providing valuable insights into the subject matter. The research objective provided guidance throughout the entire process, ensuring that the study was carried out with accuracy and precision.

3.3 Field Observations and Measurements

The next step in the research process was fieldwork. This included observing the geological structures and features and taking photos of them during excavation. The geology and geotechnical data collected helped to characterise the rock mass and identify any variations between Lift 1 and Lift 2. Additionally, the rock mass condition was evaluated to define the ground control district for the project. The data collection process involved gathering data on rock types, joint data like dip and strike and photographs that showed the support conditions. This serves as a critical point of discussion during the research study's subsequent results and discussion phase. This approach underscored the importance of collecting accurate and relevant data to ensure that the research study was carried out effectively and efficiently. In order to gain a broad understanding of the behaviour and stability of the rock mass in the crusher chamber location sites, core samples of the crusher site from diamond drill holes were collected. These core samples were then carefully reviewed and analysed, providing valuable insights into the underlying geological conditions and expected rock mass behaviour. Intact rock strength data were collected from laboratory testing of intact rock, which was conducted prior to the commencement of this research study.

3.4 Laboratory Analysis

Uniaxial Compressive Strength (UCS) tests and Triaxial Compressive Strength (TCS) tests were conducted by the CSIR and Rocklab on selected core samples to define the rock strength characteristics for the crusher chamber lithologies. In a uniaxial compression test, a well-ground core specimen with a height-to-diameter ratio of about 2:1 to 2.5:1 was loaded under two parallel platens under a constant loading rate until failure. The rock specimen was a piece of core or “right circular cylinder", with the ends ground or lapped parallel and to within 0.02 mm.

A minimum of three specimens were tested. The elastic modulus and Poisson ratio measurements were done by both vertical and lateral strain gauges (Chen, 2009). Rock tensile strength was considered an essential measure of one of the weakness modes of failure. A cylinder with a width-to-diameter ratio of about 0.5:1 was used in tensile strength tests. Usually, a minimum of three specimens should be tested for each rock type. The specimen was placed in the compression testing machine such that the load was applied across the diameter of the sample and perpendicular to the core axis and the bedding planes (if any). The specimen was loaded to failure.

Two types of UCS testing were conducted on the drilled core.

- UCM tests - UCS with elastic modulus, Young's modulus and Poisson’s ratio
- UCP tests - Uniaxial pre- and post-failure test with axial and lateral deformation.

Two types of TCS testing were conducted on the core collected from boreholes drilled at the crusher chamber site.

- TCS tests - TCS per one confining pressure at a maximum of 70 MPa.
- TCP tests - Triaxial Compression tests with post-failure behaviour.

The UCM (UCS, elastic modulus & Poisson's ratio, stress–strain curve) test was conducted using a Servo-controlled hydraulic compression testing machine. The rock core cylinder with a height to diameter ratio between 2.5:3.0 is placed between the testing machine's top and bottom loading platens. A constant loading rate was applied until the specimen fails. Both axial and lateral deformations were monitored by computerised instrumentation via strain gauges. The parameters UCS, elastic Modulus and Poisson’s ratio were calculated based on the measured information and specimen size.

The UCP (UCS, elastic modulus & Poisson's ratio, stress-strain curve) test was conducted using a Servo-controlled hydraulic stiff-compression testing machine. The rock core cylinder with a Height to diameter ratio between 2.5:3.0 was placed between the testing machine's top and bottom loading platens. A constant loading rate was applied until the test was completed. Both axial and lateral deformations were monitored by computerised instrumentation via an extensometer. The UCS, elastic modulus and Poisson’s ratio were calculated based on the measured information and specimen size. The residual strength was also calculated from the information.

TCP (TCS, elastic modulus and Poisson's ratio, stress-strain curve) test was conducted using a Servo-controlled hydraulic stiff-compression testing machine. The rock core cylinder with a height to diameter ratio between 2.0:2.5 was placed between the testing machine's top and bottom loading platens according to ISRM standards. A constant loading rate was applied until the test was completed. Both axial and lateral deformations were monitored by computerised instrumentation via an extensometer. The parameters TCS, elastic modulus and Poisson's ratio were calculated based on the measured information and specimen size. The residual strength was also calculated from the information.

3.5 Empirical Analysis

Laubscher’s Rock Mass Rating (Laubscher,1990), Bieniawski’s RMR (Bieniawski, 1989) and the Q system (NGI, 2022), were used to classify the rock mass based on data collected from field mapping and drilled holes. Rock Quality Designation (RQD) was logged directly from the core and was evaluated using the approaches of Deere *et al.,* (1967) and Palmström (2001). The stress reduction factor (SRF) was evaluated using the approach of Peck (2000) for high-stress conditions in jointed rock, i.e., where the ratio of UCS to major principal stress s associated with the advancing mining front depth or mining depth.

3.6 Numerical Analysis

The study utilised RS2 finite element software to conduct a simple numerical analysis in two dimensions (2D) and validate both empirical and analytical results. RS2 offers a wide range of support modelling options for various geotechnical structures such including underground excavations (RocScience, 2021b). RS2 allows for the installation of support units in stages and provides detailed analysis results for each element to ensure that support loads are within acceptable parameters. Similarly, the researcher chose this RS2 because it is simple to use. It was of utmost importance to carefully select the appropriate numerical modelling package RS2 and methodology to conduct accurate numerical simulations. Once this crucial step is completed, the next phase involves gathering input parameters from various sources such as literature review, laboratory testing, instrumentation and underground observations. The inputs required for numerical simulation include geometry, in-situ stresses, elastic properties of the rock mass, strength properties and joint or fault properties. For the numerical modelling conducted in this study, the input parameters used are in-situ stress and rock mass properties. The in-situ stress data were obtained through overcoring methods in 2017 by Groundworks (Handley & Piper, 2017) and were available prior to the commencement of the study.

The stress-strain behaviour of the ground and support systems was estimated using a finite element model. The numerical analysis results were then compared to predefined failure and stability evaluation criteria, such as stress concentration ($\frac{\sigma_1}{\sigma_c}$), shear failure potential, Mohr-Coulomb failure criteria and Hoek-Brown failure criteria. Through this process, the study was able to accurately identify the potential for failure and instability, which will be of great significance in the development of future numerical simulations. Combining these various approaches achieved a detailed and comprehensive picture of the rock mass behaviour and stability, helping to achieve the study's objectives. The detailed methodology for designing Lift 2 crusher chamber support is summarised in Figure 3-1.

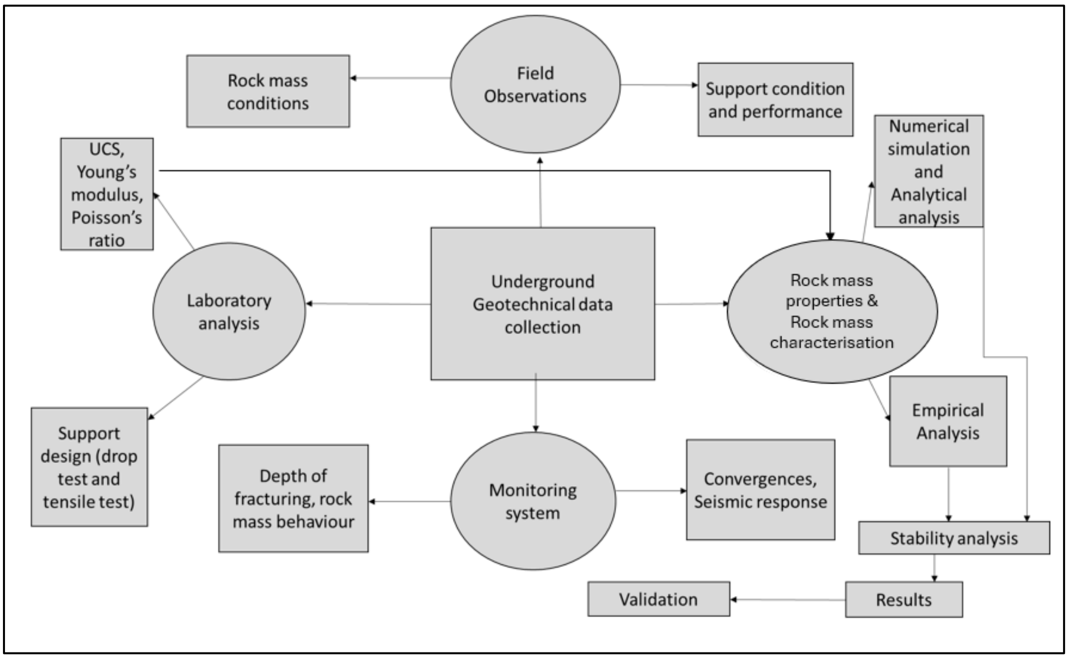

Figure 3-1: The methodology followed to design support for Lift 2 crusher chambers.

3.7 Research Design

When conducting research, the research design is critical to achieving positive results. Christensen (1985) defines a *research design* as a procedure for seeking an answer to a research problem that defines how the procedure will be formulated. Mouton (2001) asserts that a research design is akin to a strategic blueprint for conducting your research. Similarly, Leedy & Ormrod (2001) state that a research design is crucial for conducting research, as it provides the foundational framework for collecting and analysing data. Achieving desirable results is contingent upon thoroughly planned research methodology (Leedy, 1993). This research study adopted qualitative and quantitative research approaches. Triangulation is sometimes used as a term for combining qualitative and quantitative approaches, according to De Vos (2002). As the researcher seeks to develop a support system for crusher chambers, a combination of qualitative and quantitative research design approaches was the most appropriate to increase the reliability of the study.

These approaches allowed the researcher to obtain geological information from underground observations for stability assessment. These research designs allowed the researcher to collect data and thoroughly assess the rock mass behaviour which aided in designing the Lift 2 crusher chambers.

3.8 Data Collection Process

This research gathered information through underground observations and a comprehensive literature review. In addition to primary data obtained through underground observations and secondary data collected from the literature review, the researcher utilised case studies and personal experience as resources for gathering information. Mouton & Marais (1994) state that several resources of documentary data can be effectively utilised for gathering data for any study. Such sources could be records, documents, library collections or mass media material.

It is imperative to utilise a range of data collection methods when conducting qualitative research, as emphasised by Leedy & Ormrod (2001). As Leedy (1993) aptly notes, extensive planning is fundamental to obtaining favourable research results. Therefore, researchers must carefully consider and select the appropriate data collection techniques to ensure the validity and reliability of their findings. This requires a comprehensive understanding of the research problem, questions and objectives, which can be achieved through thorough planning and preparation. The source of data collected for this study is described as follows:

- Peer-reviewed journals were used for the literature review;
- The textbooks and handbooks prescribed during lectures were used in addition to peer-reviewed publications;
- Literature review on ground support design for crusher chambers;
- Benchmarking with other crusher chambers in similar operations was done and it considered the mining depth, ground conditions, stress regime and chamber dimensions when comparing ground support regimes.
    - This included underground visual observations on the type of support used for Lift 1 crusher chambers;
- In this study, the engineering properties of rock masses were defined from field and laboratory studies for each domain;

- Support systems for the crusher chambers were designed based on the rock mass properties and excavation dimensions;
- The suggested support systems by empirical and analytical design approaches were subjected to numerical analysis to evaluate their predicted performance; and
- A database with geotechnical information from site investigations (geotechnical boreholes) at PMC were analysed as part of the rock mass characterisation.

3.9 Data validation process

Data validation plays a pivotal role in any research study as it ensures that the conclusions and insights drawn from data are reliable and accurate. Through data validation, researchers can identify potential errors, inconsistencies, or anomalies in their data, thus minimizing the risk of false conclusions or unreliable findings. This is particularly important as data quality directly impacts the quality of research outcomes. In essence, data validation serves as a critical safeguard against the propagation of unreliable research findings.

Mine data was utilised for this research project. The data collected included operational data based on daily face mapping. The accuracy of the data was ensured through daily checks conducted by the Geotech Engineers and subsequently verified by line management. Numerical models was validated through observational methods as data becomes available during the development process of the Lift 2 crusher chambers. Results of analytical and empirical analysis (rock mass behaviour, expected mode of failure and support requirements) were validated by numerical simulation. Peer-reviewed journals were used to compare the study's results with the previous work. Therefore, a correlation or disagreement were outlined and the reason documented.

3.10 Data analysis approach

According to Mouton & Marais (1994), research findings enable researchers to draw well-supported and informed conclusions by thoroughly analysing the data collected. Leedy & Ormrod (2001) support this view and outline the four steps of the data analysis, stating that these steps are crucial in effectively processing data and obtaining meaningful insights. This study followed the steps described as follows:

- To make the data easier to analyse, the researcher sorted the data and grouped them into relevant categories;
- The researcher comprehensively understood all the information collected through field observation, literature reviews and case studies by examining the data. After reviewing the data a few times, the researcher made initial notes and reflected on the findings;
- The researcher then categorised the data and identified relationships and themes by breaking them into units;
- The researchers gathered and organised information by forming ideas and statements and presenting them visually through tables and graphs.

According to Mouton & Marais (1994), data analysis is a powerful method for addressing complex problems. Additionally, Mouton & Marais (1994) show that this technique involves breaking down data into smaller components and scrutinising them to understand the issue better. By reviewing the data, analysts can identify patterns, connections and discrepancies that may not be apparent when considering the entire dataset. This systematic approach enables researchers to develop more comprehensive and accurate solutions to challenging problems (Mouton & Marais, 1994). On the other hand, Vithal & Jansen (2019) show that in research, data must be scanned, cleaned and rearranged by three specific steps involved in the analysis process. These steps include;

- Carefully examining and revising the data to ensure accuracy;
- Analysing the data to identify trends and patterns and;
- Interpreting the data to draw meaningful conclusions.

By adhering to these best practices, researchers can ensure that their findings are accurate, reliable and actionable. To effectively process research data, it was crucial to present it in an organised and easily understandable manner. This process entailed structuring data into tables, graphs and statistical summaries, enabling study details to be emphasised (Vithal & Jansen, 2019). In this study, rock mass classification was presented in tables and support design charts were used for support selection. The rock mass response was visualised using numerical modelling simulations.

3.11 Chapter Summary

The purpose of this chapter was to provide an overview of the research design and to discuss methods used to ensure the reliability and validity of the research, including data collection and data analysis. This research study adopted qualitative and quantitative research design methods, which was the most appropriate as the researcher aimed to develop a support system for crusher chambers. The rock mass was qualitatively assessed using common rock mass classification systems, i.e., the Barton et al. (1974) Q-system (NGI, 2022) and RMR Bieniawski (1989). The reliability of the research was ensured through the use of multiple data collection methods, desktop study, literature review and field observations. The methods employed for analytical, empirical, laboratory and numerical analysis were also discussed. The validity of the data was ensured through daily checks conducted by Geotechnical Engineers. Only competent personnel employed by the mine, were used to map underground exposures and these were confirmed by the head of the Geotechnical department. Laboratory testing was performed by reputable service providers such CSIR and Roclab. Similarly, numerical modelling analysis was used to check empirical and analytical solutions against field data.

4 DATA COLLECTION AND ANALYSIS

4.1 Introduction

This section presents data collected for this study. This data includes various aspects such as rock types, joint properties, infill types, joint frequency and orientation and photographs depicting support conditions. Additionally, the core and depth of failure measurements are also presented. It is essential to emphasize the importance of reliable and detailed data in any research study to ensure accurate results. The aim of the research study is to design a support approach for the Lift 2 crusher chambers. Using the data presented in this chapter will facilitate the establishment of an appropriate ground support approach for Lift 2 crusher chambers by determining the expected rock mass quality and potential failure mechanism.

4.2 Field observations and measurements

Physical observations were conducted on the excavation near the Lift 2 crusher chamber sites. The sites were subdivided into Site A and Site B. The photographs presented show the observed conditions of the excavations within the two-excavation site of the study area. The excavations that were evaluated on both Sites had uniform dimensions of 5 meters in width and 5 meters in height. The geological conditions of the rock mass and rock mass properties are the key factors for the empirical stability assessments. A detailed description of the rock mass conditions encountered during the fieldwork is reported in the subsections.

4.2.1 Field observation Site A

Site A is situated along the eastern part of the Lift 2 footprint (known as Crusher 5 complex). Although it is bounded by dolerite dykes, it has been positioned such that the excavation is not placed along the contact plane, which would affect the stability of the crusher. It was observed that the excavations within Site A exhibit numerous geological conditions as expected from the borehole data assessments. The rock mass at the eastern crusher complex comprises a combination of micaceous pyroxenite (MPY), foskorite (FOS) and carbonatite (TCB& BCB). The geological conditions observed in the rocks include joint sets, faulting and fracturing. Most excavations developed within MPY exhibit both the presence of weathering and jointing (Figure 4.1). Moreover, the mica content seems to have weakened and disintegrated the rock mass. Observations showed that Site A is mostly supported by welded mesh and roof bolts and use of cable anchors linked with Osro straps in the DOL contacts (see Figure 4-1). For corrosion control, supports units are covered with a layer of fibre reinforced shotcrete. The measured bolt spacing was 1.4 m by 1.4 m and the shotcrete thickness measured 50 mm. Site A is characterised by closely jointed rock mass with the dominant rock type being FOS and it is bounded by DOL dykes.

Figure 4-1: Heading with FOS host rocks and calcite veins (Site A) (Masole, 2022).

Figure 4-2 illustrates a typical example of the jointed rock mass. Support integrity in long-term excavations can be negatively impacted by corrosion particularly in areas where groundwater is intersected (Figure 4-3). Although the excavation is covered with shotcrete, it is the authors view that the water seepage was along a geological contact traversing the excavation. Typical example of spalling or slabbing and cracking of shotcrete associated with high induced stresses is shown in Figure 4-4.

Figure 4-2: Shows Site a jointed rock mass (Masole, 2022).

Figure 4-3: Illustrates influence of water on stability of excavations (Masole, 2022).

Figure 4-4: Illustrates an excavation with loose shotcrete held by mesh (Masole, 2022).

4.2.2 Field observations Site B

Site B is located on the western side of the Crusher 6 complex, within the Lift 2 footprint. Field observations showed that Site B has less jointing and no significant geological structures. The primary rock types found were transgressive and banded carbonatite host rocks. Roof bolts and a layer of shotcrete were used to support the site and excavation was mostly dry (Figure 4-5).

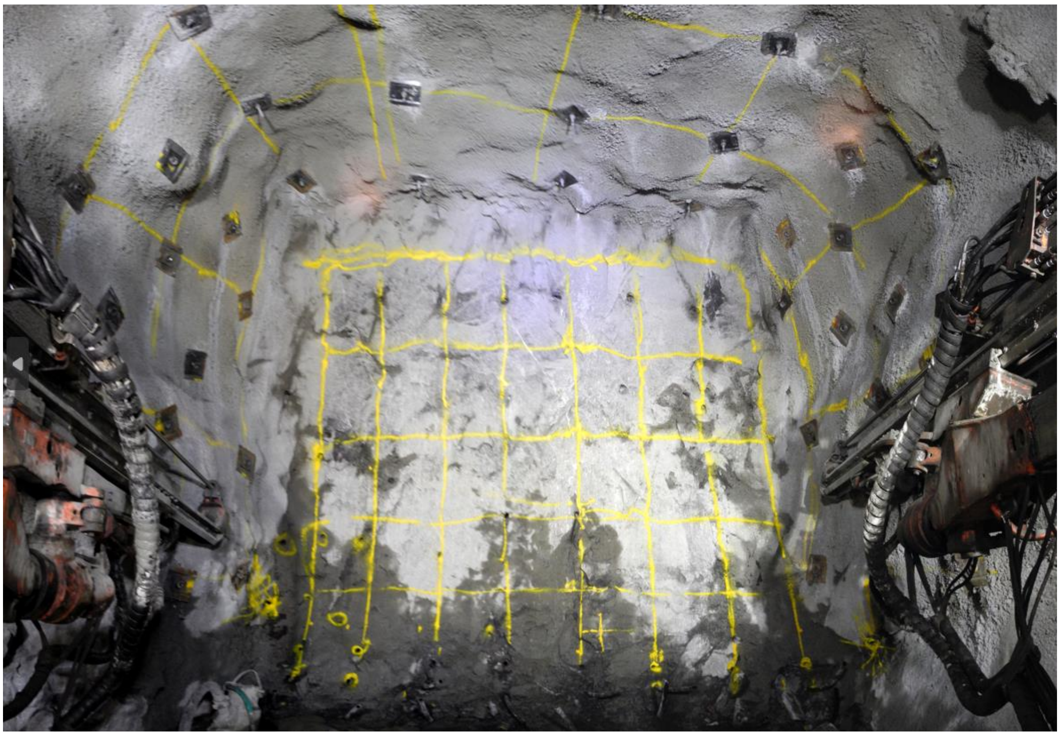

Figure 4-5: Illustrates an excavation supported with shotcrete and roof bolts (Masole, 2022).

4.2.3 Rock mass behaviour of Lift 1 excavations

The failure mechanism for the Lift 1 excavations in the production level ranged from spalling of highly stressed brittle rock mass to squeezing. In an intermediate stress environment (approximately to 1600 m depth) the rock-mass response is expected to be nonelastic and hence stability is controlled by the stress-induced damage in the chamber walls. Extensive monitoring around excavations on the Lift 1 extraction level using tape extensometers and visual observations has shown a consistent pattern of rock mass damage associated with irregular draw, particularly at the central most part of the cave footprint a typical example is shown in Figure 4-6.

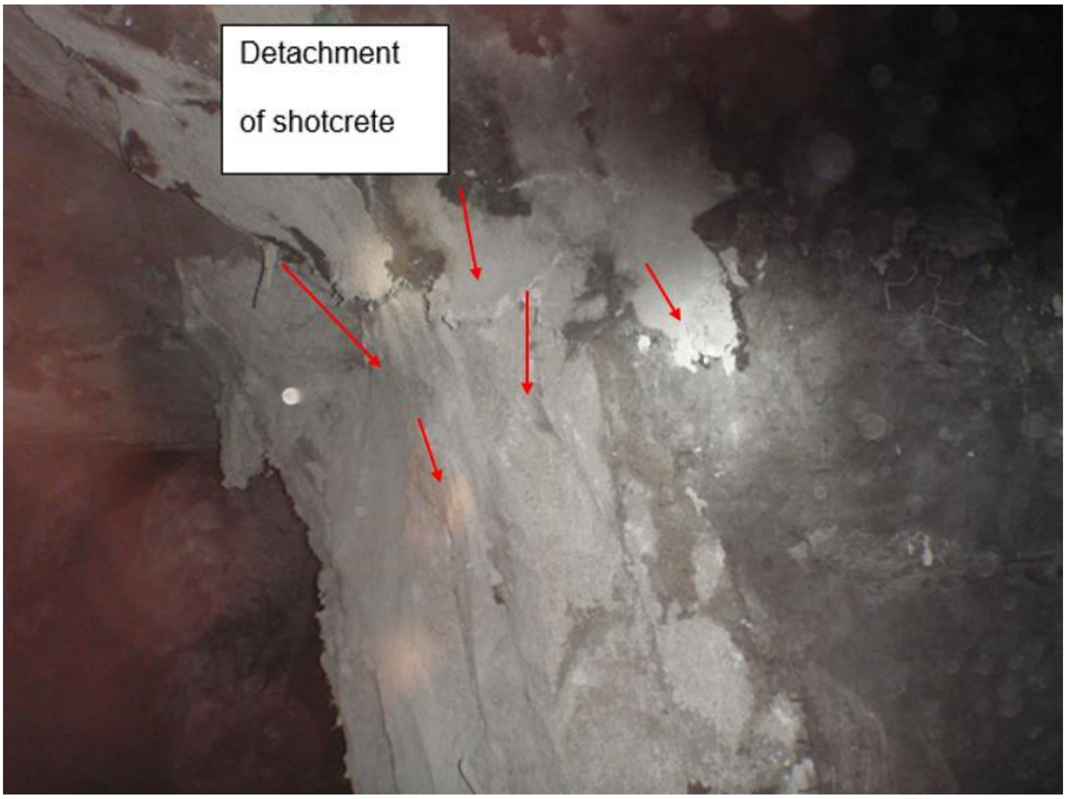

Figure 4-6: Illustrates shotcrete detachment and cracks in Lift 1 Production footprint (Masole, 2022).

Lift 1 crusher chambers were supported with 2.4 m long rock bolts, 6m cable anchors and 100 mm layer of fibre reinforced shotcrete. The installed support had been stable since the crusher development at the start of the mine. Although these crushers are located close to the cave (at 80 m from the Lift 1 production footprint), they have not been affected by caving. There has been no significant movement and seismic related damages recorded to date. This suggests that the support that was installed is adequate.

4.3 Geological mapping

Face mapping was carried out as part of the stability assessment. Mapping reports of excavations near the crusher chamber site have been reviewed and assessed. Three joint sets have been recognized in the TCB and FOS rock. These joints have a reasonably consistent orientation with depth. However, marked differences were noted in intensity of fracturing between FOS and TCB. The geology surrounding the crusher chambers is predominately FOS with an average uniaxial compressive strength (UCS) of 100 MPa and an average rock density of 3100 kg/m^3. FOS is a coarse-grained to pegmatoidal basic rock consisting of partially serpentinised olivine, magnetite and apatite (Palabora, 2015). Geotechnical mapping of blasted excavations near the crusher chamber area showed rock mass with TCB veins in some areas. A typical example of the mapped face is shown in Figure 4-7. Joint data is presented in Table 4-1.

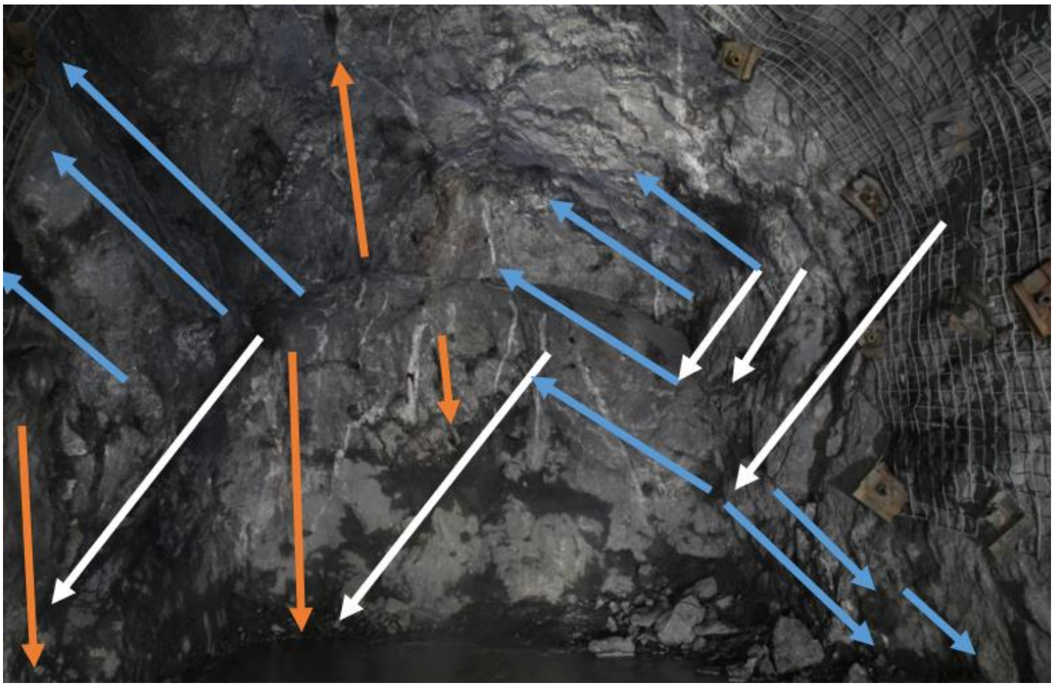

Figure 4-7: Illustrates mapped face in Site A (Masole, 2022).

Table 4-1: Mapped joint data **(Masole, 2022).**

Location ID	**Rock Type**	**UCS (MPa)**	**Dip angle (°)**	**Dip direction (°)**
Site A	TCB	120	80	256
Site A	TCB	120	70	71
Site A	TCB	120	75	66
Site A	TCB	120	60	86
Site A	TCB	120	55	76
Site A	TCB	120	55	56
Site A	TCB	120	75	81
Site A	TCB	120	50	66
Site A	TCB	120	80	61
Site A	TCB	120	60	56

Location ID	Rock Type	UCS (MPa)	Dip angle (°)	Dip direction (°)
Site A	TCB	120	60	56
Site A	TCB	120	85	51
Site A	DOL	320	65	56
Site A	TCB	120	75	21
Site B	TCB	120	45	76
Site B	TCB	120	80	110
Site B	TCB	120	70	115
Site B	TCB	120	65	120
Site B	TCB	120	60	120
Site B	TCB	120	70	310
Site B	TCB	120	40	320
Site B	TCB	120	70	90
Site B	TCB	120	65	285
Site B	TCB	120	35	325
Site B	TCB	120	45	120
Site B	TCB	120	80	90
Site B	TCB	120	70	85
Site B	TCB	120	60	120
Site B	TCB	120	80	90
Site B	TCB	120	85	270
Site B	TCB	120	80	290
Site B	TCB	120	75	105
Site B	TCB	120	50	120
Site B	TCB	120	65	315
Site B	TCB	120	60	305
Site B	TCB	120	80	320
Site B	TCB	120	85	330
Site B	TCB	120	55	343
Site B	TCB	120	50	345
Site A	FOS	100	80	49
Site A	FOS	100	70	219
Site A	FOS	100	70	224

Location ID	Rock Type	UCS (MPa)	Dip angle (°)	Dip direction (°)
Site A	FOS	100	80	229
Site A	FOS	100	65	34
Site A	FOS	100	55	49
Site A	FOS	100	80	14
Site A	FOS	100	65	19
Site A	FOS	100	85	89
Site A	FOS	100	70	239
Site A	FOS	100	60	219
Site A	FOS	100	65	59
Site A	FOS	100	70	59
Site A	FOS	100	50	49
Site B	TCB	120	80	29
Site B	TCB	120	60	34
Site A	TCB	120	80	39
Site A	FOS	100	70	120
Site A	FOS	100	45	320
Site A	FOS	100	60	135
Site A	FOS	100	80	265

4.4 Core Logging

As part of the geotechnical characterisation, the Geotechnical Department at PMC has created and maintains a database containing geotechnical information from site investigations, specifically geotechnical boreholes. Representative cores of the main geotechnical units at the crusher chamber site location were identified based on geotechnical logging of cores from geotechnical holes HD020, HD031 and HD051. All the holes were drilled using 46 mm (NX) double tube core barrels. These holes were drilled sub horizontally from the excavation walls to provide cover for excavations within and around the Lift 2 crusher chamber site. A summary of the drill hole information is shown in Table 4-2. The major structure log is shown in Table 4-3. Depth below surface is given in relation to a reference surface elevation for PMC of 374 m above mean sea level.

Table 4-2: Drill hole information (Palabora, 2017).

Hole ID	From (m)	To (m)	Orientation	Collar X (m)	Collar Y (m)	Collar Z (m)
HD020	0.00	303.34	sub horizontal	23860	-13300	-1239.43
HD039	0.00	270.90	sub horizontal	23850	-13900	-1239.43
HD051	0.00	300.02	sub horizontal	23800	-12950	-1239.43

Table 4-3: Summary of major structure log (Palabora, 2017).

Hole ID	From (m)	To (m)	Structure	Comments
HD20	0.00	15.13	None	The rock mass is weakened by alteration or strong fracturing.
	141.00	142.00	None	Fractured zone
	169.38	169.98	Dolerite stringer	Fractured zone
	208.63	260.75	Dolerite dyke zone	
HD039	0.00	13.59	None	Discing and fractured zone present. Highly weathered FOS, Crushed zone
	21.70	27.90		
	35.8.03	36.65		
	65.03	129.40	dolerite dyke intersected	Highly jointed zone
	96.90	100.00	dolerite dyke intersected	Highly jointed zone
	186.2 0	227.40	dolerite dyke intersected	Poor ground conditions are expected at the contact between Foskorite and the Dolerite dyke
HD051	0.00	5.60	None	Fractured zone
	260.66	268.55	None	Fractured zone

HD020

Drill hole HD020 was drilled from North Outer Cubby and the total drilled depth was 303.34 m. The hole intersected Foskorite (FOS), Bended Carbonatite (BCB), Micaceous Foskorite (MFOS), DOL (Dolerite), MPY (Micaceous Pyroxenite) and Transgressive Carbonatite (TCB). The core from HD020 was competent but highly jointed within the dolerite zones. Two major dykes were intersected from 70 m to 141 m and 208.63 m to 260.75 m, whereas a minor dyke was intersected from 169.38 m to 169.98 m. Discing zones were observed from 3 m to 9.25 m. Evidence of fracturing was also observed in the discing zone. The discing zone indicates area of higher stress to rock strength ratio and can result in slabbing. Photographs of the core illustrating dolerite, discing, weathered and fractured zone are shown in Figure 4-8 to Figure 4-11. The geological summary and major structure log of HD020 are Table A-3 and Table A-4 (see APPENDIX).

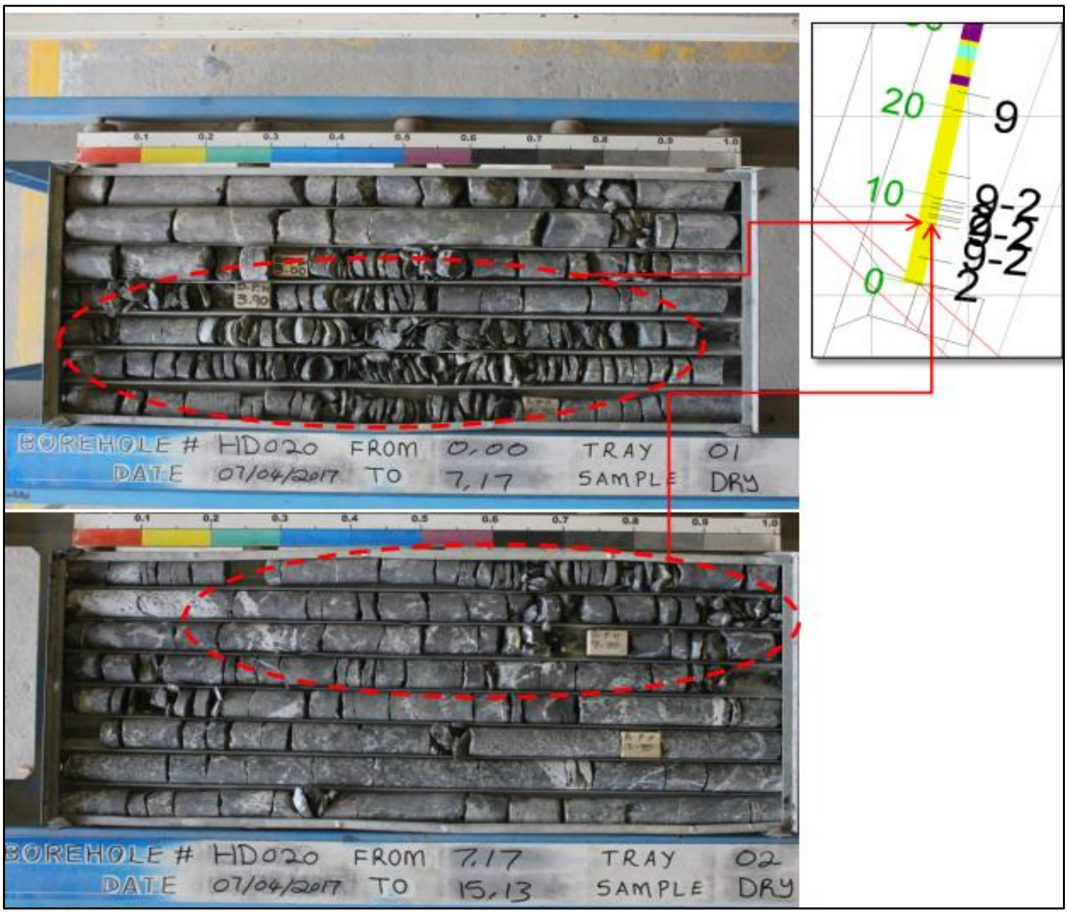

Figure 4-8: Illustrates drill hole HD020 discing and fractured zone (Palabora, 2017).

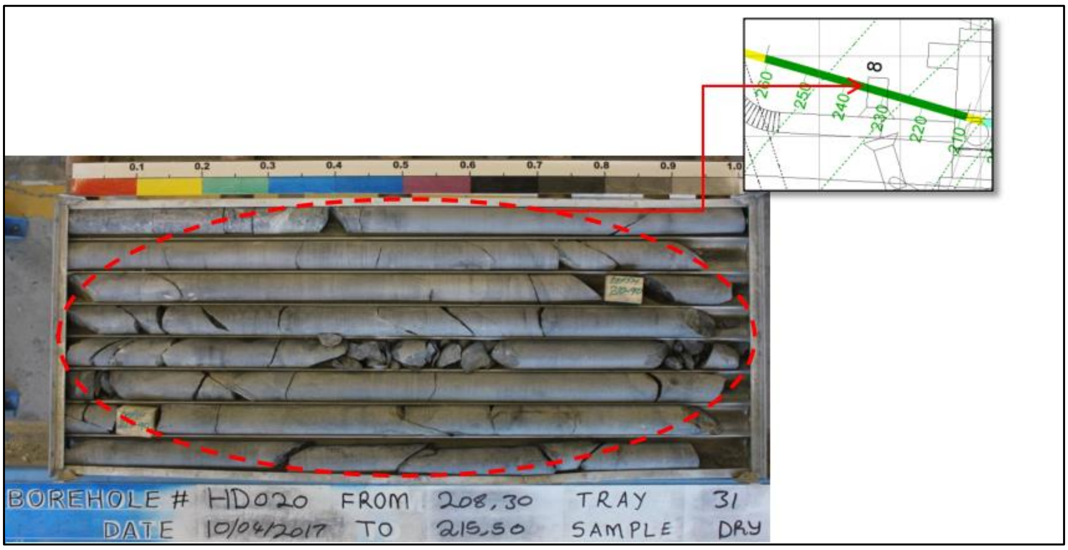

Figure 4-9: Illustrates a jointed dolerite zone (Palabora, 2017).

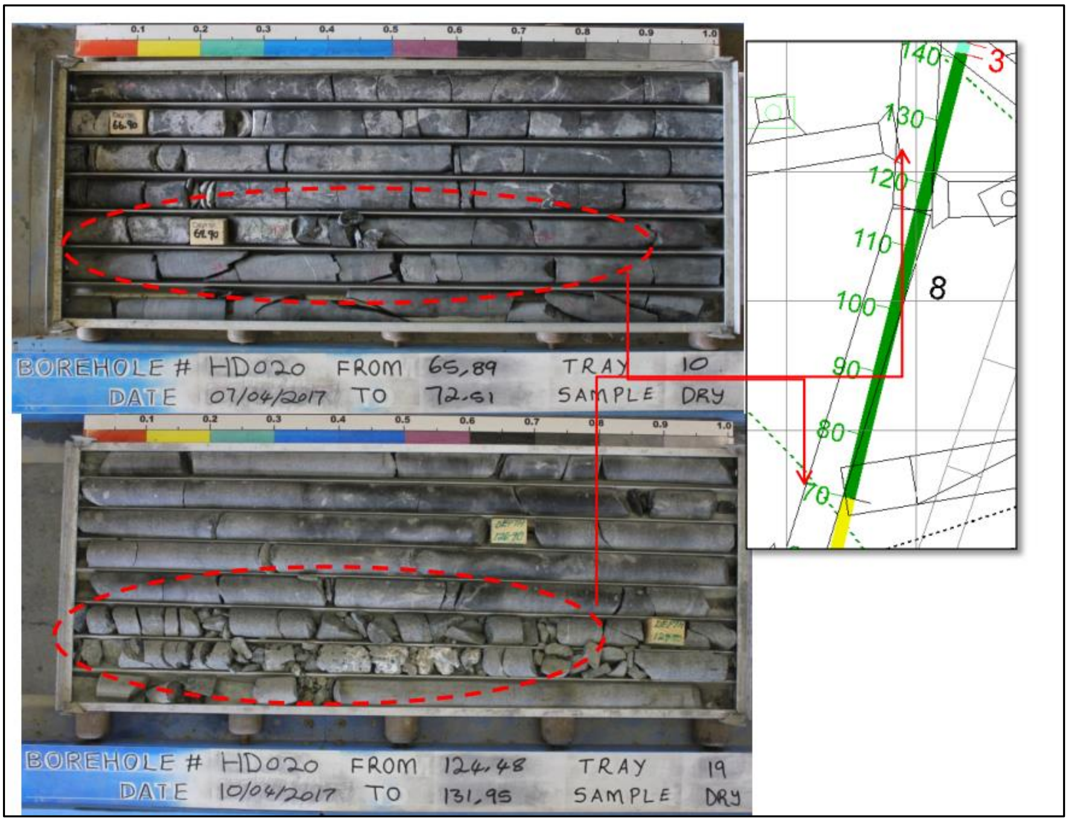

Figure 4-10: Illustrates HD020 highly jointed dolerite zone (Palabora, 2017).

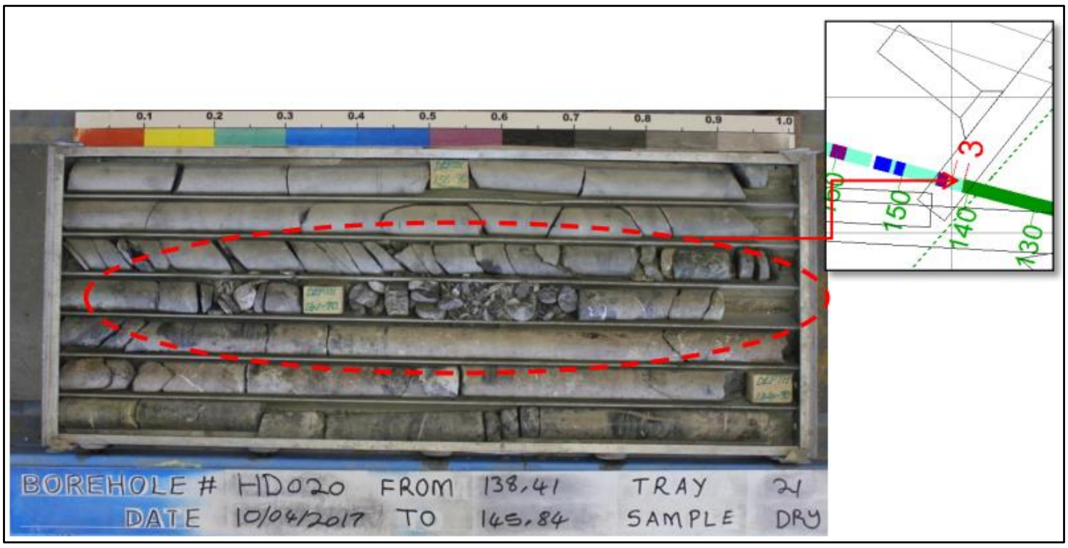

Figure 4-11: Illustrates HD020 crushed zone of MFOS (Palabora, 2017).

HD039

Drill hole HD039 was drilled from North Outer Cubby, drilled to a depth of 270.9 m. The hole intersected FOS, BCB, MFOS, DOL, MPY and TCB. The core from HD039 is competent and fractured in certain sections. The dolerite dykes exhibited both competent and jointed zones. Two major dykes were intersected from 65.03 m to 129.4 m and 186.2 m to 227.4 m. Photographs of the core illustrating discing, highly weathered and fractured zone are shown from Figure 4-12 to Figure 4-14. The geological summary and major structure log of HD039 are shown in Table A-5 and Table A-6 (see APPENDIX).

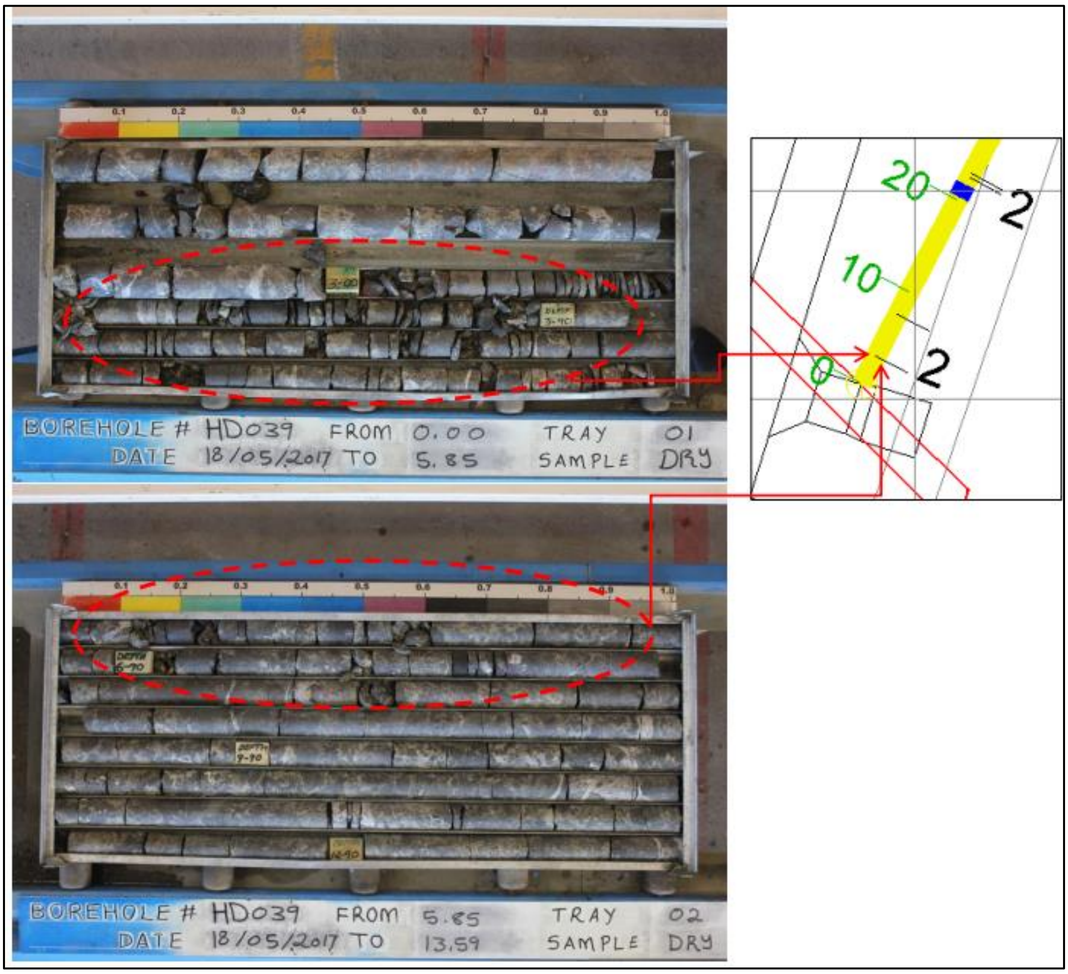

Figure 4-12: Illustrates HD039 discing and fractured zone (Palabora, 2017).

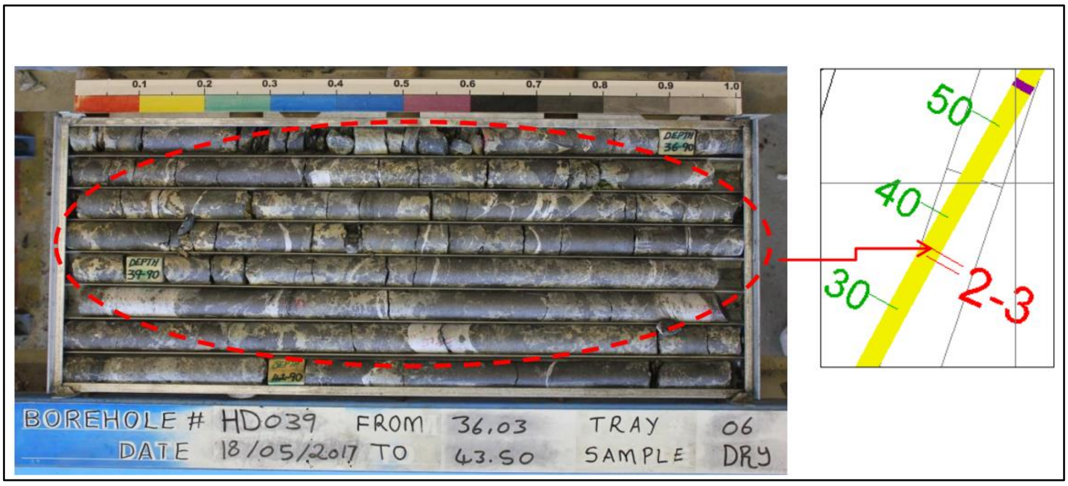

Figure 4-13: Illustrates HD039 a highly weathered FOS (Palabora, 2017).

Figure 4-14: Illustrates HD039 dolerite dyke intersected (Palabora, 2017).

HD051

Drill hole HD051 was drilled from North Outer SP1, to a depth of 300.02m. The hole intersected BCB, TCB, FOS, DOL and MFOS. The core from HD051 was competent, with fractured zones encountered between 3.64-6.78 m, 69.8-71.2 m, 134.08-138.62 m and 264.66-265.41m. Photographs of the core illustrating discing and fractured zone are shown from Figure 4-15 to Figure 4-16. The geological summary and major structure log of HD051 are shown in Table A-8 and Table A-7 (see APPENDIX).

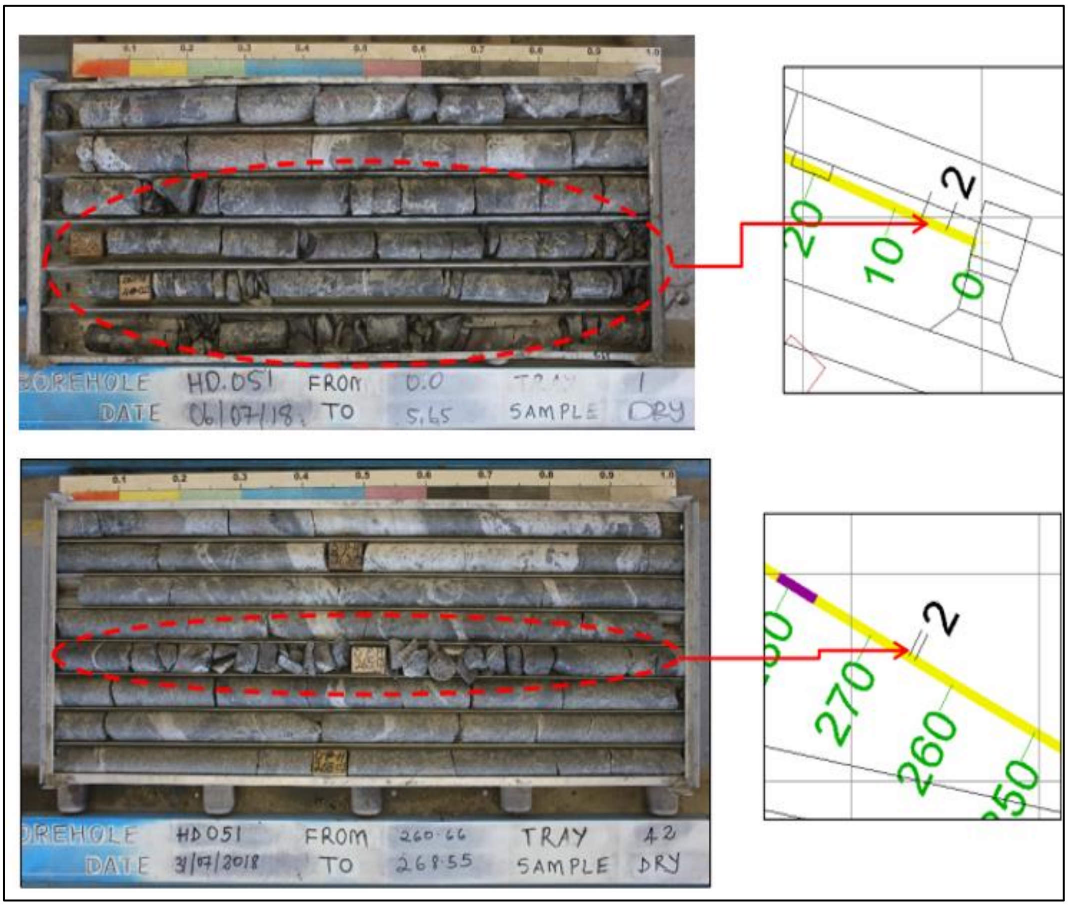

Figure 4-15: Illustrates drill hole HD051 fractured zone (Palabora, 2017).

Figure 4-16: Illustration of HD051 discing and fracture zones (Palabora, 2017).

4.5 In-situ stress

4.5.1 Lift 1

A significant variation in the principal stress magnitudes and orientations was observed in previous studies of the PMC stress regime for Lift 1. Two campaigns of stress measurement were carried out during the exploration for the underground orebody. An additional campaign was carried out, using hollow inclusion cells, from the lateral development on the production level outside the orebody. These measurements have indicated that the vertical stress is approximately equal to the overburden pressure measured from the original free surface (i.e., pre-open pit mining) assuming a rock specific weight of 3.1 t/m^3. The maximum horizontal stress ratio was indicated to be of the order of 1.2 x the vertical stress acting approximately horizontally in a Northwest/Southeast direction. A numerical sensitivity analysis of the PMC North Wall failure showed the horizontal to vertical stress ratio to be 2:1 in Lift 1 (Sainsbury, 2008). The final Lift 1 study accepted that the in-situ state of stress at the Lift 1 elevation was hydrostatic and approximately equal to the overburden load of 38 MPa (Palabora, 2015).

4.5.2 Lift 2

Observations of stress-induced damage throughout Lift 1 infrastructure and initial Lift 2 development led to the recalibration of model input parameters during the early development of Lift 2 infrastructure; for Lift 2, a revised in-situ stress regime with 1.2:1 horizontal to vertical stress ratio was adopted (Sainsbury *et al.,* 2016). The in-situ stress results at Lift 2 were revised based on stress measurements done using overcoring techniques in 2017 by Groundwork Consulting (Handley & Piper, 2017) and the results are shown in Table 4-4. The stress conditions will vary as the cave develops.

Table 4-4: Lift 2 in-situ stress data (Handley & Piper, 2017)

Line Item	Description	Orientation (°)	Magnitude (MPa)
$\sigma 1$	pgh	90	48.66
$\sigma 2$	0.93 $\sigma 1$	48	45.25
$\sigma 3$	0.39 $\sigma 1$	138	18.98

4.5.3 Stress damage assessment

Discing in core indicates that the stress levels in the planned crusher chambers are high and therefore rock failure around the excavation can be expected. Literature shows that when a type of rock that is brittle such as dolerite dyke is subjected to stress levels that range from 0.3 to 0.4 times its uniaxial compressive strength (UCS), it is highly likely that the rock will fracture, (Kaiser, et al., 1995); (Martin *et al.,* 1998). It is worth noting that the UCS of different types of rocks at PMC varies, with Micaceous Pyroxenite having a UCS of 80 MPa and Dolerite having a UCS of 320 MPa. As stated by Kaiser *et al.* (1995), when the stress ratio σmax/UCS exceeds 0.4, significant damage is expected to occur. Based on stress measurements obtained from the Lift 2 excavations, it has been determined that the major principal stress level is 49 MPa. This level falls within the range that suggests significant fracturing is likely to occur (Kaiser, et al., 1995); (Barton & Grimstad, 2014). Table 4-5 illustrates the stress damage assessment as described by Martin *et al. (*1998).

Table 4-5: Definition for stress damage assessment (Martin *et al.,* 1998)

σ_{max} /UCS	Description	Comment
<0.3	No fracturing	
0.3-0.35	Onset of fracturing	
0.35-0.4	Localized slabbing	
0.4-0.5	Widespread slabbing but not deep	Development stage
0.5-0.75	Walls broken into the blocks	Development stage
>0.75	Spalling starts to occur/ rock-burst in brittle rock	During undercutting and caving

4.5.4 Depth of fracturing assessment

A rule of thumb is that rock mass deterioration at PMC starts at 33 MPa which is one third of the UCS of the rock (Palabora, 2015). Severe rock mass fracturing occurs when the stress levels exceed half the UCS and this has been supported by the general observations and numerical simulation conducted in the past. The extent of fracturing needs to be determined for support design as cited by Kaiser *et al.* (1995). Figure 4-17 and Figure 4-18 show that the fractured zone extends up to 3.6 m into the rock mass. These boreholes were drilled into the side wall of the 4.5 m x 4.5 m excavation. The hole diameter and length were 41 mm and 9 m respectively.

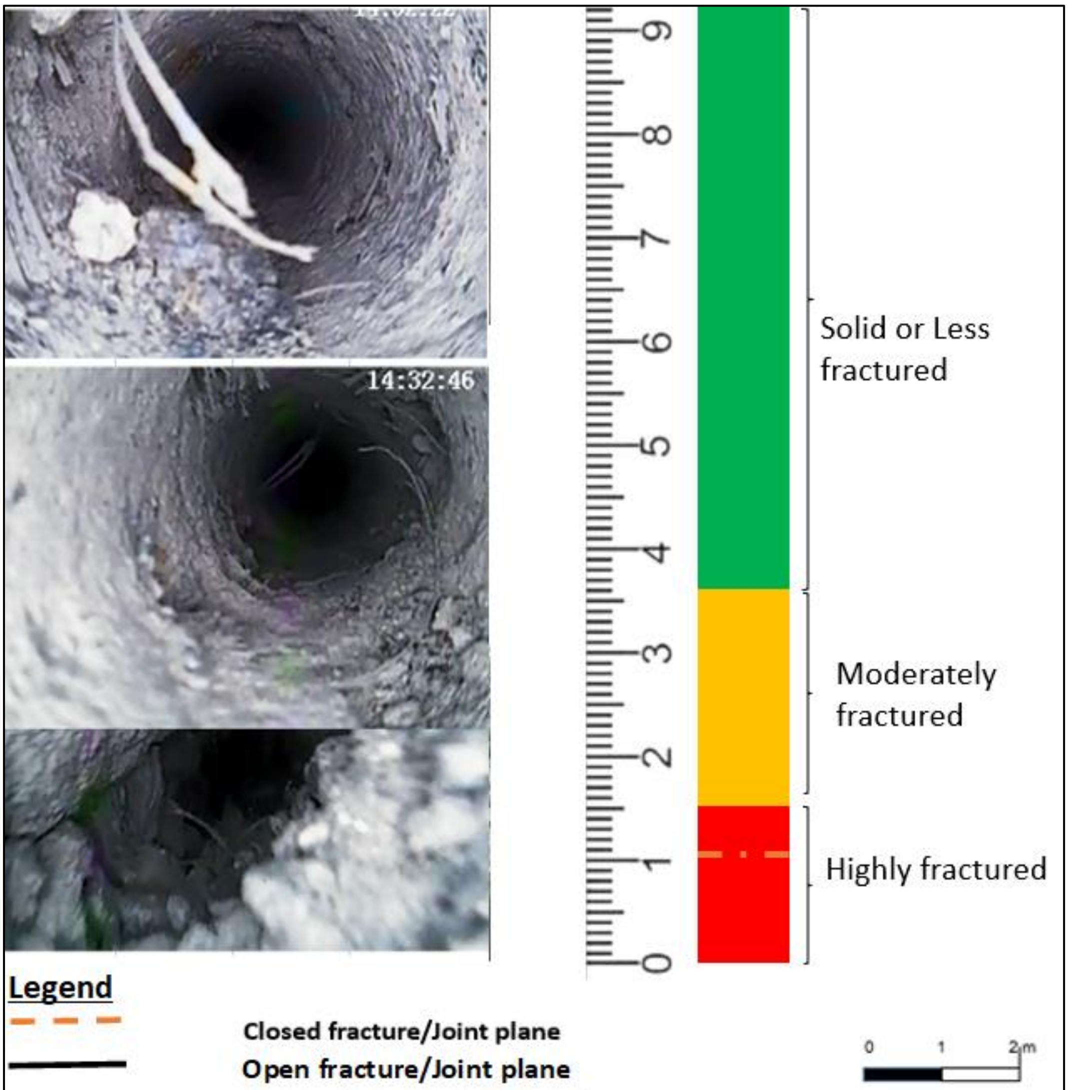

Working Place: Around Crusher 5	Borehole ID: A1				
Logger: Nyeleti Masole	Face Borehole			Pillar	X
Drilling Completion Date	10/05/2022	Date Logged: 10/05/2022			

Figure 4-17: Illustrates borehole camera assessment at Site A (Masole, 2022).

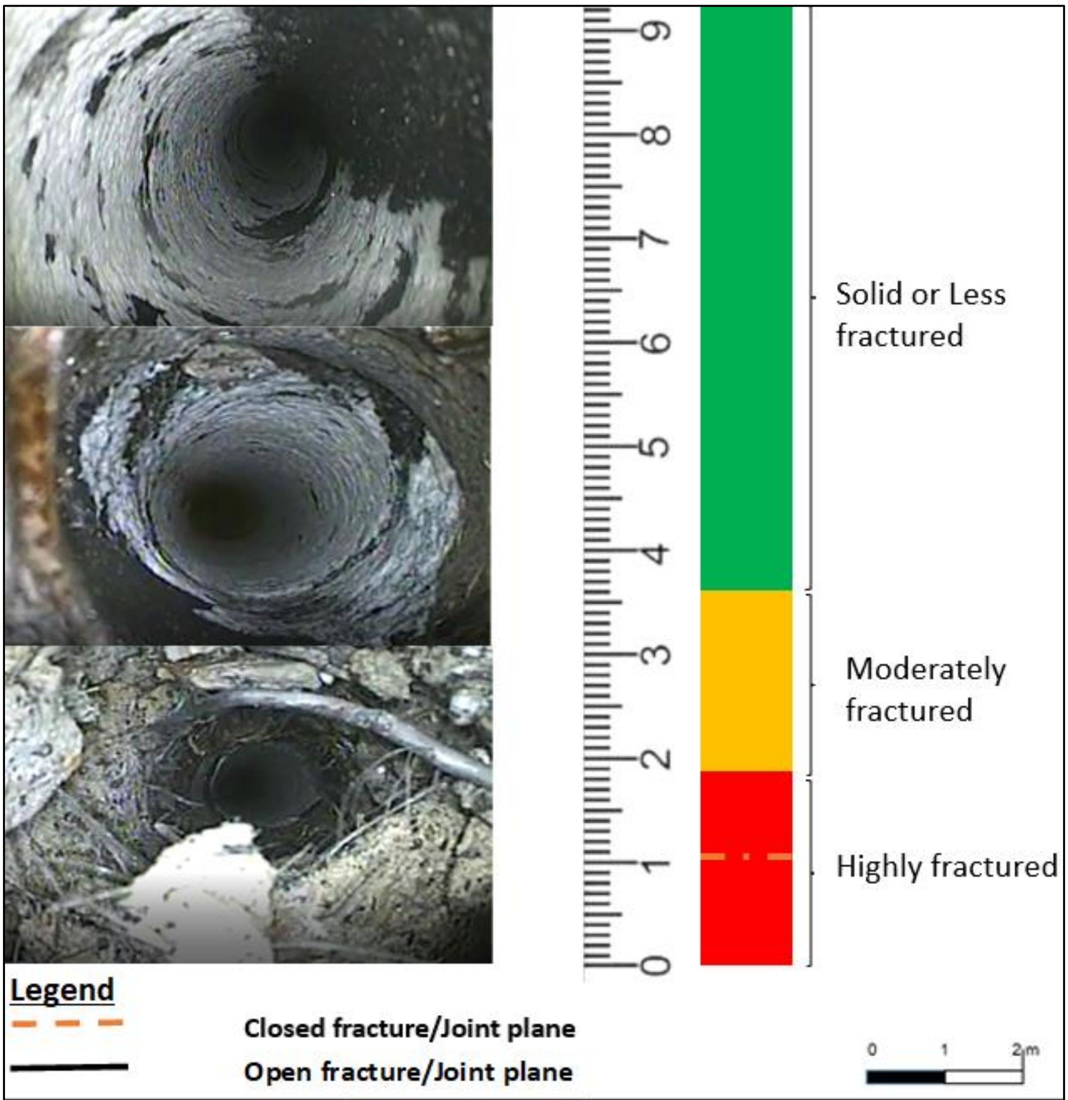

Working Place: Around Crusher 6	Borehole ID: A2				
Logger: Nyeleti Masole	Face Borehole			Pillar	X
Drilling Completion Date	10/05/2022	Date Logged: 10/05/2022			

Figure 4-18: Illustrates borehole camera assessment at Site B (Masole, 2022).

5 SUPPORT DESIGN FOR LIFT 2 CRUSHER CHAMBERS

5.1 Introduction

This chapter examines the design of the Lift 2 crusher chambers' support system by utilising a combination of analytical, numerical, and empirical design methods. The analytical analysis is conducted using Unwedge, which helped identify potential wedges and their failure mechanisms. Based on the identified failure mechanisms, the necessary support units were designed. Empirical analysis, on the other hand, was employed to determine the required length and spacing of the support units. RS2 was used to simulate the level of stress and deformation imposed on the crusher chambers and to confirm the analytical and empirical findings.

5.2 Kinematic analysis

The purpose of kinematic analysis was to identify the mechanism of block failure and based on the structural data gathered from crusher chamber vicinity, an Unwedge analysis was completed. The program allows the user to input an excavation shape and orientation, major joint set orientations, various reinforcement bolt systems and shotcrete liner.

5.2.1 Modelling procedures

Joint set orientation and excavation geometry are inputs for wedge failure assessment. The procedure involved defining the geometry of the excavation and specifying its trend and plunge. The geometry of the crusher chamber was constructed with a trend and plunge of 0°/0°. The rock was assumed to have a density of 3.1 t/m^3 (Palabora, 2015). Water was not accounted for in the analysis. The joints were conservatively assumed to have zero cohesion, tensile strength of zero and a friction angle of 35° for a fair rock mass (Bieniawski, 1989). These joints were assessed and flagged if they created wedges with FoS of less than 1.5. Results were output as FoS, apex height, mode of failure, volume and wedge weight. The main joint set orientation and mean true joint spacings for the dominant rock type surrounding the Lift 2 Crusher Chambers is shown in Table 5-1.

Table 5-1: Summary of prominent joint sets analysis

Joint set	Dip	Dip direction	Spacing (m)
1	84°	167°	0.41
2	80°	84°	0.65
3	26°	264°	0.28

5.2.2 Unwedge results and interpretation

In the Unwedge analysis program on joint sets for the crusher chamber walls, a potentially unstable block was predicted, having an apex height of 3.8m and that failure mechanisms involving sliding, crushing and squeezing should be expected. The intersection of the three joint planes, as determined through Unwedge analysis, is expected to cause possible wedge failure at the hanging wall. It can be noted that the sidewall has a high probability of failure when compared to the hanging wall and this is associated with the excavation height.

The apex height for the roof wedge is 3.92 m. Figure 5-1 shows the great circle simulating the three major joint sets. The simulated wedges shown in Figure 5-2 are not the only wedges that are simulated to occur when developing the Lift 2 crusher chambers. It is the author’s view that throughout the length of the crusher chambers, similar wedges will be exposed.

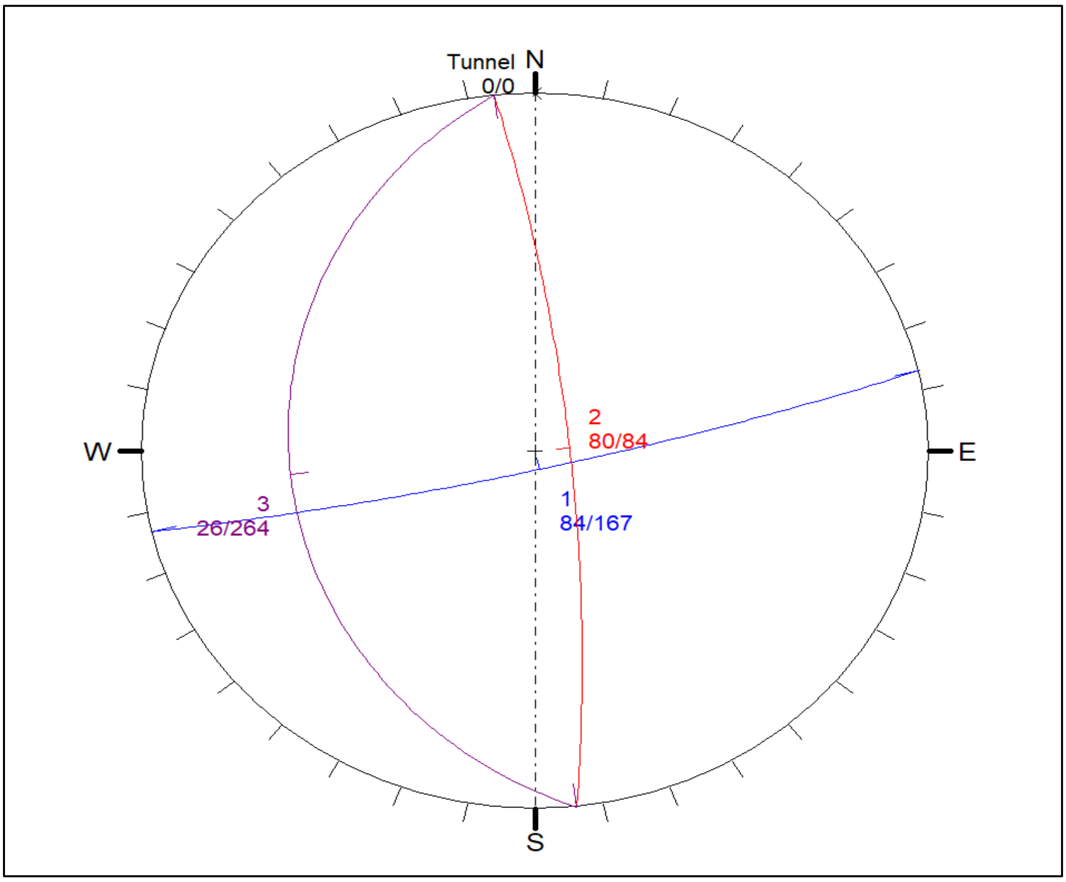

Figure 5-1: Great circle representing the three joint sets

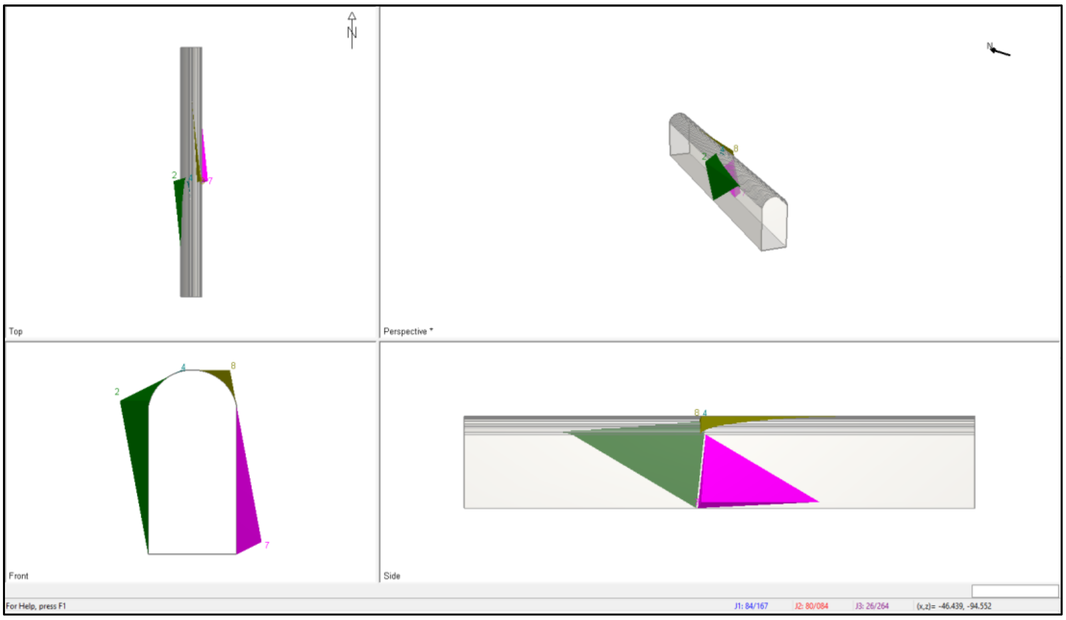

Figure 5-2: Simulated wedges in the rock mass surrounding the Lift 2 crusher chambers

5.3 Numerical modelling analysis

As part of the stability assessment, the crusher chamber was modelled using the geotechnical finite element method (FEM) code RS2 by RocScience (2021b). RS2 is a 2D finite element software package designed to analyse geotechnical structures in civil and mining applications. It can simulate the behaviour of the structure in response to various loading conditions, allowing the user to identify potential failure modes and take corrective measures. It can also model detailed designs for tunnels and supports, as well as evaluate slope and excavation stability. In addition, it can model groundwater seepage, consolidation and other essential parameters related to the structure (Rocscience, 2021b).

For this study, numerical analysis was conducted with the aim of correlating empirical and analytical results as well as estimating the depth of failure, bolt length and thickness of shotcrete based on the results of empirical and analytical analyses. Both elastic and plastic analyses were done using the Mohr-Coulomb failure criteria to estimate the depth of failure and determine under what stress conditions failure will occur. Table 5-2 shows the system's strengths and limitations.

Table 5-2: Strength and limitations of RS2 (Rocscience, 2021b)

Numerical Modelling code	**Advantages**	**Disadvantages**
2D Finite Element Method	Easy to use and enable nonlinear systems, with yield and large strain to be solved efficiently	It is a 2D program

5.3.1 Input Parameters

The Mohr-Coulomb constitutive model was chosen for this analysis as aforementioned and the advantage of this failure criterion is that it considers the increase in rock strength due to the presence of confining stresses. The onset of fracturing was assumed to be 3 mm/m based on laboratory testing (Chen, 2009). Rock mass properties and in situ stress are in puts into the numerical modelling.

Rock Mass Properties

An estimate of the intact rock strength parameters is required as input for numerical modelling and rock mass classification. The rock properties used for the design and analyses of the crusher chambers were based on rock mass classification and rock property data obtained from fieldwork and laboratory testing. The data was also obtained through back analysis of the North Wall failure done by Itasca. The Mohr-Coulomb criterion was used to define the peak strength of the rock mass based on least-square fit to the Hoek-Brown envelope from estimates of GSI, σ_{ci} and m_i. A summary of the peak rock properties of the dominant rock units is shown in Table 5-3 (Palabora, 2015).

Table 5-3. **Rock material properties applied in the model (Palabora, 2015).**

Domain	**Density Kg/m^3**	**UCS (MPa)**	**GSI**	**C (MPa)**	**Friction angle (°)**	**E (GPa)**	**σ_t (MPa)**	**v**
BCB	2865	114	73	3.2	35	40.1	0.8	0.21
TCB	2887	110	73	3.2	35	39.4	0.8	0.21
MPY	3037	78	76	3.2	35	39.5	1.2	0.21
DOL	3055	277	73	3.2	35	62.4	1.6	0.21
FOS	3530	93	74	3.2	35	38.4	0.8	0.21

5.3.2 Model geometry and sequence

A two-dimensional cross-section of the crusher chamber was created in the RS2 software and the chamber area was constructed, followed by model boundaries. The in-situ stresses were applied and gravitational acceleration was assumed to be 9.81m/s^2. Figure 5-3 illustrates the model outline.

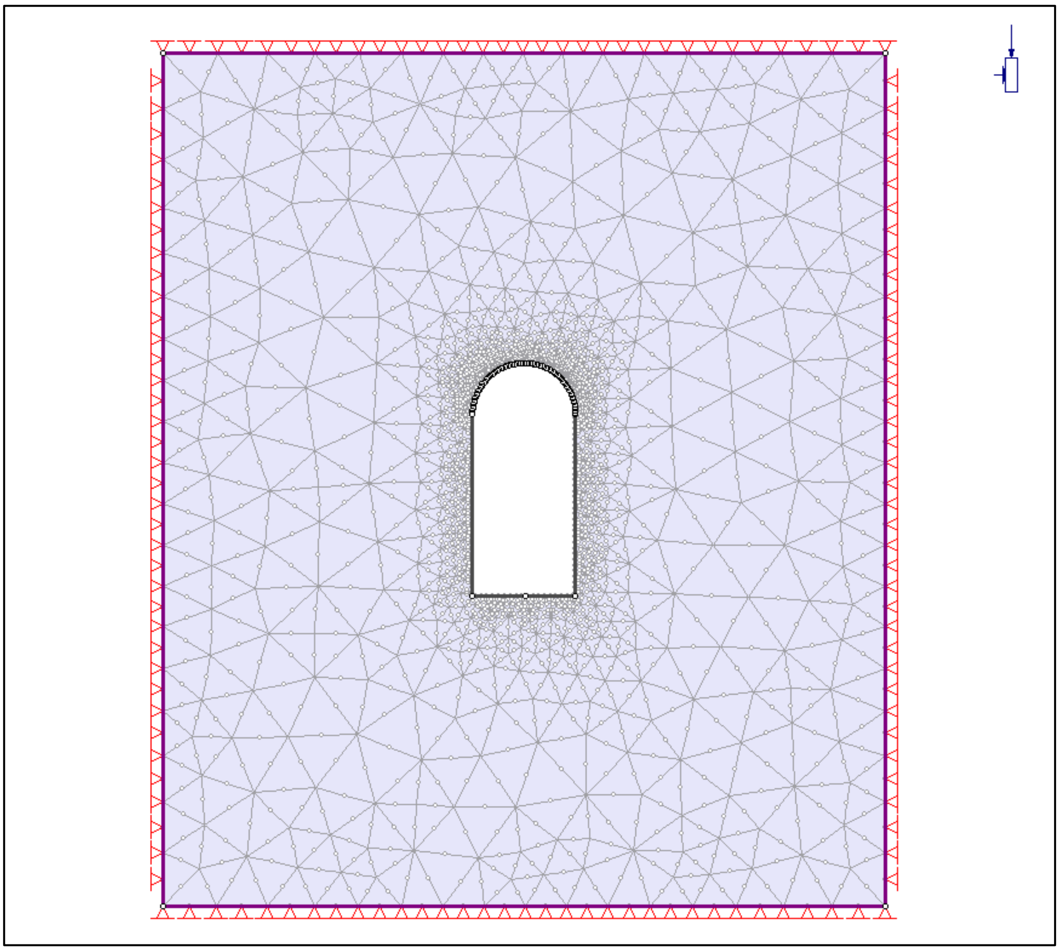

Figure 5-3: RS2 Model Outline

5.3.3 Boundary conditions and model initialisation

The boundary should be applied to the model such that they are far enough away from the core of the model, so they do not influence the results significantly. In RS2 it is automatically created which is approximately 3 times the diameter of the excavation, however the requirement is that the boundary should be 5 to 10 times the diameter of the excavation. Initial conditions define the in-situ state of stress. Initialising stress in all the zones in the model is achieved by assigning vertical stress and horizontal stress magnitude in Table 4-4. Elastic properties dictate the type of response the model will display upon excavation or disturbance, these were also assigned to all zones in model and the model was initialised.

5.3.4 Results of Numerical Analysis

When the model is computed, the resultant Factor of Safety (FoS) is indicated by strength factor as stated by Ledesma *et al.* (2016). The strength ratio for the crusher chamber walls and height lies mostly on 1.26 (Figure 5-4), indicating that from the strength factor point of view, the crusher chamber will be unstable without support.

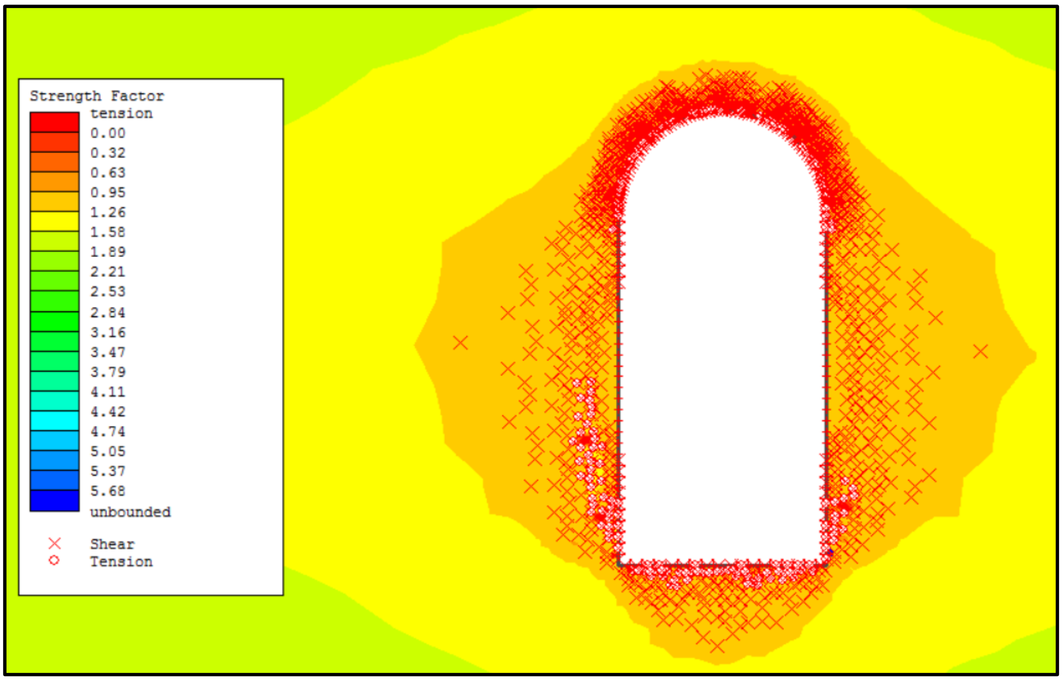

Figure 5-4: Contours of Strength Factor.

The yield limit for the hanging wall is 2.23 m and 3.3 m on the sidewalls (Figure **5-5**). This implies that the estimated cable bolt length of 6 m to 9 m will be able to anchor back the yield zone.

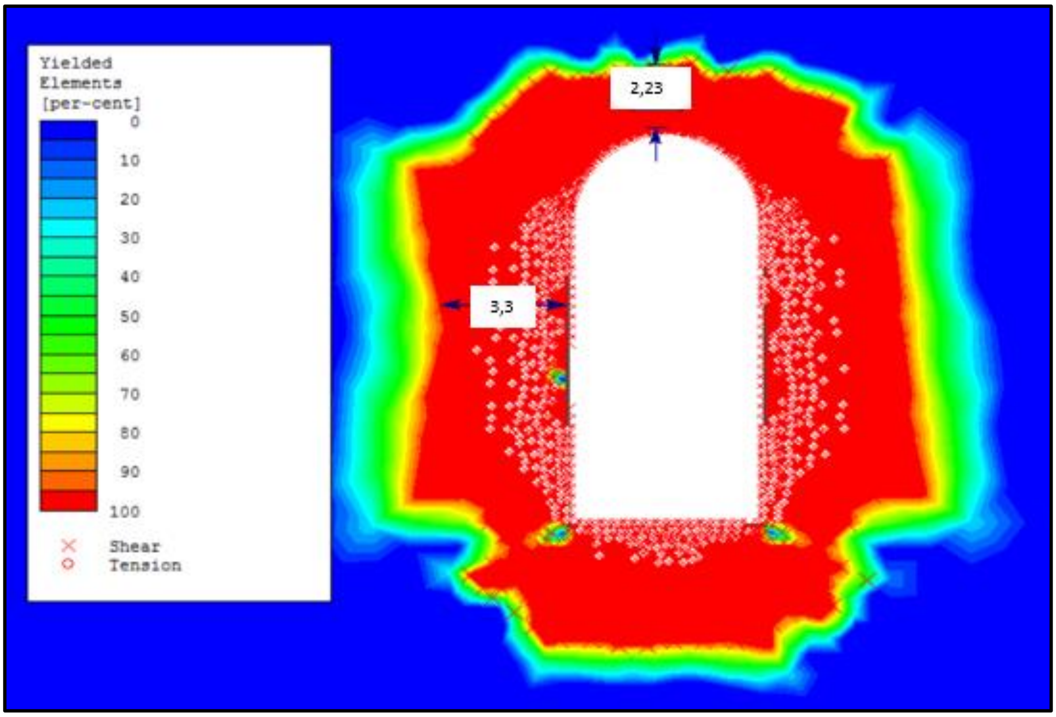

Figure 5-5. Simulated Yield Zone

The major principal stress magnitude is 39 MPa and minor principal stress magnitude is 13 MPa as shown in Figure 5-6 and Figure 5-7 respectively. Similarly, the high tensile stresses on the sidewall, confirm the loosening of the rock mass that is predicted to occur. These results are expected to vary with the rock type and also increase during Lift 2 undercutting process. The UCS of FOS is 100 MPa, therefore, the ratio of $(\frac{\sigma_1}{\sigma_c})$ is 0.39 which implies that localised slabbing will occur when developing the crusher chambers (Martin *et al.,* 1998).

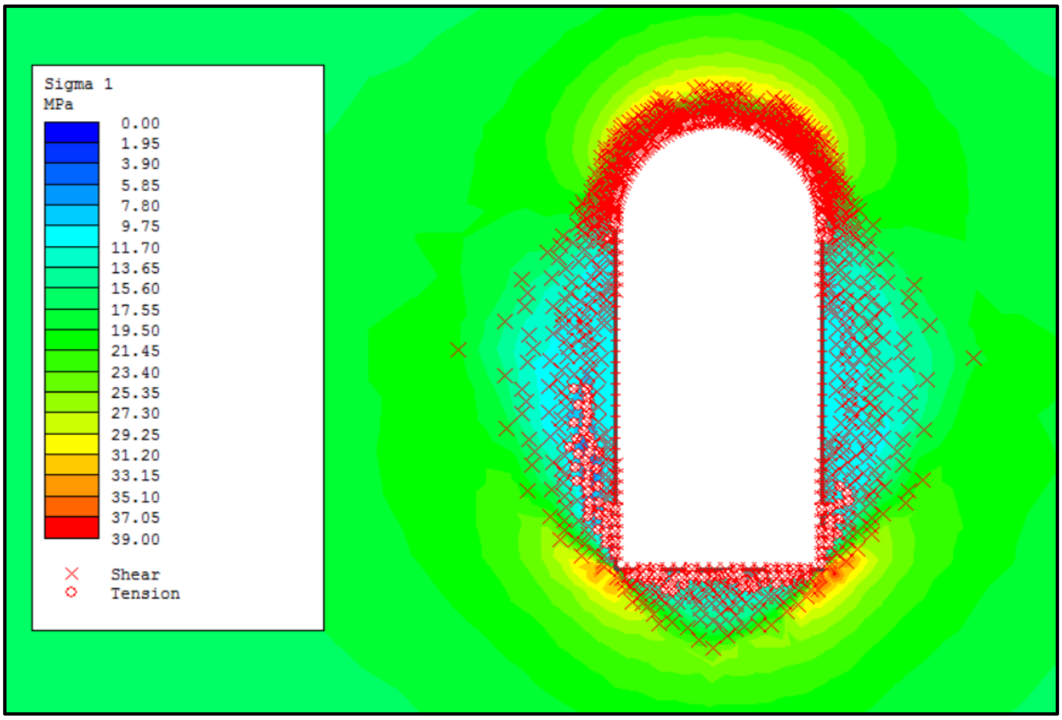

Figure 5-6. Major Principal Stress.

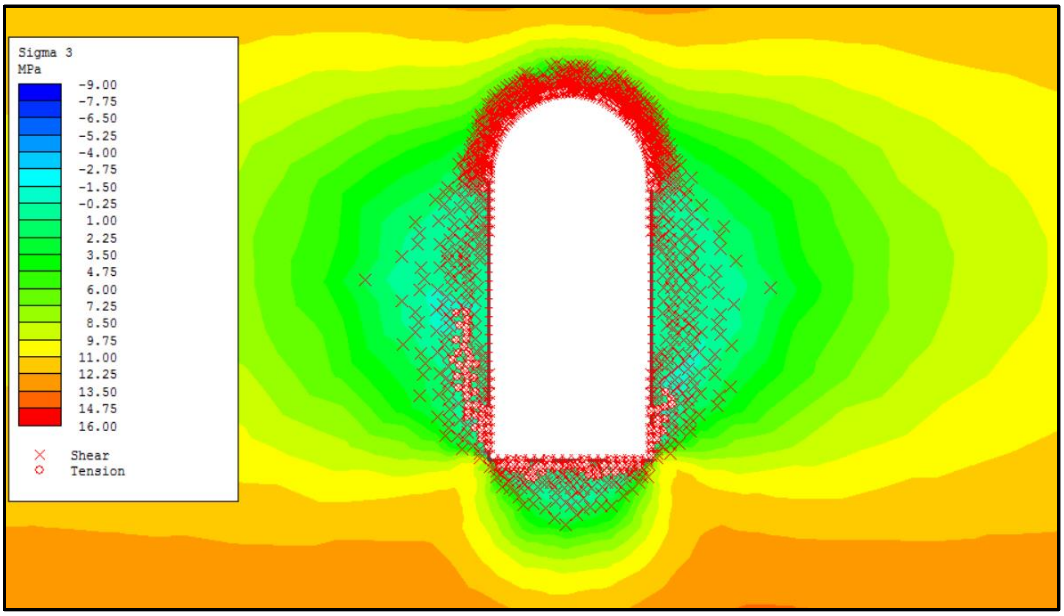

Figure 5-7: Minor Principal Stress.

The vertical dispalcement is simuated to reach 6 mm (Figure 5-8). The value is compatible with the ones obtained from a 3-pin convergence stations installed underground to monitor tunnel convergence. The convergence may increase with redistribution of stress and stress changes related to caving.

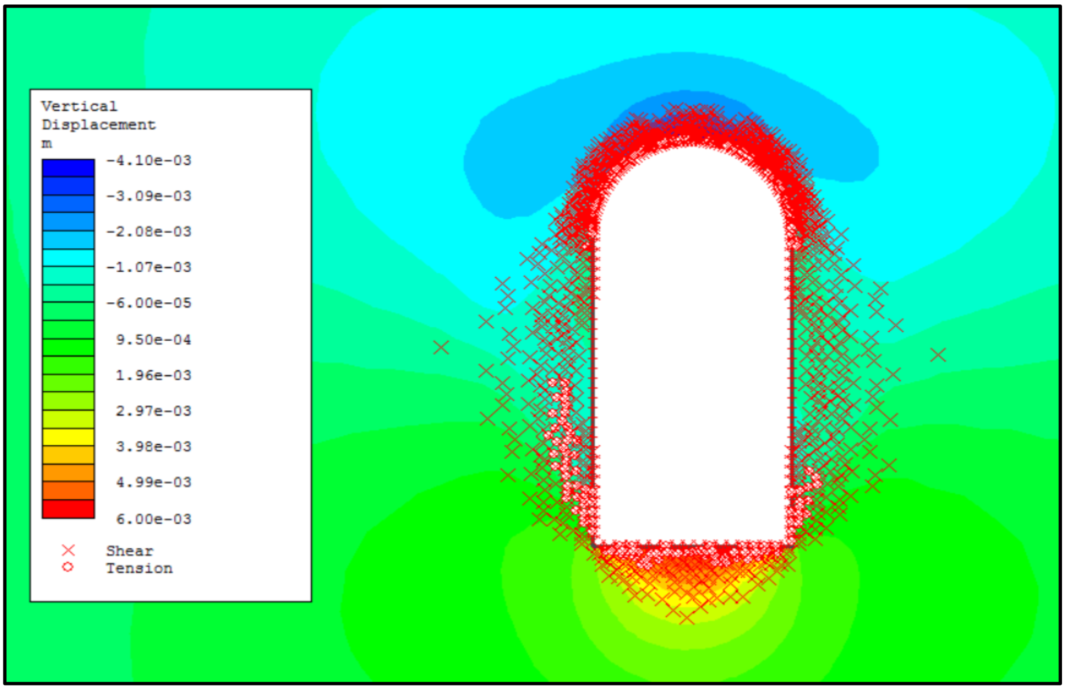

Figure 5-8: Vertical Displacement.

Figure 5-9 shows the simulated results with support. The support consisted of 9 m long cable bolts and 150 mm fibre-reinforced shotcrete. The maximum shear strain shown in Figure 5-9 (a) is below the 3 mm/m criteria to cause damage. The total displacement is simulated to be less than 2 mm Figure 5-9 (b). The major and minor principal stress are shown in Figure 5-9 (c) and Figure 5-9 (d). There is a slight decrease in the depth of yield as a result of installed support as shown in Figure 5-9 (e). From these results, no high stress feature such as dog-earing and spalling/ scaling of sidewalls or bucking of the pillar should be pronounced and this could be validated from the Lift 1 crusher chambers.

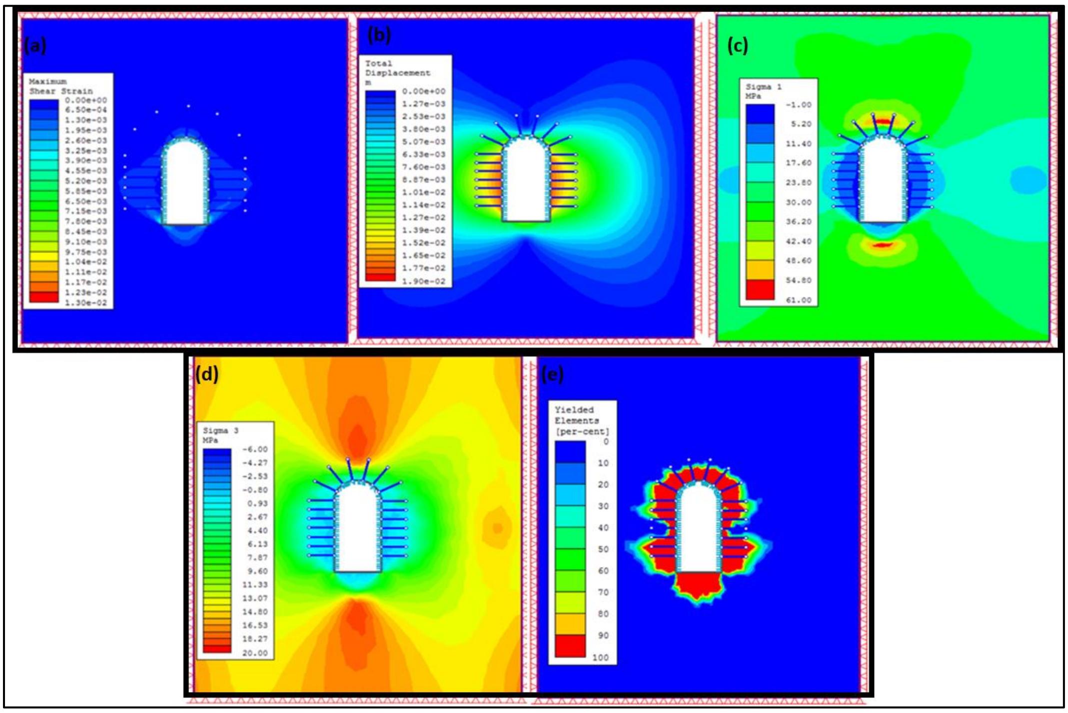

Figure 5-9: (a) Maximum shear strain, (b) Total displacement, σ_1 (c), σ_3 (d), Yield zone (e).

5.4 Rock Mass Rating and Support Selection

Rock mass rating has been conducted for the Lift 2 crusher chambers based on geotechnical mapping of blasted excavation within the Lift 2 crusher chambers and the results are shown in Table 5-4. These results catergorise the rock mass as being Fair which suggests that the crusher chambers require support to maintain a long-term stability.

Table 5-4: ***Rock Mass Rating for each rock type***

Rock type	Average Q value	Classes	Average RMR value	Classes	Average MRMR value	Class
BCB	4.4	Fair	57	Fair	49	Fair
DOL	5.2	Fair	59	Fair	50	Fair
FOS	4.2	Fair	57	Fair	46	Fair
MPY	3.5	Fair	55	Fair	44	Fair
TCB	4	Fair	56	Fair	48	Fair
Overall	4	Fair	57	Fair	47	Fair

Based on the Q-value of 4 and ESR of 0.5, support required to support a 12 m wide span plots between category number 5 and 6. This suggests that the required support is bolting plus fibre reinforced shotcrete (90-120 mm thick) with an energy absorption of 700 J as shown in Figure 5-10.

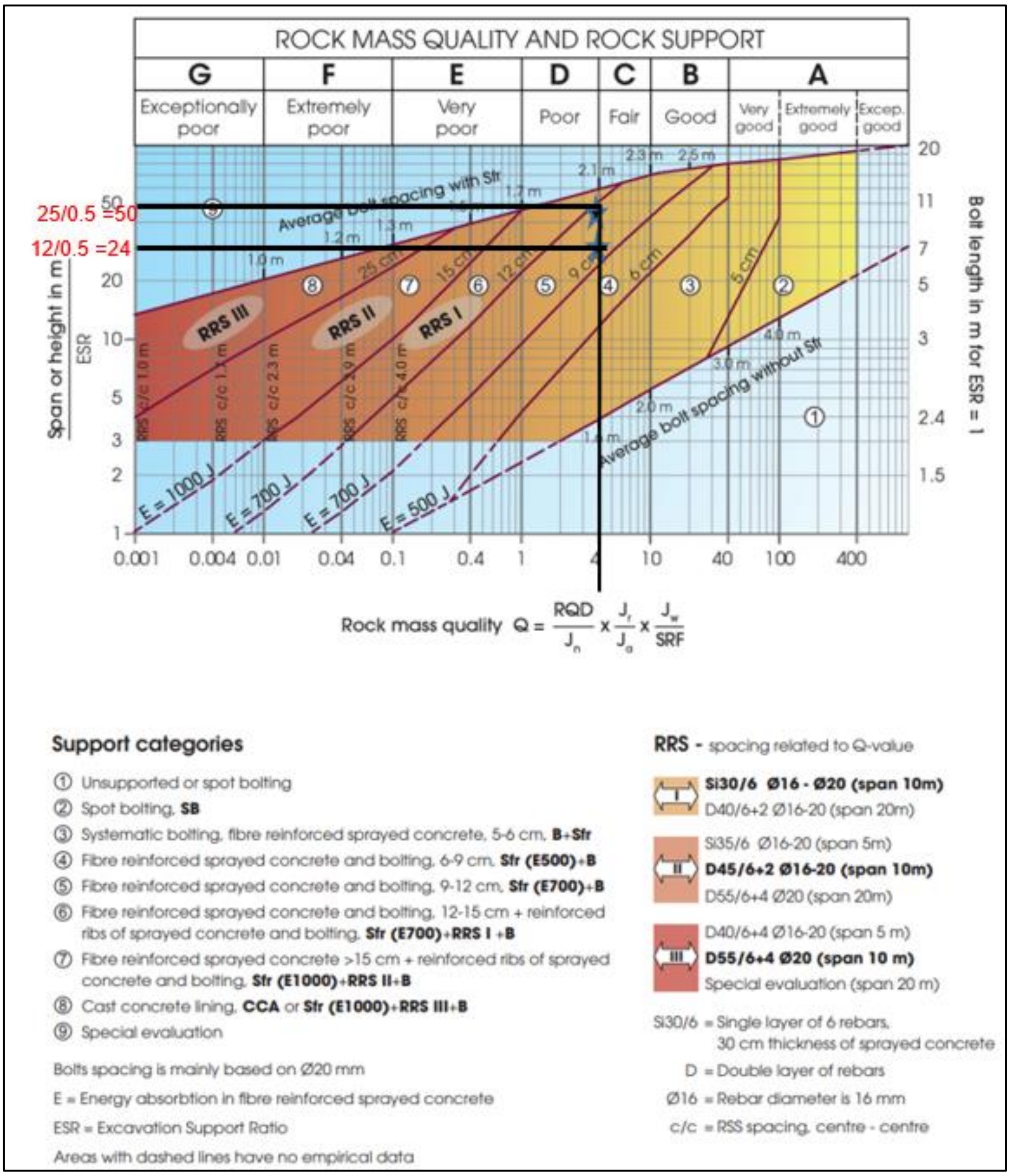

Figure 5-10: Support design chart as a function of Q (NGI, 2022).

The averaged Q value of 4 was used to assess the stability of the crusher chambers in terms of the factor of safety. The recommended safety factor according to the industry best practice for large excavation should be at least 1.5

and the chamber falls below the minimum recommended value predicting unstable ground conditions (Figure 5-11).

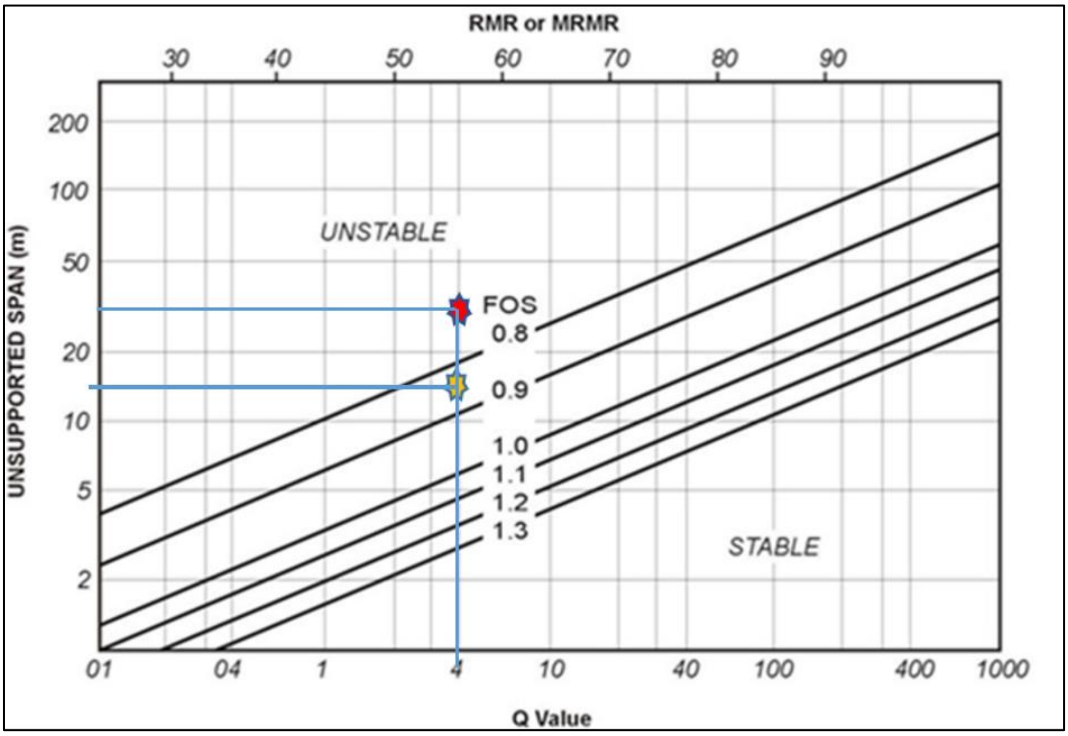

Figure 5-11: Unsupported span vs Q/RMR of the 12 and 25m span (from Stacey, 2001)

5.5 Support calculations

The crusher chamber dimensions are 12 m wide by 25 m high and 61 m long. Considering the high-class safety requirement of crusher chamber project, an ESR of 1.6 was chosen. From the calculation done, it was noted that the roof bolt length of 3 m is required on the hanging wall, with 4 m length bolts on the sidewall of the excavation. The calculation is shown below.

L *(12 m span)*	=	*2 + 0.15 x B/ESR*
	=	2 + 0.15 x 12/1.6
	=	3 m
L (25 m span)	=	2 + 0.15 x B/ESR
	=	2 + 0.15 x 25/1.6
	=	4 m

5.5.1 Cable bolt Length

Cable bolt length was calculated as follows;

L (hanging wall)	=	$0.7S^{0.7} + 2$ m
	=	$0.7 \times 12^{0.7} + 2$
	=	6 m
L (side wall)	=	$0.7S^{0.7} + 2$ m
	=	$0.7 \times 25^{0.7} + 2$
	=	9 m

5.5.2 Ground support demand/ support resistance

Wedge stability analysis showed that the wedges have the probability of failure and will require support to prevent a fall of ground. The support resistance required to prevent the rocks from falling was calculated using Equation b where; p is the density of rock (3.1 t/m^3), f is the factor of safety 1.6, h is the apex height from Unwedge analysis conducted earlier (3.9 m) and g is the gravitational acceleration 9.81 m/s^2.

SR = p g h f

Therefore:

SR = $3.1\ t/m^3 \times 9.81\ m/s^2 \times 3.92\ m \times 1.6$

= $190.73\ kN/m^2$

Assuming a bolt length with a yield load of 18 t, the required bolt spacing is calculated below. The calculated spacing is 1.0 m x 1.0 m and this gives a FoS of approximately 1.5.

(Roof bolt spacing)	=	$\sqrt{}176.58\ kN/190.73\ kN/m^2$
	=	1.0 m x 1.0 m
At 3.90 m thickness	=	$1\ m^2 \times 3.1 kg/m^3 \times 3.90\ m$
	=	12.09 t (Load to be supported)
Strength of bolt	=	18 t
FoS at 1.2 m x 1.2 m	=	18 t/12.35 t
	=	1.5

(Cable bolt spacing) = $\sqrt{372.78 \text{ kN}/190.73 \text{ kN/m}^2}$

Assumed cable anchor strength = 38 t

= 1.4 m x 1.4 m

5.5.3 Dynamic load calculation

Assumptions:

- Gravity 9.81 m/s^2
- Rock density 3100 Kg/m^3
- Ejection height 1.5 m
- Velocity 3 m/s
- Ejection distance "H" 0.2m (block that is allowed to fall, Palabora (2015)

Mass of block = base area x ejection height x density

= (1 x 1) m^2 x 1.5m x 3100 kg/m^3

= 4650 kg

Energy Absorption (hanging wall) = ($^1/_2$ x mass x velocity^2) + (mass x gravity x H)

= ($^1/_2$ x 4650 kg x (3 m/s)^2) + (4650 kg x 9.81 m/s^2 x 0.2 m)

= 20925 J/m^2 + 9123.3 J/m^2

= 30048.3 J/m^2

= 30 kJ/m^2

Required Energy Absorption (sidewall) = 0.5 mv^2

= 0.5 x 4650 kg x (3 m/s)^2

= 20925 J/m^2

= 20.9 kJ/m^2

Assuming that the roof bolt to be used is a Par 1, currently being used in the mine. The energy absorption for a Par 1 yielding bolt is 46 kJ/m^2 based on Palabora (2015) derated to fit underground conditions. FoS provided by Par 1 bolts is calculated to be 1.5 on the hanging wall and 2.2 on the sidewall. The calculated

FoS meets the acceptable criteria of 1.5 to 2 as described by Hoek (2007). FoS (hanging wall) = Energy absorption provided/Energy absorption required

= 46 kJ/m^2/30 kJ/m^2

= 1.5

Safety factor (sidewall) = 46 kJ/m^2/20.9 kJ/m^2

= 2.2

5.5.4 Calculating the number of cables required

Based on empirical tool for assessing the number of cable bolts required to support the 12 m wide span (hanging wall) is given below, assuming a FoS of 1.5 for permanent excavation:

The mass of rock contained within the parabolic arch is given of the crusher chamber by Equation 2-15:

$$Mass = Density\ x\ \frac{Minimum\ span^2}{3} (tons)$$

If the density of the material is 3.1 t/m^3 and the width of the crusher chamber is 12 m. Therefore;

mass = 3.1 (t/m^3) * 12^2/3

= 148.8 t

$$Number\ of\ Cables = \frac{Mass\ x\ FoS}{Cable\ bolt\ strength}$$

= (148.8 t x 1.5)/38 t per cable

= 6 cables per linear metre

Number of bolts required to support the wedge with a weight of 100 t, assuming an ultimate bolt strength of 250 kN/m^2 with a Fos of 1.5 is calculated as follows:

$$N_{bolt} = FoS \frac{W_g}{P_{ult}}$$

$$N_{bolt} = 1.5 \frac{100t * \frac{9.81m}{s}}{250 \frac{kN}{m^2}}$$

$$N_{bolt} = 6$$

5.5.5 Ground support for lift 2 crusher chambers

Preliminary support required to support the 12 m wide by 25 m high by 61 m long Lift 2 crusher chambers is presented in Table 5-5 and Figure 5-12. Underground geotechnical mapping will be important for the collection of structural data required to validate current structural interpretations and for analysis of the structural influences on the stability of the Lift 2 Crusher chambers. Shotcrete shall be fibre-reinforced (FRS).

Table 5-5: Selected Ground Support for Lift 2 Crusher Chambers

	Item	Pattern	Comments
Lift 2 Crusher	Length of roof bolts	3.0 m	25 mm diameter, 2.9 m inside the support hole
	Spacing of roof bolts	1.0 m x 1.0 m	
	Shotcrete	75 mm	40 MPa 700J (Efnarc), from floor to floor (First pass)
	Welded Mesh	5.6 mm x 100 mm x 100 mm	Over the shotcrete (300 mm overlap)
	Cable Length	9 m	Single bulbed strand (18 mm and 7 strand)
	Cable spacing	1.4 m x 1.4 m	
	Shotcrete	75 mm	40 MPa 700 J (Efnarc), from floor to floor Over support units (Second pass)

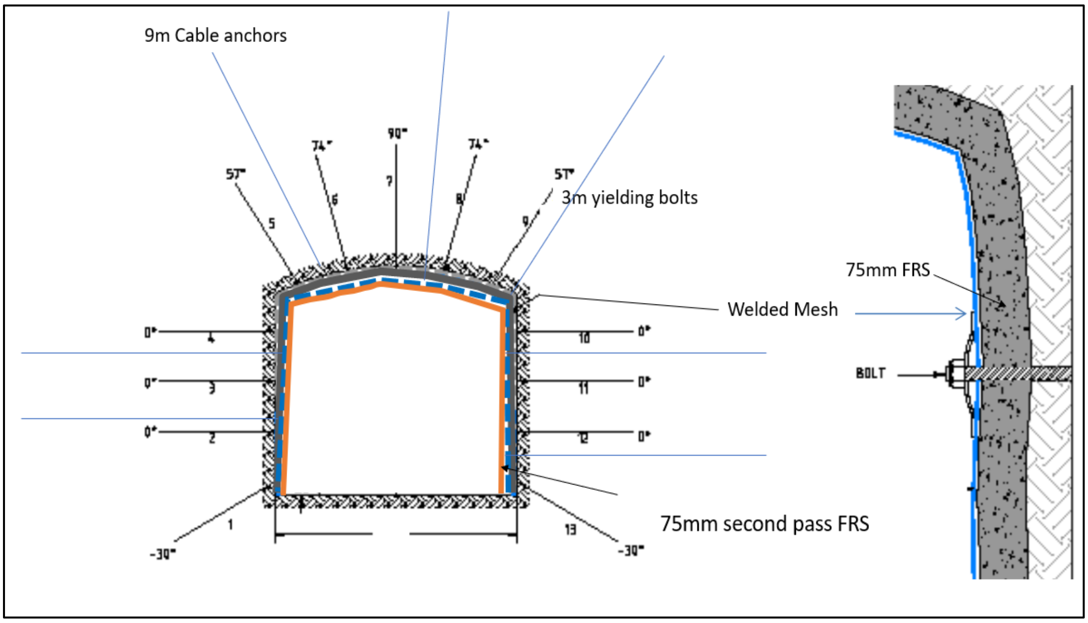

Figure 5-12: Proposed Support Standard for Lift 2 Crusher Chambers.

6 CONCLUSIONS AND RECOMMENDATIONS

This research study aimed to develop a support system for Lift 2 crusher chambers. Underground observations were conducted to collect geotechnical data and assess the performance of the Lift 1 crusher chambers. The geotechnical data collection process allowed for the prediction of rock mass behaviour, characterisation of the rock mass and identification of any differences between Lift 1 and Lift 2 in terms of rock mass characterisation, classification and ground control district. Lift 2 geotechnical zones have been defined according to rock mass properties that are primarily a function of rock type and major structures.

Field observations were conducted to assess the Lift 1 crusher chamber support performance and the observations showed that the rock types and structural data for Lift 2 do not differ significantly from those in Lift 1. However, Lift 2 displays significant fracturing and the rock mass mining through MPY tends to be highly disintegrated due to the mica content. A borehole camera was used to determine the depth of failure using a borehole camera, where 9 m boreholes were drilled into the sidewall of 5 m wide by 5 m high excavations. The site was categorised as Site A (around Crusher 5) and Site B (around Crusher 6) of the planned crusher site. Based on the borehole camera assessment, the depth of failure extends up to 3.5 m into the rock mass for both sites. The fractured zone may increase further into the rock mass due to an increase in stress levels associated with the development of the Lift 2 block cave.

Similarly, a literature review was conducted to establish the commonly used support design methods. The three distinct design methods chosen by the researcher, namely empirical, analytical and numerical analysis, are employed to design support for excavations such as the Lift 2 crusher chambers. A support system for the Lift 2 crusher chamber was determined based on empirical, analytical and numerical evaluations of the rock mass. The study showed that the creation of large crusher chambers necessitates the implementation of a combination of design approaches. Therefore, the recommended support design approach for Lift 2 is a combination of empirical, analytical and numerical design methods. Empirical techniques in conjunction with analytical and numerical modelling methods were employed to predict the stresses the crusher chambers will be subjected to and whether this level of stress will cause failure. Support systems have been developed taking account of the expected mode of failure, the excavation size and operational requirements. Rock mass classification by NGI (2022) and Bieniawski (1989) were used to classify the quality of the rock mass and support design charts by these authors are then used to specify the support requirements. The results obtained from analytical and empirical analysis were further validated using RS2 software. The geotechnical parameters of various lithological units within the planned crusher chamber site were defined using the rock mass classification systems. The dominant joint sets to be exposed when developing the Lift 2 crusher chambers were also determined. These joint sets were used in the kinematic analyses to evaluate the effect of discontinuity and the risk of wedge instability using the Unwedge software package from RocScience (RocScience, 2022). It also provided the basis for determining the maximum expected apex height of the simulated wedges for the establishment of appropriate support required to anchor beyond the unstable rock mass.

Unwedge results showed that four wedges are simulated to occur and their mode of failure is falling and sliding. The apex height is 3.9 m, slightly higher than the borehole data suggested. For the design of Lift 2 crusher chambers, preliminary numerical studies were conducted using the RS2 package. The results showed that the principal stress level is expected to reach 39 MPa, with tensile and shear damage simulated to occur on the crusher chamber excavation walls. For large excavations such as the Lift 2 crusher chambers, the highest stress concentration is expected in the corners where the stresses are tangentially orientated. Additionally, the stress levels are expected to vary with rock. The stress levels predicted by RS2 are expected to increase more than three times during the undercutting and cave propagation process, as seen with Lift 1 excavations. The yield zone or the extent of fracturing is simulated to be approximately 2.3 m on the hanging wall and 3.3 m into the sidewall. These were slightly lower than what the borehole camera assessment projected. Moreover, the numerical analysis also indicated that the estimated cable bolt length of between 6-9 m at 1.4 m spacing is adequate to support the expected yield limit. Core logging was conducted on boreholes, namely HD020, HD039 and HD051.

These boreholes were drilled at the northern side of the footprint and were drilled flat. Core logging data revealed a combination of poor, ‘Fair’ and ‘Good’ ground conditions, with highly jointed rock mass and discing on the core. Discing signifies high stress, which may induce seismicity (Cai & Kaiser, 2018). Similarly, the literature showed that using energy-absorbing rock bolts is one of the most effective support methods for burst-prone rock masses (Cai & Kaiser, 2018); (Kaiser & Cai, 2013); (Kaiser et al., 1995). For that reason, the selected ground support for the crusher chamber accounts for dynamic loading conditions (see Table 5-5). Thus, the rock mass conditions summarised in this study are only inferred based on current information derived from drilling within and around the crusher chamber sites, including the interpretation of the regional geology of the mine. Similarly, all predictions and recommended ground support must only be regarded as indicative. Additional ground support must be installed where required as per field mapping and visual inspection after each blast.

6.1 Recommendation for Future Work

Based on the knowledge of the structural geology of the area where the Lift 2 crusher chambers will be developed, it is not expected that major structures will affect the stability of the excavations. However, if there is any major structure that passes through the excavations, it is recommended to design a special support for that part of the excavation. In order to accurately simulate the mining sequence and geometry of the crusher chambers, a 3D numerical modelling approach is necessary. This will provide a deeper understanding of the failure mechanism and allow for improved confidence in the results. To achieve this, additional work is required, specifically the use of a numerical modelling package that can effectively model discontinuities, such as 3DEC. It is worth noting that such discontinuities cannot be adequately simulated using the RS2 software. Therefore, a more comprehensive approach is needed to ensure accurate and reliable results. As part of monitoring excavation performance once fully developed, multi-point borehole extensometers need to be installed around the crusher chamber, sidewalls as well as in the hanging wall. This will help to monitor both the elastic and non-elastic deformation. This is crucial to understanding the performance of various geotechnical units once an excavation is constructed in that particular domain.

REFERENCE LIST

Barton, N., 2002. Some new Q-value correlations to assist in site characterization and tunnel. *International journal of Rock Mechanics and Mining Sciences,* Volume 39, pp. 185-216.

Barton, N. & Grimstad, E., 2014. 40 years of Q-system lessons. *Tunnelling Journal,* 6(4), pp. 189-236.

Barton, N., Lien, R. & Lunde, J., 1974. Engineering Classification of Rock Masses for the Design of Tunnel Support. *Rock Mechanics,* 6(4), pp. 189-236.

Bieniawski, Z., 1976. Rock mass classification in rock engineering. *In Proceedings of the Symposium on Exploration for Rock Engineering,* 1-5 November.pp. 97-106.

Bieniawski, Z., 1992. *Design Methodology in Rock Engineering.* Rotterdam: A.A. Balkema.

Bieniawski, Z. & Lowson, A., 2013. Proceedings of the SME, Rapid Excavation and Tunnelling Conference. In: *Critical assessment of rmr based tunnel design practices: A practical engineer's.* Washington, DC, USA: Society for Mining, Metallurgy, and Exploration (SME), pp. 180-198.

Bieniawski, Z. T., 1973. Engineering Classification of Jointed Rock Masses. *South African Institute of Civil Engineers,* 15(12), pp. 335-344.

Bieniawski, Z. T., 1989. *Engineering Rock Mass Classifications: A Complete Manual for Engineers and Geologists in Mining.* New York: Wiley & Sons.

Bless, C. & Higson-Smith, C., 2000. *Fundamentals of Social Research Methods: An African Perspective.* Cape Town: Juta and Company.

Brown, E., 2012. Progress and Challenges in Some Area of Deep Mining. *Deep Mining 2012: Proceedings of the Sixth International Seminar on Deep and High Stress Mining,* 1(1), pp. 1-24.

Budavari, S., 1983. *Rock Mechanics in Mining Practice.* Johannesburg: South African Institute of Mining and Metallurgy Monograph Series M5.

Cai, M. & Kaiser, P., 2018. *Rockburst phenomenon and support characteristics,.* Sudbury, Canada: MIRARCO–Mining Innovation.

Campbell, A., Lilley, C., Waters, S. & Jones, P. A., 2013. Geotechnical Analysis and Ground Support Selection for the Ernest Henry crusher Chamber. *Ground Support 2013: Proceedings of the Seventh International Symposium on Ground Support in Mining and Underground Construction,* 1(1), pp. 437-450.

Carter, T. & Marinos, V., 2014. Use of GSI for rock engineering design. *In Proceedings of 1st international conference on applied empirical design methods in mining,* Volume 1, pp. 1-19.

Celada, B., Tardáguila, I., Varona, P., Rodríguez, A. & Bieniawski, Z.T., 2014. Innovating tunnel design by an improved experience-based RMR system. *Proceedings of the World Tunnel Congress 2014 – Tunnels for a better Life. Foz do Iguaçu, Brazil,* pp. 1-9.

Chen, J., 2009. *RockLab: Palabora Rock properties test results,* Phalaborwa: Internal Report.

Chen, S., Xiao, M. & Chen, J., 2020. *Failure Process and Stability Analysis of Rock Blocks in a Large Underground Excavation Based on a Numerical Method.* [Online] Available at: https://doi.org/10.1155/2020/4280428 [Accessed 04 01 2023].

Choquet, P. & Hadjigeorgiou, J., 1993. The design of support for underground excavations. *Comprehensive Rock Engineering: Principles, Practice & Projects,* Volume 4, p. 313–348.

Christensen, L., 1985. *Experimental Methodology.* 3 ed. Boston: Allyn and Bacon.

De la Vergn, J., 2014. *Hard Rock Miner’s Handbook.* 5 ed. Canada: Stantec Consulting.

De Vos, A., 2002. *Research at grass roots.* 4 ed. Pretoria: Van Schaik.

Deere, 1964. Technical description of rock cores. *Rock Mechanics Engineering Geology,* Volume 1, pp. 16-22.

Deere, D., Hendron, A., Patton, F. & Cording, E., 1967. Design of surface and near surface construction in rock. In: *Proceedings of the 8th U.S. Symposium on Rock Mechanics–.* New York: American Institute of Mining, Metallurgical and Petroleum Engineers Inc, pp. 237-302.

Diering, T., Ngidi, S., Bezuidenhout, J. & Paetzold, H., 2018. Palabora Lift 1 block cave: understanding the grade behaviour. *Caving 2018: Proceedings of the Fourth International Symposium on Block and Sublevel Caving,* pp. 91-106.

Fernandez, F., Evans, P. & Gelson, R., 2010. Design and Implementation of a Damage Assessment System at Argyle Diamond's Block Cave Project. *Caving 2010: Proceedings of the Second International Symposium on Block and Sublevel Caving,* Volume 2, pp. 65-81.

Fu, X., Sheng, Q. & Zhang, Y., 2013. Stepwise Excavation Process of Underground Caverns of Hydropower Station Using DDA. *Rock and Soil Mechanics,* 34(2), pp. 568-574.

Goel, R., Jethwa, J. & Paithankar, A., 1996. Correlation Between Barton's Q and Bieniawski's RMR A New Approach. *International Journal Rock Mechanics, Mining Sciences and Geomechanics,* 33(2), pp. 179-181.

Handley, M. & Piper, P., 2017. *Palabora Lift 2 Stress measurement: Internal Report,* Phalaborwa: Internal Report.

Hills, P., Raymond, N. & Doyle, M., 2015. 'Empirical ground support and reinforcement design at Challenger Gold Mine', in Y Potvin (ed.). *Design*

Methods 2015: Proceedings of the International Seminar on Design Methods in Underground Mining, pp. 385-398.

Hoek, E., 1994. Strength of rock and rock masses. *ISRM News Journal ,* Volume 2, p. 4–16.

Hoek, E., 2007. *Practical rock engineering.* [Online] Available at: www.rocscience.com [Accessed 23 January 2023].

Hoek, E. & Bieniawski, Z., 1965. Brittle fracture propagation in rock under compression. *International Journal of Fracture Mechanics,* 1(3), pp. 137-155.

Hoek, E. & Brown, E., 1980. *Underground excavation in rock.* 1 ed. London: CRC Press.

Hoek, E. & Brown, E., 2019. The Hoek-Brown failure criterion and GSI -2018 Edition. *Journal of Rock Mechanics and Geotechnical Engineering,* Volume 11, pp. 445-463.

Hoek, E., Carranza-Torres, C. & Corkum, B., 2002. Hoek-Brown failure criterion - 2002 Edition. *Proceedings of the 5th North American Rock Mechanics Symposium and 17th Tunnelling Association of Canada Conference: NARMS-TAC 2002,* Volume 1, pp. 267-273.

Hoek, E., Carter, T. & Diederichs, M., 2013. Quantification of the Geological Strength Index Chart. In: *Proceedings of the 47th US Rock Mechanics/Geomechanics Symposium.* San Francisco, CA, USA: ARMA, pp. 13-672.

Hoek, E. & Diederichs, M., 2006. Empirical estimation of rock mass modulus. *International Journal of Rock Mechanics & Mining Sciences,* Volume 43, pp. 203-215.

Hoek, E., Kaiser, P. & Bawden, W., 1995. *Support of Underground Excavations in Hard Rock.* Rotterdam, The Netherlands: AA Balkema.

Hutchinson, D. J. & Diederichs, M. S., 1996. *Cablebolting in Underground Mines.* Richmond: Bi Tech Publishers.

Kaiser, P. K. & Cai, M., 2013. Critical Review of Design Principles for Rock Support in Burst-Prone Ground – Time to Rethink. *Ground Support 2013: Proceedings of the Seventh International Symposium on Ground Support in Mining and Underground Construction,* 1(1), pp. 3-36.

Kaiser, P., McCreath, D. & Tannant, D., 1995. *Canadian Rockburst Research Program 1990-1995.* Sudbury: Geomechanics Research Centre.

Laubscher, D., 1994. Cave mining – the state of the art. *Journal of the South African Institute of Mining and Metallurgy,* 94(10), p. 279–293.

Laubscher, D. H., 1990. Mine Design: A Geomechanics Classification System for the Rating of Rock Mass in Mine Design. *Journal of the South African Institute of Mining & Metallurgy,* 90(10), pp. 257-272.

Laubscher, D. & Jakubec, J., 2001. Underground Mining Methods - Engineering Fundamentals and International Case Studies. In: A. Hustrulid W & R. Bullock, eds. *The MRMR rock mass classification for jointed rock masses.* Colorado, USA: Society for Mining, Metallurgy, and Exploration (SME), pp. 475-481.

Laubscher, D. & Page, C., 1990. The design of rock support in high stress or weak. In: *Proceedings of 92nd Canadian Institute of Mining & Metallurgy.* Ottawa: AGM, p. Paper # 91.

Laubscher, D. & Taylor, H., 1976. The importance of geomechanics of jointed rock masses in mining operations. *In: Proceedings of the Symposium on Exploration for Rock Engineering,* pp. 119-128.

Ledesma, O., Medive, I. & Sfriso, A., 2016. *Factor of safety by the strength-reduction technique applied to the Hoek-Brown model.* [Online] Available at:https://dxi97tvbmhbca.cloudfront.net/upload/user/image/ONLedesma_IM endive_ASfriso_Enief_201620191128191005047.pdf [Accessed 14 October 2022].

Leedy, P., 1993. *Practical Research: Planning and Design.* 5 ed. New York: Mackmillan.

Leedy, P. & Ormrod, J., 2001. *Practical Research Planning and Design.* 7 ed. Upper Saddle River, NJ and Thousand Oaks,CA: Merrill Prentice Hall and SAGE Publications.

Leedy, P. & Ormrod, J., 2005. *Practical Research Planning and Design.* Upper Saddle River, NJ: Prentice Hall.

Li, C., 2017. Principle of Rockbolting Design. *Journal of Rock Mechanics and Geotechnical Engineering,* 9(3), pp. 396-414.

Lorig, L. G. & Varona, P., 2013. 'Guidelines for numerical modelling of rock support for mines', in Y Potvin & B Brady (eds). *Ground Support 2013: Proceedings of the Seventh International Symposium on Ground Support in Mining and Underground Construction,* pp. 81-105.

Martin, C., Kaiser, P. & McCreath, D., 1998. Hoek–Brown parameters for predicting the depth of brittle failure around tunnels. *Canadian Geotechnical Journal,* Volume 36, pp. 136-151.

Masole, N., 2022. *Site Visit and Borehole Camera Assessment Report,* Phalaborwa: Internal Report.

Mathews, K., Hoek, E., Wyllie, D. & Stewart, S., 1981. *Prediction of stable excavations for mining at depths below 1000 metres in hard rock. CANMET report DSS Serial No. OSQ80-00081,* Ottawa: Department of Energy, Mines and Resources.

Mikula, P. A. & Lee, M. F., 2007. Empirical Performance Chart for Ground Support in Seismic Conditions at Mt Charlotte. *Deep Mining: Proceedings of the*

Fourth International Seminar on Deep and High Stress Mining,Australian Centre for Geomechanics, 1(1), pp. 324-334.

Morissette, P. & Hadjigeorgiou, J., 2019. Ground support design for dynamic loading conditions: A quantitative data-driven approach based on rockburst case studies. *Journal of Rock Mechanics and Geotechnical Engineering,* Volume 11, pp. 909-919.

Moss, A. & Kaiser, P., 2022a. Deformation-based support design for highly stressed ground with a focus on rockburst damage mitigation. *Journal of Rock Mechanics and Geotechnical Engineering,* 14(1), pp. 50-66.

Moss, A. & Kaiser, P., 2022b. Operational Approach to Ground Control in Deep Mines. *Journal of Rock Mechanics and Geotechnical Engineering,* 14(1), pp. 67-81.

Mouton, J., 2001. *How to Succeed in Your Master's and Doctoral Studies: A South African Guide and Resource Book.* Pretoria: Van Schaik.

Mouton, J. & Marais, H., 1994. *Basic concepts in the methodology of the social sciences.* Pretoria: HSRC.

NGI, 2022. *Using the Q-system: Rock mass classification and support design.* Norway: NGI.

Obert, L., 1973. Opening and development. In: *Mining Engineering Handbook.* Volume 1 ed. New York: Society of Mining Engineers (SME), pp. 10.2-10.4.

Pakalnis, R., 2015. Empirical design methods in practice. *Underground Design Methods 2015: Australian Centre for Geomechanics,* pp. 37-56.

Pakalnis, R., 2015. Empirical design methods in practice, in Y Potvin (ed.). *Proceedings of the International Seminar on Design Methods in Underground Mining,* pp. 37-56.

Palabora, 2015. *Palabora Copper Feasibility Study Lift II Base Case,* Phalaborwa: Internal Report.

Palabora, 2017. *Lift 2 Cover Drilling Report.* Phalaborwa: Internal report.

Palmström, A., 1982. The volumetric joint count - a useful and simple measure of the degree of jointing. *Proceedings of International Association of Engineering Geology. IAEG Congress,* Volume 2, pp. V.221- V.228.

Palmström, A., 2001. Measurement and characterization of rock mass jointing. In: V. Sharma & K. Saxena, eds. *In-situ Characterization of Rocks.* Oslo, Norway: A.A. Balkema , pp. 49-97.

Palmstrom, A. & Broch, E., 2006. Use and misuse of rock mass classifications systems with particular reference to the Q-system. *Tunnelling Underground Space Technology,* Volume 21, p. 575–593.

Pariseau, W., 2007. *Design analysis in rock mechanics,.* Balkema: Taylor & Francis.

Peck, W., 2000. Determining the stress reduction factor in highly stressed jointed rock. *Australian Centre for Geomechanics,* 35(2), pp. 57-60.

Potvin, Y. & Hadjigeorgiou, J., 2015. Empirical ground support design of mine drives, in Y Potvin (ed.). *Design Methods 2015: Proceedings of the International Seminar on Design Methods in Underground Mining,* pp. 419-430.

Potvin, Y. & Hadjigeorgiou, J., 2020. Ground Support for underground mines. In: *Numerical modelling for ground support design – mining applications.* Australia: Australian Centre for Geomechanics, p. 237.

Potvin, Y., Wesseloo, J. & Heal, D., 2010. An interpretation of ground support capacity submitted to dynamic loading. *Mining Technology,* 119(4), pp. 233-245.

Rahimi, B., Sharifzad, M. & Feng, X.-T., 2020. Ground behaviour analysis, support system design and construction strategies in deep hard rock mining -Justified in Western Australian’s mines. *Journal of Rock Mechanics and Geotechnical Engineering,* 12(1), pp. 1-20.

Rehman, H., Naji, A., Kim, J.-J. & Yoo, H.-K., 2018. Empirical Evaluation of Rock Mass Rating and Tunneling Quality Index System for Tunnel Support Design. *Applied Sciences,* 8(5), pp. 426-791.

RocScience, 2020. *3D Modelling of Underground Excavations with EX3 and RS3.* [Online] Available at: https://www.rocscience.com/learning/3d-modelling-of-undergroud-excavations-with-ex3-and-rs3 [Accessed 15 July 2023].

Rocscience, 2021b. *RS2 version 11.018,* Toronto: Rocscience Inc.

RocScience, 2021a. *Rocscience.* [Online] Available at: https://rocscience.com/software/dips [Accessed 25 July 2023].

RocSience, 2022. *Latest Features in Unwedge.* [Online] Available at: https://www.rocscience.com/learning/latest-features-in-Unwedge [Accessed 14 June 2023].

Sainsbury, B., Pierce, M. & Mas Ivars, D., 2008. Analysis of Caving Behaviour Using a Synthetic Rock Mass- Ubiquitous Joint Rock Mass Modelling Technique, , in Y Potvin, J Carter, A Dyskin & R Jeffrey (eds). *SHIRMS 2008: Proceedings of the First Southern Hemisphere International Rock Mechanics Symposium,* pp. 243-253.

Sainsbury, D.P., Sainsbury, B.L., Paetzold, H-D., Lourens, P. & Vakili, A., 2016. Caving induced subsidence behaviour of Lift 1 at the Palabora Block Cave mine. *Seventh International Conference & Exhibition on Mass Mining,* pp. 1-12.

Sharrock, G. B., Ooi, J. & Baasanjav, B., 2022. 'Geotechnical Analysis and Ground Support Selection for the Oyu Tolgoi Crusher Chamber #2', Y Potvin (ed.).

Caving 2022: Fifth International Conference on Block and Sublevel Caving, 1(1), pp. 227-240.

Sjöberg, J., 2020. Solving Rock Mechanics Issues Through Modelling: Then, Now, and In the Future. *UMT 2020: Proceedings of the Second International Conference on Underground Mining Technology,* 3-4 November, 2(1), pp. 27-46.

Somodi, G., Bar, N., Kovács, L., Arrieta, M., Török, Á. & Vásárhelyi, B., 2021. Study of Rock Mass Rating (RMR) and Geological Strength Index (GSI) Correlations in Granite, Siltstone, Sandstone and Quartzite Rock Masses. *Applied Sciences,* 28 February, 11(8), p. 3351.

Southwood, M. & Cairncross, B., 2017. The Minerals of Palabora, Limpopo Province, South Africa. *Rock & Minerals,* 92(5), pp. 426-453.

Speakman, R., 2022. 'A mixed-method approach for major excavation ground support evaluation', in Y Potvin (ed.). *Caving 2022: Fifth International Conference on Block and Sublevel Caving,* Volume 1, pp. 279-288.

Stacey, T., 2009. Design a Strategic Issue. *Journal of the South African Institute of Mining and Mertallugy,* 109(3), pp. 157-162.

Stacey, T., 2015. Rock engineering design — the importance of process, prediction of behaviour, choice of design criteria, review and consideration of risk. *Design Methods 2015: Proceedings of the International Seminar on Design Methods in Underground Mining,* pp. 57-76.

Stacey, T., 2016. *Innovative and controversial support for rockbursting conditions,* Lulea, Sweden.: Innovative and controversial support for rockbursting conditions.

Stacey, T. & Page, C., 1986. *Practical Handbook for Underground Rock Mechanics.* Johannesburg: Trans Tech Publications.

Stacey, T. R., 2001. *Best Practice Rock Engineering Handbook for “Other” Mines.* Braamfontein: The Safety in Mines Research Advisory Committee (SIMRAC).

Stacey, T. & Wesseloo, J., 2022. Design and Prediction in Rock Engineering: The Importance. *Rock Mechanics and Rock Engineering of Mechanisms of Failure, with Focus on High Stress, Brittle Rock Conditions,* Volume 55, p. 1517–1535.

Talu, M. & Wilson, A., 2004. Innovative Mining Method and Related Support systems and Quality Assurance for a Large Underground Crusher Excavation: De Beers Finsch Mine, South Africa. *In Proceedings of Massive Mining 2004,* pp. 356-361.

Talu, S., 2011. *Lift 2 underground study: Lift 2 decline and portal support recommendations,* Phalaborwa: Internal Report.

Terron-Almenara, J., Holter, K. & Høien, A., 2023. A Hybrid Methodology of Rock Support Design for Poor Ground Conditions in Hard Rock Tunnelling. *Rock Mechanics and Rock Engineering,* Volume 56, p. 4061–4088 .

Unteregger, D., Fuchs, B. & Hofstetter, G., 2015. Damage plasticity model for different types of intact rock. *International Journal of Rock Mechanics and Mining Sciences,* Volume 80, pp. 402-411.

Van As, A. & Guest, A., 2020. The design & operating philosophies of panel vs block caving. *MassMin2020: Proceedings of the Eighth International Conference & Exhibition on Mass Mining,* pp. 207-220.

Verwoerd, W. J., 1986. Mineral deposits associated with carbonatites and alkaline rocks. *In Mineral deposits of Southern Africa: Geological Society of South Africa,* 2(21), pp. 73-91.

Vithal, R. & Jansen, J., 2019. *Designing Your First Research Proposal: A Manual for Beginning Researchers.* 2 ed. Cape Town: Juta.

Zhao, C., Zhu, W., Li, S. & Yu, S., 2016. Stability Analysis of Caverns Surrounding Rock Mass by Improved Discontinuous Deformation Analysis Method. *Journal of Central South University of Science and Technology,* 47(2), pp. 593-598.

A. APPENDIX

Shown in Figure A- 1 is an illustration of the six parameters of the Q system after (NGI,2022).

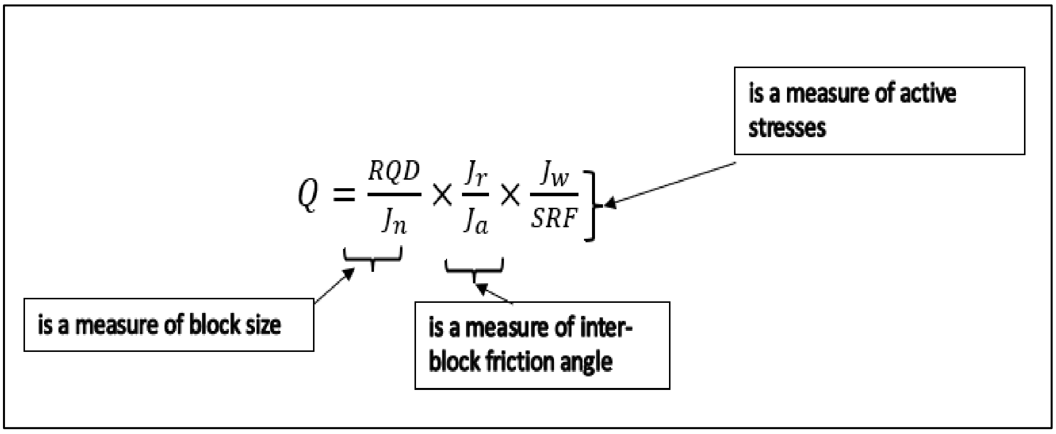

Figure A- 1: Q system (NGI,2022)

Figure A-2 shows the orientation guide adopted at PMC.

Orientation Guide

Strike and Dip of Joints Relative to Tunnel Direction

Parallel to the Tunnel

Perpendicular to the Tunnel

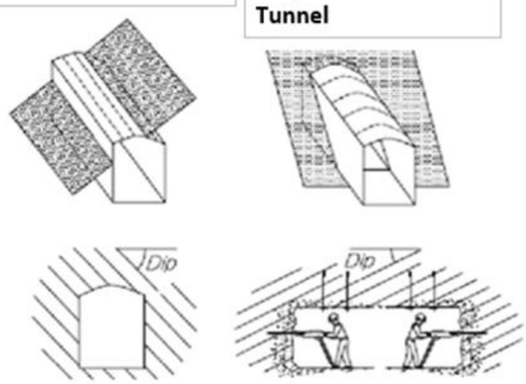

Note:
- **Crusher chambers are to be developed along the North-South Direction.**
- **Therefore, Joints dipping along the crusher chamber will influence stability more.**

Dip (degrees)	Dip parallel to Tunnel	Dip with Tunnel	Dip Against Tunnel
60 - 90	Very favorable	Very favorable	Fair
45 - 60	Fair	Favorable	Unfavorable
0 - 45	Fair	Very unfavorable	Very unfavorable

Figure A- 2: Orientation guide (Bieniawski, 1989)

Table A-1: RMR parameters and rating (Bieniawski, 1989)

A. CLASSIFICATION PARAMETERS AND THEIR RATINGS									
	Parameter		Range of Values						
1	Strength of intact Rock Material	Point Load Strength Index	>10 MPa	4-10 MPa	2-4 MPa	1-2MPa	For this low range- uniaxial compressive test is preferred		
		Uniaxial Compressive Strength	>250 MPa	100-250 MPa	50-100 MPa	25-50 MPa	5-25 MPa	1-5 MPa	<1 MPa
	Rating		15	12	7	4	2	1	0
2	Drill core Quality RQD		90%-100%	75%-90%	50%-75%	25%-50%	<25%		
	Rating		20	17	13	8	3		
3	Spacing of Discontinuities		>2m	0.6m-2m	200-600mm	60-200mm	<60mm		
	Rating		20	15	10	8	5		
4	Condition of Discontinuities (See E)		Very rough surfaces; Not continuous; No separation; Unweathered wall rock	Slightly rough surfaces; Separation <1mm; Slightly weathered walls	Slightly rough surfaces; Separation <1mm; Highly weathered walls	Slickensided surfaces or Gouge <5mm thick or Separation 1-5mm; Continuous	Soft gouge >5mm thick or Separation >5mm; Continuous		
	Rating		30	25	20	10	0		
5	Groundwater	Inflow / 10m tunnel length (l/m)	None	<10	10-25	25-125	>125		
		(Joint water press.) / (Major principal stress)	0	<0.1	0.1-0.2	0.2-0.5	>0.5		
		General Conditions	Completely Dry	Damp	Wet	Dripping	Flowing		
	Ratings		15	10	7	4	0		

B. RATING ADJUSTMENT FOR DISCONTINUITY ORIENTATIONS (See F)						
Strike And Dip Orientations		Very Favourable	Favourable	Fair	Unfavourable	Very Unfavourable
Ratings	Tunnels and Mines	0	-2	-5	-10	-12
	Foundations	0	-2	-7	-15	-25
	Slopes	0	-5	-25	-50	-

Table A-2: Cont... RMR parameters and rating (Bieniawski, 1989)

C. ROCK MASS CLASSES DETERMINED FROM TOTAL RATINGS					
Rating	100 ← 81	80 ← 61	60 ← 41	40 ← 21	<21
Class Number	I	II	III	IV	V
Description	Very Good Rock	Good Rock	Fair Rock	Poor Rock	Very Poor Rock
D. MEANING OF ROCK CLASSES					
Class Number	I	II	III	IV	V
Average Stand-Up Time	20yrs for 15m span	1yr for 10m span	1 week for 5m span	10hrs for 2.5m span	30min for 1m span
Cohesion of Rock Mass (kPa)	>400	300-400	200-300	100-200	<100
Friction Angle of Rock Mass (°)	>45	35-45	25-35	15-25	<15
E. GUIDELINES FOR CLASSIFICATION OF DISCONTINUITY CONDITIONS					
Discontinuity Length (Persistence)	<1m	1-3m	3-10m	10-20m	>20m
Rating	6	4	2	1	0
Separation (Aperture)	None	<0.1mm	0.1-1.0mm	1-5mm	>5mm
Rating	6	5	4	1	0
Roughness	Very Rough	Rough	Slightly Rough	Smooth	Slickensided
Rating	6	5	3	1	O
Infilling (Gouge)	None	Hard Filing <5mm	Hard Filling >5mm	Soft Filling <5mm	Soft Filling >5mm
Rating	6	4	2	2	0
Weathering	Unweathered	Slightly Weathered	Moderately Weathered	Highly Weathered	Decomposed
Rating	6	5	3	1	0

F. EFFECT OF DISCONTINUITY STRIKE AND DIP ORIENTATION IN TUNNELING			
Strike Perpendicular to Tunnel Axis		Strike Parallel to Tunnel Axis	
Drive with Dip: Dip 45°- 90°	Drive with Dip: Dip 20°- 45°	Dip 45°- 90°	Dip 20°- 45°
Very Favourable	Favourable	Very Unfavourable	Fair
Drive against Dip: Dip 45°- 90°	Drive against Dip: Dip 20°- 45	Dip 0°- 20°: Irrespective of Strike	
Fair	Unfavourable	Fair	

A typical load deformation curve of a 25mm threaded bar is shown in Figure A-3.

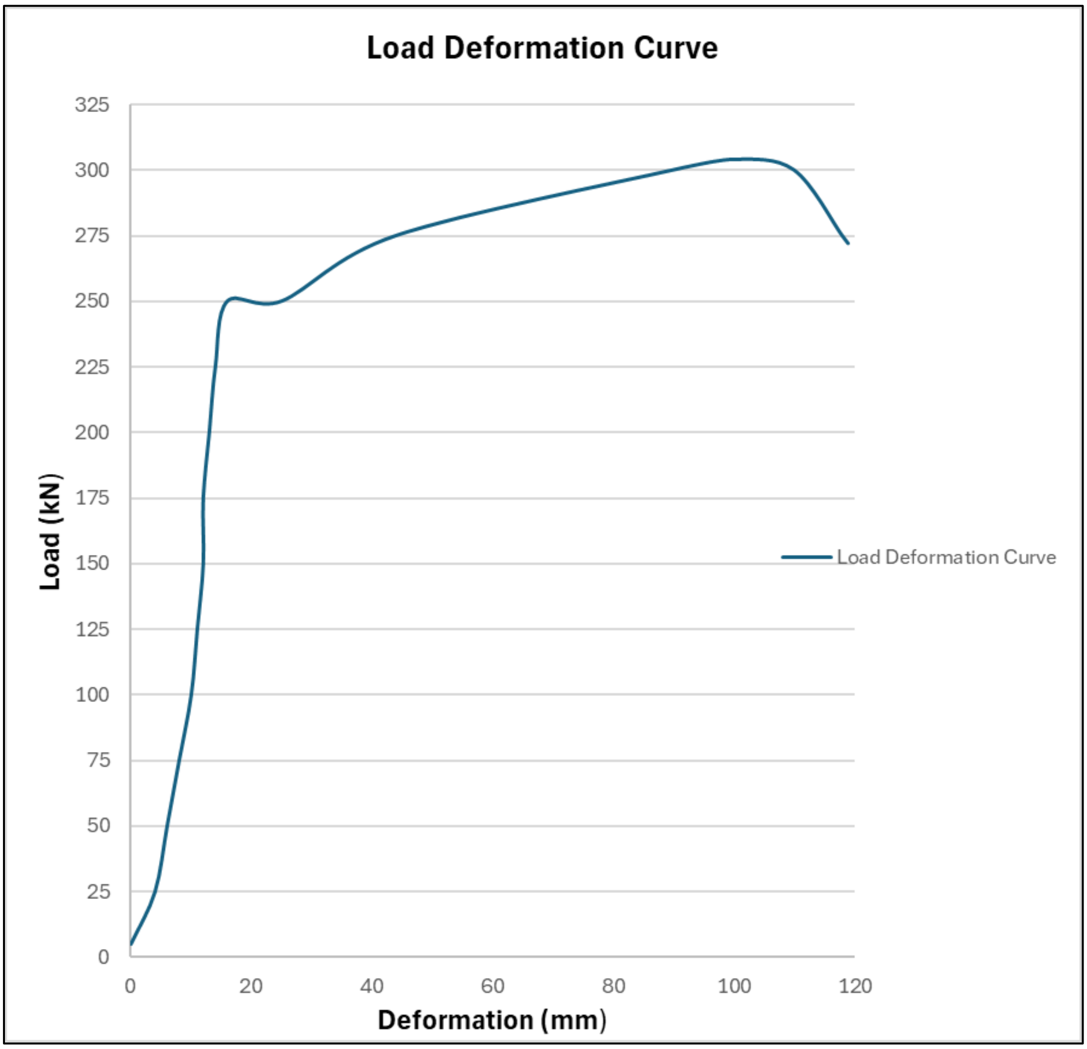

Figure A- 3: Typical loding deformation curve of a 25mm threaded bar.

A stress vs strain curve of a 18mm 7 strands cable bolt is shown in Figure A-4.

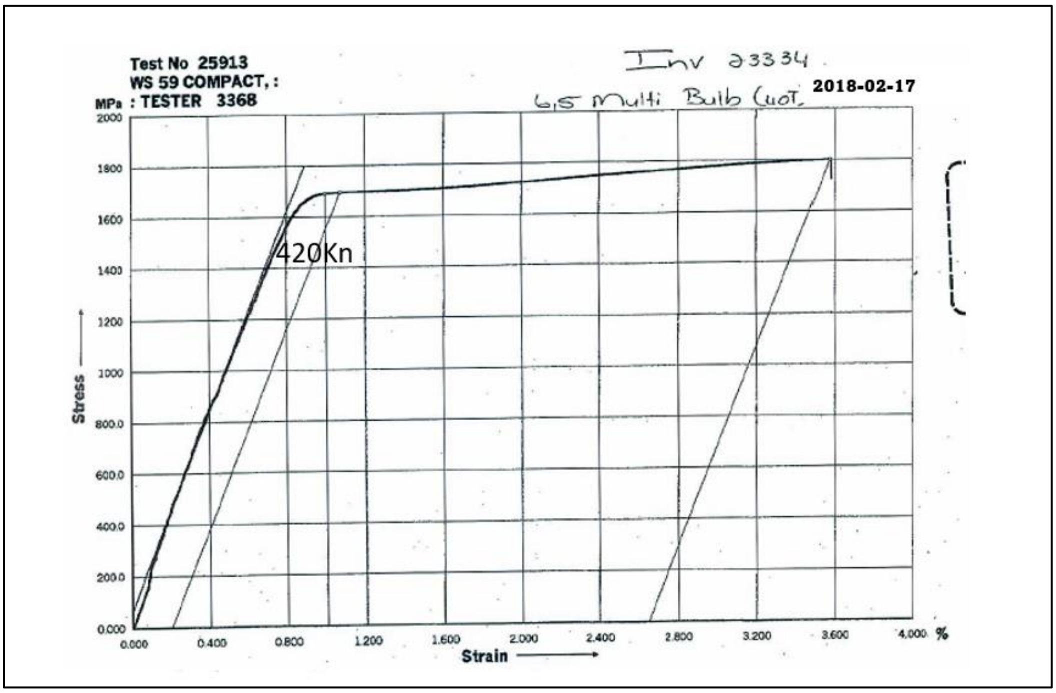

Figure A- 4: Strength /strain curve for 18mm 7 strand cable bolt.

The following geological conditions were observed from the core sample extracted from the borehole: Discing, fracture, discing-fracture, dyke, and crushed zone. A comprehensive overview of the geological summary of the borehole is provided in Table A-3 to TableA-8.

Table A-3: : Geological summary of HD020 (Palabora, 2017)

Ins	Drill Hole ID	Project	Geology From	Geology To	Priority	Logged By	Rock Type	Top Contact	Bottom Contact	Dip	Texture	Alteration	Structure	Grain Size	Colour
1	HD020	2ndLft_Cov	0	23.66	1	SM	FOS	TOH	GRADATIONAL		MELA	S_ALT	NONE	MG	OLIVE_GREY
2	HD020	2ndLft_Cov	23.66	24.72	1	SM	MPY	GRADATIONAL	GRADATIONAL		MESO	NONE	NONE	CG	MED_BROWN
3	HD020	2ndLft_Cov	24.72	25.67	1	SM	FOS	GRADATIONAL	GRADATIONAL		MELA	NONE	NONE	CG	OLIVE_GREY
4	HD020	2ndLft_Cov	25.67	27.18	1	SM	MFOS	GRADATIONAL	GRADATIONAL		MESO	NONE	FRAC	CG	GREEN_BROW
5	HD020	2ndLft_Cov	27.18	27.73	1	SM	FOS	GRADATIONAL	GRADATIONAL		MELA	NONE	NONE	CG	OLIVE_GREY
6	HD020	2ndLft_Cov	27.73	34.61	1	SM	MPY	GRADATIONAL	GRADATIONAL		MESO	NONE	NONE	CG	DARK_BROWN
7	HD020	2ndLft_Cov	34.61	36.2	1	SM	MFOS	GRADATIONAL	GRADATIONAL		MESO	NONE	NONE	CG	DARK_BROWN
8	HD020	2ndLft_Cov	36.2	38.82	1	SM	MPY	GRADATIONAL	BROKEN		MESO	NONE	NONE	MG	MED_BROWN
9	HD020	2ndLft_Cov	38.82	46.56	1	SM	FOS	BROKEN	GRADATIONAL		MELA	NONE	NONE	CG	OLIVE_GREY
10	HD020	2ndLft_Cov	46.56	48.9	1	SM	MPY	GRADATIONAL	BROKEN		MESO	NONE	JOINT	CG	GREEN_BROW
11	HD020	2ndLft_Cov	48.9	50.26	1	SM	MFO	BROKEN	SHARP	55	MESO	NONE	NONE	CG	OLIVE_GREY
12	HD020	2ndLft_Cov	50.26	50.87	1	SM	MPY	SHARP	GRADATIONAL		MESO	NONE	JOINT	CG	GREEN_BROW
13	HD020	2ndLft_Cov	50.87	52.11	1	SM	MFO	GRADATIONAL	SHARP	50	MESO	NONE	NONE	CG	GREEN_BROW
14	HD020	2ndLft_Cov	52.11	70	1	SM	FOS	SHARP	SHARP	53	MESO	NONE	NONE	CG	MED_GREY
15	HD020	2ndLft_Cov	70	141	1	SM	DOL	SHARP	BROKEN		HOMO	NONE	JOINT	FG	LIGHT_GREY
16	HD020	2ndLft_Cov	141	143.4	1	SM	MFOS	BROKEN	GRADATIONAL		MESO	S_ALT	FRAC	CG	OLIVE_GREY
17	HD020	2ndLft_Cov	143.4	144.95	1	SM	MPY	GRADATIONAL	GRADATIONAL		MESO	NONE	NONE	CG	MED_BROWN
18	HD020	2ndLft_Cov	144.95	149.92	1	SM	MFOS	GRADATIONAL	GRADATIONAL		MESO	NONE	NONE	CG	LIGHT_GREY
19	HD020	2ndLft_Cov	149.92	151.32	1	SM	BCB	GRADATIONAL	SHARP	83	LEUCO	NONE	JOINT	MG	WHITE
20	HD020	2ndLft_Cov	151.32	151.99	1	SM	MFOS	SHARP	SHARP	80	MELA	NONE	NONE	CG	DARK_GREY
21	HD020	2ndLft_Cov	151.99	154.39	1	SM	BCB	SHARP	GRADATIONAL		LEUCO	NONE	JOINT	MG	WHITE
22	HD020	2ndLft_Cov	154.99	158.81	1	SM	MFOS	GRADATIONAL	SHARP	54	MESO	NONE	NONE	CG	GREEN_BROW
23	HD020	2ndLft_Cov	158.81	161	1	SM	MPY	SHARP	SHARP	40	MESO	NONE	NONE	CG	GREEN_BROW
24	HD020	2ndLft_Cov	161	162.29	1	SM	MFOS	SHARP	BROKEN		MESO	NONE	NONE	CG	DARK_GREY
25	HD020	2ndLft_Cov	162.29	163.89	1	SM	MPY	BROKEN	GRADATIONAL		MESO	NONE	JOINT	MG	GREEN_BROW
26	HD020	2ndLft_Cov	163.89	165.11	1	SM	MFOS	GRADATIONAL	GRADATIONAL		MESO	S_ALT	JOINT	MG	DARK_BROWN
27	HD020	2ndLft_Cov	165.11	166.44	1	SM	MPY	GRADATIONAL	SHARP	35	MESO	NONE	NONE	CG	GREEN_BROW
28	HD020	2ndLft_Cov	166.44	167.37	1	SM	MFOS	SHARP	GRADATIONAL		MESO	NONE	NONE	CG	DARK_BROWN
29	HD020	2ndLft_Cov	167.37	169.38	1	SM	FOS	GRADATIONAL	SHARP	65	MESO	NONE	NONE	CG	OLIVE_GREY
30	HD020	2ndLft_Cov	169.38	169.98	1	SM	DOL	SHARP	SHARP	66	HOMO	NONE	JOINT	FG	DARK_GREY
31	HD020	2ndLft_Cov	169.98	172.77	1	SM	FOS	SHARP	SHARP	51	MELA	NONE	NONE	CG	DARK_GREY
32	HD020	2ndLft_Cov	172.77	175.51	1	SM	TCB	SHARP	SHARP	47	LEUCO	NONE	NONE	CG	WHITE
33	HD020	2ndLft_Cov	175.51	180.03	1	SM	FOS	SHARP	SHARP	70	MESO	NONE	NONE	CG	OLIVE_GREY
34	HD020	2ndLft_Cov	180.03	180.59	1	SM	TCB	SHARP	SHARP	86	LEUCO	NONE	JOINT	MG	WHITE
35	HD020	2ndLft_Cov	180.59	181.61	1	SM	MPY	SHARP	SHARP	50	MESO	NONE	NONE	CG	GREEN_BROW
36	HD020	2ndLft_Cov	181.61	189.46	1	SM	FOS	SHARP	SHARP	49	MELA	NONE	NONE	CG	OLIVE_GREY
37	HD020	2ndLft_Cov	189.46	190.72	1	SM	BCB	SHARP	SHARP	65	LEUCO	NONE	NONE	MG	WHITE
38	HD020	2ndLft_Cov	190.72	192.32	1	SM	FOS	SHARP	SHARP	45	MELA	NONE	JOINT	CG	OLIVE_GREY
39	HD020	2ndLft_Cov	192.32	193.84	1	SM	MPY	SHARP	GRADATIONAL		MESO	NONE	NONE	CG	GREEN_BROW
40	HD020	2ndLft_Cov	193.84	194.63	1	SM	FOS	GRADATIONAL	GRADATIONAL		MELA	NONE	NONE	CG	BLACK
41	HD020	2ndLft_Cov	194.63	195.59	1	SM	MPY	GRADATIONAL	GRADATIONAL		MESO	NONE	NONE	CG	DARK_BROWN
42	HD020	2ndLft_Cov	195.59	196.96	1	SM	MFOS	GRADATIONAL	SHARP	35	MESO	NONE	JOINT	CG	LIGHT_GREY
43	HD020	2ndLft_Cov	196.96	197.55	1	SM	MPY	SHARP	SHARP	90	MESO	NONE	NONE	CG	GREEN_BROW
44	HD020	2ndLft_Cov	197.55	198.11	1	SM	TCB	SHARP	SHARP	55	LEUCO	NONE	NONE	CG	WHITE
45	HD020	2ndLft_Cov	198.11	199.92	1	SM	MPY	SHARP	SHARP	70	MESO	NONE	JOINT	CG	GREEN_BROW
46	HD020	2ndLft_Cov	199.92	204.38	1	SM	MFOS	SHARP	GRADATIONAL		MELA	NONE	NONE	MG	LIGHT_BROWN
47	HD020	2ndLft_Cov	204.38	208.68	1	SM	FOS	GRADATIONAL	SHARP	59	MELA	NONE	NONE	CG	OLIVE_GREY
48	HD020	2ndLft_Cov	208.68	260.75	1	SM	DOL	SHARP	SHARP	34	HOMO	NONE	JOINT	FG	DARK_GREY
49	HD020	2ndLft_Cov	260.75	303.34	1	SM	FOS	SHARP	EOH		MELA	NONE	JOINT	CG	MED_GREY

Table A-4: Summary of major structure log of HD020 (Palabora, 2017)

Ins	Drill Hole ID	Project	Date	Logged By	Priority	Geology From	Geology To	Major Structure Type	Major Structure Desc	Infill Quality	Infill Type	Alteration
1	HD020	2ndLft_Cov	10-Apr-2017 06:18:38	SM	1	0	3	2	4	3	No_Infill	2
2	HD020	2ndLft_Cov	10-Apr-2017 06:18:38	SM	1	3	6.9	9-2	4	5	No_Infill	2
3	HD020	2ndLft_Cov	10-Apr-2017 06:18:38	SM	1	7.62	7.95	9-2	6	5	No_Infill	2
4	HD020	2ndLft_Cov	10-Apr-2017 06:18:38	SM	1	8.67	9.25	2	4	3	No_Infill	1
5	HD020	2ndLft_Cov	10-Apr-2017 06:18:38	SM	1	9.83	12.7	9-2	6	5	No_Infill	1
6	HD020	2ndLft_Cov	10-Apr-2017 06:18:38	SM	1	19.86	21.93	9	3	5	No_Infill	3
7	HD020	2ndLft_Cov	10-Apr-2017 06:18:38	SM	1	70	141	8	3-4	3-4	Calcite	1
8	HD020	2ndLft_Cov	10-Apr-2017 06:18:38	SM	1	141	142.8	3	3	2	No_Infill	3
9	HD020	2ndLft_Cov	10-Apr-2017 06:18:38	SM	1	169.38	169.98	8	3	4	No_Infill	1
10	HD020	2ndLft_Cov	10-Apr-2017 06:18:38	SM	1	208.68	260.75	8	3	4	Calcite	1

Table A-5: Geological summary of HD039 (Palabora, 2017)

Ins	Project	Geology From	Geology To	Priority	Logged By	Rock Type	Top Contact	Bottom Contact	Dip	Texture	Alteration	Structure	Grain Size	Colour
1	2ndLft_Cov	0	16.13	1	NM	FOS	GRADATIONAL	GRADATIONAL		MELA	HW	FRAC	MG	OLIVE_GREY
2	2ndLft_Cov	16.13	18.02	1	NM	FOS	GRADATIONAL	GRADATIONAL		MELA	NONE	NONE	CG	BLACK
3	2ndLft_Cov	18.02	20.33	1	NM	FOS	GRADATIONAL	GRADATIONAL		MESO	HW	FRAC	CG	OLIVE_GREY
4	2ndLft_Cov	20.33	21.7	1	NM	BCB	GRADATIONAL	GRADATIONAL		LAY	NONE	NONE	FG	LIGHT_GREY
5	2ndLft_Cov	21.7	54	1	NM	FOS	GRADATIONAL	GRADATIONAL		MESO	HW	FRAC	MG	OLIVE_GREY
6	2ndLft_Cov	54	54.84	1	NM	MPY	GRADATIONAL	GRADATIONAL		MESO	NONE	NONE	FG	GREEN_BROWN
7	2ndLft_Cov	54.84	65.03	1	NM	FOS	GRADATIONAL	SHARP	80	MELA	S_ALT	FRAC	CG	GREEN_GREY
8	2ndLft_Cov	65.03	129.4	1	NM	DOL	SHARP	SHARP	47	HOMO	NONE	FRAC	MG	MED_GREY
9	2ndLft_Cov	129.4	132	1	NM	FOS	SHARP	GRADATIONAL		MELA	NONE	NONE	MG	DARK_GREY
10	2ndLft_Cov	132	133.4	1	NM	TCB	GRADATIONAL	SHARP	56	MESO	S_ALT	FRAC	FG	LIGHT_GREY
11	2ndLft_Cov	133.4	147.71	1	NM	FOS	SHARP	GRADATIONAL		MELA	NONE	NONE	MG	DARK_GREY
12	2ndLft_Cov	147.71	149.56	1	NM	MPY	GRADATIONAL	SHARP	50	MESO	NONE	NONE	FG	MED_BROWN
13	2ndLft_Cov	149.56	150.84	1	NM	BCB	SHARP	SHARP	70	LAY	NONE	NONE	MG	WHITE
14	2ndLft_Cov	150.84	152.94	1	NM	MFOS	SHARP	GRADATIONAL		MELA	NONE	NONE	CG	RED_BROWN
15	2ndLft_Cov	152.94	153.67	1	NM	BCB	GRADATIONAL	BROKEN		LEUCO	NONE	NONE	FG	WHITE
16	2ndLft_Cov	153.67	177.05	1	NM	FOS	BROKEN	SHARP	85	MELA	HW	NONE	CG	DARK_GREY
17	2ndLft_Cov	177.05	186.2	1	NM	FOS	GRADATIONAL	SHARP	85	MELA	NONE	NONE	CG	DARK_GREY
18	2ndLft_Cov	186.2	227.4	1	NM	DOL	SHARP	SHARP	40	HOMO	S_ALT	FRAC	MG	MED_GREY
19	2ndLft_Cov	227.4	237.9	1	NM	FOS	SHARP	GRADATIONAL		MELA	NONE	NONE	CG	DARK_GREY
20	2ndLft_Cov	237.9	240.1	1	NM	FOS	GRADATIONAL	GRADATIONAL		MELA	NONE	NONE	FG	GREEN_GREY
21	2ndLft_Cov	240.1	251.64	1	NM	FOS	GRADATIONAL	SHARP	68	MESO	NONE	NONE	CG	GREEN_GREY
22	2ndLft_Cov	252.64	253.6	1	NM	BCB	SHARP	SHARP	85	LEUCO	NONE	NONE	MG	WHITE
23	2ndLft_Cov	253.6	259.14	1	NM	FOS	SHARP	GRADATIONAL		MESO	NONE	NONE	MG	MED_GREY

Table A-6: Summary of Major Structure log of HD039 (Palabora, 2017)

Ins	Drill Hole ID	Project	Date	Logged By	Priority	Geology From	Geology To	Major Structure Type	Major Structure Desc	Infill Quality	Infill Type	Alteration
1	HD039	2ndLft_Cov	21-Apr-2017 13:23:18	NM	1	3	7.53	2	3	3	No_Infill	2
2	HD039	2ndLft_Cov	21-Apr-2017 13:23:18	NM	1	22.48	22.9	2	3	3	No_Infill	2
3	HD039	2ndLft_Cov	21-Apr-2017 13:23:18	NM	1	35.8	36.65	2-3	4	2-3	No_Infill	2
4	HD039	2ndLft_Cov	21-Apr-2017 13:23:18	NM	1	60.73	61.4	2	3	2-3	No_Infill	2
5	HD039	2ndLft_Cov	21-Apr-2017 13:23:18	NM	1	65.03	129.4	8	3-4	3-4	No_Infill	1
6	HD039	2ndLft_Cov	24-Apr-2017 13:23:18	NM	1	186.2	227.4	8	3	3-4	Calcite	2

Table A-7: **Geological Summary of HD051 (Palabora, 2017)**

Ins	Drill Hole ID	Geology From	Geology To	Priority	Rock Type	Top Contact	Bottom Contact	Dip	Texture	Alteration	Structure	Grain Size	Colour
1	HD051	0	47	1	FOS	TOH	GRADATIONAL		MELA	S_ALT	NONE	CG	GREEN_GRE
2	HD051	47	69.94	1	FOS	GRADATIONAL	SHARP	50	MELA	NONE	NONE	CG	GREEN_GRE
3	HD051	69.94	131.52	1	DOL	SHARP	SHARP	65	MELA	NONE	FRAC	FG	MED_GREY
4	HD051	131.52	138.32	1	MPY	SHARP	SHARP	85	MELA	S_ALT	FRAC	MG	GREEN_BRO
5	HD051	138.32	148.94	1	FOS	SHARP	GRADATIONAL		MESO	NONE	NONE	CG	BLACK
6	HD051	148.94	150.75	1	MPY	GRADATIONAL	BROKEN		MELA	NONE	NONE	MG	GREEN_BRO
7	HD051	150.75	152	1	FOS	BROKEN	SHARP	45	MELA	NONE	NONE	MG	DARK_GREY
8	HD051	152	152.55	1	MPY	SHARP	SHARP	55	MESO	NONE	NONE	MG	MED_OLIVE
9	HD051	152.55	153.32	1	BCB	SHARP	SHARP	65	LEUCO	NONE	NONE	FG	WHITE
10	HD051	153.32	155.37	1	MFOS	SHARP	GRADATIONAL		MESO	NONE	NONE	MG	OLIVE_GREY
11	HD051	155.37	157.75	1	BCB	GRADATIONAL	SHARP	25	LEUCO	NONE	NONE	FG	LIGHT_GREY
12	HD051	157.75	159.23	1	MPY	SHARP	SHARP	40	MESO	NONE	NONE	MG	GREEN_BRO
13	HD051	159.23	160.39	1	FOS	SHARP	SHARP	45	MELA	NONE	NONE	CG	BLACK
14	HD051	160.39	161.54	1	BCB	SHARP	SHARP	30	LEUCO	NONE	NONE	FG	WHITE
15	HD051	161.54	163.8	1	MPY	SHARP	GRADATIONAL		MESO	NONE	NONE	MG	GREEN_BRO
16	HD051	163.8	168	1	FOS	GRADATIONAL	SHARP	35	MESO	NONE	NONE	CG	MED_GREY
17	HD051	168	170.95	1	MPY	SHARP	SHARP	30	MESO	NONE	NONE	MG	GREEN_BRO
18	HD051	170.95	172.95	1	FOS	SHARP	SHARP	50	MELA	NONE	NONE	CG	DARK_GREY
19	HD051	172.95	175.48	1	MPY	SHARP	GRADATIONAL		MESO	NONE	NONE	MG	GREEN_BRO
20	HD051	175.48	202.37	1	FOS	GRADATIONAL	GRADATIONAL		MESO	S_ALT	FRAC	CG	GREEN_GRE
21	HD051	202.37	246.52	1	DOL	GRADATIONAL	SHARP	40	MELA	NONE	NONE	MG	DARK_GREY
22	HD051	246.52	276.84	1	FOS	SHARP			MELA	S_ALT	FRAC	CG	GREEN_GRE
23	HD051	276.84	281.41	1	MPY	SHARP	GRADATIONAL	40	MELA	NONE	NONE	MG	GREEN_BRO
24	HD051	281.41	284.5	1	FOS	GRADATIONAL	SHARP	60	MELA	S_ALT	NONE	MG	GREEN_GRE
25	HD051	284.5	286.16	1	MPY	SHARP	GRADATIONAL		MESO	NONE	FRAC	FG	GREEN_BRO
26	HD051	286.16	294.3	1	FOS	GRADATIONAL	SHARP	35	MELA	NONE	NONE	MG	GREEN_GRE
27	HD051	294.3	295.63	1	TCB	SHARP	SHARP	35	LEUCO	NONE	NONE	FG	WHITE
28	HD051	295.63	300.02	1	MPY	SHARP	EOH		MESO	NONE	NONE	CG	GREEN_BRO

Table A-8: Summary of major structure log of HD051 (Palabora, 2017)

Ins	Drill Hole ID	Project	Date	Logged By	Priority	Geology From	Geology To	Major Structure Type	Infill Type	Alteration
1	HD051	2ndLft_Cov	29-Jun-2018 12:19:46	NM	1	3.64	6.78	2	No_Infill	2
2	HD051	2ndLft_Cov	29-Jun-2018 12:19:46	NM	1	69.8	71.2	2	No_Infill	1
3	HD051	2ndLft_Cov	29-Jun-2018 12:19:46	NM	1	71.2	131.52	8	No_Infill	1
4	HD051	2ndLft_Cov	29-Jun-2018 12:19:46	NM	1	134.08	138.62	2	No_Infill	2
5	HD051	2ndLft_Cov	11-Jul-2018 12:19:46	NM	1	202.37	246.52	8	No_Infill	1
6	HD051	2ndLft_Cov	11-Jul-2018 12:19:46	NM	1	264.66	265.41	2	No_Infill	2

A detailed description of the structure types is presented in Table A-9.

Table A-9: Table codes description (Palabora, 2017)

Structure type		Alteration
2 – Fractured Zone	9 – Discing	1- No Alterations
9-2 – Discing - Fracture		2- Weaker than the IRS
8 – Dyke		3- Stronger than the IRS
3 - Crushed		